A study on the possibilities of using a coupled or schematized numerical method to determine the flow pattern downstream of a discharge sluice

An Ostend case study

T.T. Grolleman

Witteveen + Bos

TU Delft

A study on the possibilities of using a coupled or schematized numerical method to determine the flow pattern downstream of a discharge sluice

An Ostend case study

by

T.T. Grolleman

to obtain the degree of Master of Science
at the Delft University of Technology,

Student number:	4366484	
Project duration:	November 16, 2020 – October 19, 2021	
Thesis committee:	Prof. dr. ir. M. (Mark) van Koningsveld,	TU Delft
	Dr. ir, I. (Ido) Akkerman,	TU Delft
	Ir. A. J. (Arne) van der Hout,	TU Delft
	Ir. F. P. (Floor) Bakker,	TU Delft
	Ir. T. E. (Tim) van Engelen,	Witteveen+Bos

TU Delft

Nomenclature

Abbreviations

1D	One-dimensional
3D	Three-dimensional
AEM	Algebraic Eddy viscosity closure Model
AMDK	Agentschap Maritieme Dienstverlening en Kust
ASCE	American Society of Civil Engineers
COMSOL	COMSOL Multiphysics 5.6
CSM	Continental Shelf Model
D3D	Delft3D-FLOW 4
DES	Detached Eddy Simulation
DESA	Distributed Entrainment Sink Approach
EFDC	Environmental Fluid Dynamics Code
FEM	Finite Element Method
HIC	Hydrologisch Informatie Centrum
IMDC	International Marine and Dredging Consultants
JETLAG	Lagrangian Jet Model
LES	Large Eddy Simulation
MHW	Mean High Water
MLW	Mean Low Water
PIANC	Permanent International Commission for Navigation Congresses
PSU	Practical Salinity Unit
RANS	Reynolds Averaged Navier-Stokes
RNG	Re-Normalisation Group
RSM	Reynolds Stress Model
RYCO	Royal Yachtclub Oostende
SWE	Shallow Water Equations
TAW	Tweede Algemene Waterpassing
USA	United States of America
WL	Waterbouwkundig Laboratorium
ZUNO	Zuidelijke Noordzee

Greek Symbols

β	Convective velocity vector	[m/s]
Δt	Time step	[s]
Δx	Spatial step	[m]
Δy	Cross sectional length	[m]
δ	Height wall boundary layer	[m]
ϵ	Dissipation rate	[-]
ϵ	Roughness height	[m]
μ	Discharge coefficient	[-]
μ_T	Turbulent dynamic viscosity	[Ns/m^2]
ν	Kinematic viscosity	[m^2/s]
ρ	Density	[kg/m^3]
ξ	Energy loss coefficient	[-]

Roman Symbols

A	Flow surface	[m^2]
b	0.1 x distance from outflow opening	[m]
c	Diffusion coefficient	[m^2/s]
c	Magnitude of the velocity	[m/s]
C_{drag}	Drag coefficient	[-]
C_{loss}	Loss coefficient	[-]
D_H	Hydraulic diameter	[m]
D_h	Horizontal eddy diffusivity	[m^2/s]
d_{pile}	Diameter pile	[m]
F	Force	[N]
f	Resistance factor	[-]
Fr	Froude number	[-]
g	Gravitational acceleration	[m/s^2]
h	Mesh element size	[m]
h	Water depth	[m]
h_0	Water level at point 0	[m]
h_1	Water level at point 1	[m]
h_2	Water level at point 2	[m]
I_T	Turbulent intensity	[-]
k	Turbulent kinetic energy	[J]

k_s	Equivalent sand roughness height	[m]
L	Length	[m]
l_m	Mixing length	[m]
L_T	Turbulent length scale	[m]
N	Number of piles	[-]
n	Manning coefficient	[$m^{1/3}s$]
p_0	Pressure at point 0	[Pa]
p_1	Pressure at point 1	[Pa]
p_2	Pressure at point 2	[Pa]
Pe	Peclet number	[-]
Q	Discharge	[m^3/s]
Re	Reynolds number	[-]
T	Temperature	[K]
U_m	Maximum flow velocity	[m/s]
v_1	Flow velocity at point 1	[m/s]
v_2	Flow velocity at point 2	[m/s]
v_c	Cross flow velocity	[m/s]
v_h	Horizontal eddy viscosity	[m^2/s]

Preface

The following study completes my Master of Science programme in Civil Engineering in the track 'Hydraulic Engineering', concludes my time as a student at Delft University of Technology and marks the end of my educational career of 21 years. In the beginning of summer 2020, a few months after the start of the COVID-19 pandemic, I started to look for a graduation project. The first idea was to do 'something with hydrodynamics in ports'. Ports in general have fascinated me for years and are also one of the reasons why I started civil engineering. After a long search I found a graduation opportunity at Witteveen+Bos (W+B). The topic was linked to a project that W+B currently works on. W+B is a non-listed engineering consultancy firm with an international character based in the Netherlands.

I am extremely grateful that W+B offered me this opportunity in the group Hydrodynamics & Morphology. Intellectual, material and financial support was offered by W+B to enable the completion of this thesis.

Writing a master thesis during these abnormal times was not always enjoyable. After working in my bedroom for a few months, I made the decision to rent an office in Rotterdam together with my housemates. This felt like a great relief and was a good interim solution until universities and offices slowly opened again. The last few months I could work at the W+B offices. There, I really enjoyed talking to colleagues and discussing my graduation project with them.

A word of gratitude to Prof. dr. ir. Mark van Koningsveld for the trust and the aid during my thesis. His view of the bigger picture and the feedback during the progress meetings have taught me a lot. Also, to Ir. Floor Bakker for reserving time to read my work and give me valuable feedback. Besides, I would like to thank Dr. ir. Ido Akkerman for his feedback from a different angle, despite his paternity leave. A great thanks to Ir. Arne van der Hout for his critical questions that made me want to figure out everything in detail. I have always experienced our meetings as very valuable.

I would like to thank my group leader at W+B, Wim Ridderinkhof, for his infinite enthusiasm, not only on a professional level but also in a social context. I would like to thank Tim van Engelen for being my daily supervisor at W+B. By daily, I mean really every day. With every question or uncertainty I faced, I could ask him and he was always willing to make time for me. I appreciated his openness, which made me feel like I could always share everything.

I would like to say a special thanks to my housemates. The office we rented together has been very helpful to me. Besides, as we were all in the same situation, I was more able to put things into perspective. A big thanks to all my close friends and parents, who always gave me the care and support where needed. Last but definitely not least, thank you Cathelijn, for hearing all the ins and outs of my graduation project and for your support.

I have learned a lot in the last 11 months and I really enjoyed being able to contribute to a water safety project that will be carried out in a few years' time.

I hope you enjoy reading.

T.T. Grolleman
Rotterdam, October 19, 2021

Abstract

In the port of Ostend a discharge sluice is going to be constructed as part of an enforced dike ring. The proposed location of this discharge sluice is close to an already existing marina, the Royal Yachtclub Oostende (RYCO), and hindrance is expected regarding the outflow of the sluice in marina direction. When designing the sluice, an optimal balance has to be found between acceptable flow velocities in the downstream area and the capacity of the discharge sluice. It is therefore very important to be able to determine resulting flow patterns.

Formulas and rules of thumb found in literature are not sufficient to determine the resulting flow pattern of this system due to the complex geometry, including a pile row for flow velocity reduction. Other studies have shown that numerical models could simulate flow patterns of discharge sluices with much detail. However, a lot of detail in the results also requires much computational time. An example of a detailed numerical software program that is able to simulate the complete three-dimensional flow field is COMSOL Multiphysics 5.6 (COMSOL). Although it provides the most detail, simulating the flow in the entire area of interest (including the RYCO) for a complete tidal cycle in COMSOL would take too much computational time.

The objective of the present study is therefore to investigate the possibilities of determining the flow pattern downstream of a discharge sluice using a numerical method that requires less computational time but has sufficient accuracy to determine the potential impact of a discharge sluice on nautical activities.

In the present study, two options are considered to determine the flow field downstream of a discharge sluice. Method COMSOL-D3D is a coupled numerical method of a COMSOL and a coarser Delft3D-FLOW 4 (D3D) model. The other option, method D3D, uses only a D3D model and the sluice outflow is schematized by means of the general discharge relation.

As validation of the results is not possible due to a lack of measurement data, the methods are applied to a simplified case. The flow pattern resulting from each method is compared to the results obtained with a so-called baseline method. This method consists of modelling the entire domain with only a detailed numerical model, COMSOL. This is possible since, for validation purpose, the domain of the simplified case is relatively small and only stationary conditions are considered.

In conclusion, there is a lot of potential in the use of both methods in predicting the flow pattern downstream of a discharge sluice. They produce for the simplified case flow patterns similar to those obtained with the detailed method. Moreover, both methods require relatively little computational time compared to a full 3D simulation, method D3D requires the least amount. However, there are a number of conditions for the application of both methods.

The methods cannot be applied in the direct vicinity of the discharge sluice where the flow is highly three-dimensional. If one is interested in the flow in the first meters after the outflow opening or around the pile row, for example for designing the bottom protection, the two considered options are not sufficiently accurate. The flow in this area is too complex to simulate in a D3D model. In this case it is recommended to model the situation completely in COMSOL or a model similar to COMSOL. Furthermore, method D3D can only be applied if the sluice system is simple enough to correctly determine the discharge coefficient analytically/empirically and to simulate the effect of the pile row with a simplification in D3D. It is possible to accurately determine the effect of the pile row on the flow in this study with a schematized porous plate in D3D. Further research must show whether this applies to all types of pile rows.

For method COMSOL-D3D it is important that a correct coupling is made between both models. Here it is important to gradually impose the flow rates in the D3D model. Furthermore, the coupling should be made before the predicted point at which the jets starts deflecting towards the side but downstream of the area at which three-dimensional flows caused by the pile row are present.

It is important to note that due to a lack of validation data there is an uncertainty in the results following from the model approaches. Further research and the use of validation data must show how accurate the results of the considered methods are.

In this research method D3D is applied to the Ostend case. It becomes clear that flow rates exceed predetermined limits for safe operation in the marina. This applies to the entire marina and a large part of the time that the discharge sluice is discharging in marina direction. Measures will therefore have to be taken to prevent this. It is recommended to use method COMSOL-D3D to investigate the optimization between flow velocities in the marina and the discharge capacity. This is due to the fact that the design of the discharge sluice is expected to become much more complex and as a result the discharge coefficient is no longer easy to determine using formulas from literature.

Contents

Nomenclature 3

Preface 4

Abstract 5

List of figures 11

List of tables 12

1 Introduction 13
- 1.1 Introduction to Ostend case . . . 14
- 1.2 Predicting nautical impact . . . 14
- 1.3 Numerical approaches . . . 15
- 1.4 Problem definition . . . 16
- 1.5 Objective and research questions . . . 16
  - 1.5.1 Research objective . . . 16
  - 1.5.2 Research questions . . . 16
- 1.6 Methodology . . . 17
- 1.7 Thesis outline . . . 17

2 Theoretical framework 18
- 2.1 Discharge sluice flow . . . 18
  - 2.1.1 Resulting jet . . . 19
  - 2.1.2 Pile row . . . 20
- 2.2 Discharge coefficient . . . 20
- 2.3 Numerical modelling . . . 22
  - 2.3.1 Comsol Multyphysics 5.6 (COMSOL) . . . 23
  - 2.3.2 Delft3D-FLOW 4 (D3D) . . . 23
  - 2.3.3 COMSOL vs. D3D . . . 24
  - 2.3.4 Turbulence modelling . . . 24
- 2.4 Density driven flows and flow stratification . . . 25
  - 2.4.1 Flow stratification . . . 25
- 2.5 The Coanda effect . . . 25
- 2.6 Current guidelines marina design . . . 26
  - 2.6.1 Marina layout . . . 26
  - 2.6.2 Maximum flow velocities . . . 26
- 2.7 Conclusion . . . 26

3 System analysis 28
- 3.1 The port of Ostend . . . 28
  - 3.1.1 The Royal Yachtclub Ostend (RYCO) . . . 29
  - 3.1.2 The port basin . . . 29
  - 3.1.3 The Noordede River / Ghent-Ostend channel . . . 29
  - 3.1.4 The Spuikom . . . 29
- 3.2 Salinity . . . 29
- 3.3 Tidal signal . . . 30
- 3.4 The proposed discharge sluice . . . 31

4 Set-up methods, simplified model 32
4.1 Simplified case . . . 32
4.2 Baseline method . . . 32
4.2.1 Assumptions . . . 33
4.2.2 Boundary conditions . . . 34
4.2.3 Grid design . . . 35
4.2.4 Other settings . . . 35
4.2.5 Modelling process . . . 35
4.3 Method COMSOL - D3D: A modelling train consisting of a COMSOL and a D3D model . . . 35
4.3.1 COMSOL . . . 36
4.3.2 Coupling COMSOL and D3D . . . 36
4.3.3 D3D . . . 38
4.4 Method D3D: Delft3D-FLOW 4 with fixed source terms and porous plate . . . 38
4.4.1 Other settings . . . 39

5 Comparison of methods 40
5.1 Method COMSOL - D3D versus baseline method . . . 40
5.2 Method D3D versus baseline method . . . 44
5.3 Prediction flow patterns by means of formulas from literature . . . 47
5.4 Discussion and conclusion comparison of methods . . . 52
5.4.1 Baseline method . . . 52
5.4.2 Method COMSOL - D3D vs. baseline . . . 52
5.4.3 Method D3D vs. baseline . . . 53
5.4.4 Method formulas from literature . . . 53
5.4.5 Conclusion . . . 55

6 Model set-up, Ostend model 56
6.1 Port of Ostend model . . . 56
6.2 Applying method D3D to the Ostend case . . . 59

7 Potential impact on the nautical activities in the marina 60
7.1 Situation without discharge from the Noordede River / Ghent-Ostend channel . . . 60
7.2 Situation with discharge from the Noordede River / Ghent-Ostend channel . . . 62
7.3 Conclusion . . . 64

8 Discussion 65
8.1 Discussion results Ostend model . . . 65
8.2 Inaccuracies baseline method . . . 66
8.3 Coanda effect . . . 66
8.4 Discharge coefficient . . . 67
8.5 Improvement coupling COMSOL-D3D . . . 67
8.6 Limitations methods COMSOL-D3D and D3D . . . 69
8.6.1 Limitations method COMSOL - D3D . . . 69
8.6.2 Limitations method D3D . . . 69

9 Conclusions and recommendations 70
9.1 Conclusions . . . 70
9.2 Recommendations for further research . . . 73
9.2.1 Recommendations regarding the baseline method . . . 73
9.2.2 Recommendations regarding method COMSOL - D3D . . . 73
9.2.3 Recommendations regarding method D3D . . . 74
9.2.4 Recommendations regarding the literature method . . . 74
9.2.5 Recommendations regarding the realistic Ostend D3D model . . . 74

A Turbulence modelling 75

B Model specifications 77
B.1 COMSOL . . . 77
B.1.1 Physical settings . . . 77
B.1.2 Numerical settings . . . 78

B.2 D3D 79
B.2.1 Physical settings 79
B.2.2 Numerical settings 79

C Sensitivity analysis **80**
C.1 Sensitivity analyses COMSOL modelling 80
C.1.1 Grid size 80
C.1.2 Length and width upstream water body 81
C.2 Sensitivity analysis D3D modelling 83

D Validation Granddaughter model **84**

E Results extra simulation 'thin dam method' **85**

Bibliography **88**

List of Figures

1.1 Discharge sluice at Bath (van Reeken, 1988). 13
1.2 A map of the project area, adapted from Ridderinkhof et al. (2019). 14

2.1 Definition sketch of a flow through a discharge sluice, a side view. 18
2.2 Schematisation of a plane turbulent wall jet, a side view (Rajatratnam, 1976). 20
2.3 COMSOL model geometries. 22
2.4 Lock filling process with two different densities (J. Pietrzak, 2017). 25
2.5 The setup of the Coanda Effect experiments (Miozzi et al., 2010). 26

3.1 The scope area of this study. 28
3.2 Sampling locations port of Ostend (Persoone & de Pauw, 1968). 30
3.3 Salinity levels port of Ostend, x-axis: months, y-axis: salinity rate (Persoone & de Pauw, 1968). 30
3.4 Geometry proposed discharge sluice, different views. 31

4.1 The geometry that is used during the simulations with the baseline method. 33
4.2 Boundary conditions of the COMSOL model that is used in the baseline method. Sketch is not to scale. 35
4.3 Schematisation method COMSOL - D3D. 36
4.4 Geometry COMSOL domain, method COMSOL-D3D. 36
4.5 The output grid of the coupling plane, corresponding with the one in D3D, that is copied on the outflow boundary of the COMSOL model. 37
4.6 A combination of sink and source terms in D3D, left: the source terms, top and bottom: the sink terms. 38
4.7 Source terms and thin dams method D3D, top view. 39

5.1 Comparison of the jets obtained with the baseline method (top) and method COMSOL - D3D (bottom). 41
5.2 Distribution of the locations 1, 2, 3 and 4, the red crosses indicate the comparison points for method D3D. 42
5.3 Comparison of flow velocities baseline method and method COMSOL - D3D at four different locations. 43
5.4 Comparison of horizontal distribution flow velocity at three different distances from outflow opening, method COMSOL-D3D and baseline method. 44
5.5 Comparison of the jets obtained with baseline method (top) and method D3D (bottom). 45
5.6 Comparison of flow velocities baseline method and method D3D at three different locations 46
5.7 Comparison of horizontal distribution flow velocity at three different distances from outflow opening, method D3D and baseline method. 47
5.8 Flow pattern from above as assumed in literature method, figure is not to scale. 48
5.9 Flow pattern from the side as assumed in literature method, figure is not to scale. 48
5.10 Flow velocity against the distance from the the outflow opening. 49
5.11 Comparison of horizontal distribution flow velocity baseline method and literature method at four different distances from the outflow opening. 50
5.12 Comparison of vertical distribution flow velocity baseline method and the literature method at three different distances from the outflow opening. 51
5.13 Horizontal flow velocity distribution at first cell after coupling, sides of the jet. 53
5.14 Vertical distribution vertical flow velocity at first cell after coupling, centerline jet. 53
5.15 Comparison of horizontal distribution flow velocity at three different distances from outflow opening, method COMSOL-D3D, method D3D and baseline method. 55

6.1 Connection of the Ostend model with the CSM - ZUNO - Coastal Strip model train. CSM: blue. ZUNO: green. Coastal Strip: red. Ostend Mother model: black. (Dujardin et al., 2017). . . . 56
6.2 Left: Ostend Mother model (blue) and Daughter model (red). Right: Bathymetry Daughter model. (Witteveen+Bos, 2019). . . . 57
6.3 Grey: Daughter model. Blue: Granddaughter model. . . . 57
6.4 Bathymetry of the Granddaughter model. . . . 57
6.5 Set-up of the Ostend model. . . . 59

7.1 The impact on the marina in the port of Ostend, depth-averaged, 0.3 m/s contour lines, without riverine discharge. . . . 61
7.2 The impact on the marina in the port of Ostend, top layer, 0.3 m/s contour lines, without riverine discharge. . . . 61
7.3 The impact on the marina in the port of Ostend, top layer, 0.8 m/s contour lines, without riverine discharge. . . . 62
7.4 The impact on the marina in the port of Ostend, depth-averaged, 0.3 m/s contour lines, with riverine discharge. . . . 63
7.5 The impact on the marina in the port of Ostend, top layer, 0.3 m/s contour lines, with riverine discharge. . . . 63
7.6 The impact on the marina in the port of Ostend, top layer, 0.8 m/s contour lines, with riverine discharge. . . . 64

8.1 Set-up method COMSOL - D3D with extra thin dams (yellow), grid cells with source terms are indicated with a cross. . . . 68

C.1 Comparison horizontal distributions at x = 43 m, different grid sizes. . . . 80
C.2 Comparison vertical distributions at x = 43 m, different grid sizes. . . . 80
C.3 Comparison horizontal distributions at x = 50 m, different grid sizes. . . . 81
C.4 Comparison vertical distributions at x = 50 m, different grid sizes. . . . 81
C.5 Comparison horizontal distributions at x = 80 m, different grid sizes. . . . 81
C.6 Comparison vertical distributions at x = 80 m, different grid sizes. . . . 81
C.7 Comparison horizontal distributions at x = 43 m, different width and length upstream water body. . . . 82
C.8 Comparison vertical distributions at x = 43 m, different width and length upstream water body. . . . 82
C.9 Comparison horizontal distributions at x = 50 m, different width and length upstream water body. . . . 82
C.10 Comparison vertical distributions at x = 50 m, different width and length upstream water body. . . . 82
C.11 Comparison horizontal distributions at x = 80 m, different width and length upstream water body. . . . 82
C.12 Comparison vertical distributions at x = 80 m, different width and length upstream water body. . . . 82
C.13 Jets in D3D with different grid sizes. . . . 83

D.1 Comparison of water levels at corresponding location in Daughter and Granddaughter model. . . . 84
D.2 Comparison of depth-averaged flow velocities at corresponding location in Daughter and Granddaughter model. . . . 84

E.1 Comparison of flow velocities baseline method and method Comsol - D3D at four different locations, thin dam method. . . . 85

List of Tables

2.1 Distinct loss coefficients and the discharge coefficient of the system. 22
2.2 A comparison between COMSOL and D3D. 24

3.1 Tidal deflections of the water surface in the port of Ostend (AMDK, 2021). 30

B.1 Physical parameters COMSOL model. 78
B.2 Physical parameters D3D models. 79
B.3 Numerical constants applied for D3D models. 79

1

Introduction

Our planet is warming up and countries around the world are taking measures against the sea level rise (Church et al., 2013). One of these measures that governments commonly take to keep the water out is the construction of hydraulic structures such as dikes, storm surge barriers and sluices. Well-known examples are the Afsluitdijk and the Eastern Scheld Barrier (Dronkers, 2011; Konter & Klatter, 1991). In this study the focus is on one specific type of hydraulic structure, a discharge sluice (Dutch: 'Spuisluis'). An example of such a structure is depicted in Fig. 1.1. A discharge sluice both functions as a storm surge barrier as well as an opening for water to flow from one side to the other. It is intended to drain inland water, to reverse outside water and, conversely, to let outside water in (Maas, 2002).

Figure 1.1: Discharge sluice at Bath (van Reeken, 1988).

If there is a difference in water level between both sides, opening the valves in the sluice culverts results in a flow through the discharge sluice. The outflow of water on either side of the sluice can potentially have undesirable consequences. A large amount of turbulence, recognizable by the white surfaces in Fig. 1.1, is associated with the sluice outflow. In case of a poor bed protection a scour hole might be formed after some time. There is a chance that the structure ultimately may become unstable.

Another problem that may arise is when certain activities in the outflow area of the sluice are hindered by the resulting flow. Examples of this have occurred in the past and are listed below:

- In the port of Rotterdam hindrance to nautical activities was expected due to a cooling water outflow in the Maasvlakte extension. Dekker et al. (2009) assessed this effect and it was found that with a correctly functioning diffuser in front of the outflow opening resulting flow patterns would not significantly hinder the nautical activities.
- At the Krammersluizen lock system a nautical impact on arriving vessels due to the outflow from the sluice system was expected. Kranenburg et al. (2016) determined the impact and their concluding advice was not to sail in certain areas when discharging from the lock to the arrival area.

- In the Sampit River (South Carolina, USA) it was expected that a stormwater discharge would have an impact on recreational vessels. Aziz et al. (2008) investigated the resulting flow patterns and they concluded that the level of hindrance largely varies with the type of outlet opening.
- In densely populated coastal cities in Asia, wastewater outfalls are often located not far from sensitive areas such as beaches or shell fisheries. The impact and the risk were predicted both in the near field and intermediate field by Choi and Lee (2007).

Also the port of Ostend expects to experience hindrance due to the outflow of a proposed discharge sluice. The next section provides more details on this.

1.1. Introduction to Ostend case

A discharge sluice is going to be located in the eastern part of the port of Ostend (indicated by the red dotted line in Fig. 1.2) and will be part of an enforced dike ring. The dike ring has the aim to protect an inland water basin, 'The Spuikom', and the hinterland against the rising sea level (Church et al., 2013; Goossens & Moerkerke, 2019). The main purpose of the sluice is to allow excess water to flow from the hinterland to sea and to regulate water levels in the Spuikom while allowing sufficient flushing to ensure good water quality. However, the proposed location of the discharge sluice is close to an already existing marina, called the 'Royal Yachtclub Oostende (RYCO)'. The pontoon structures are indicated in light brown on the map in Fig. 1.2.

Problems with high flow velocities inside the marina due to the outflow of water can be expected. Manoeuvring a vessel in that case can be very risky. Furthermore, the moored vessels and pontoon structures inside the marina could experience large forces due to the flow velocities. It is therefore very important to determine downstream flow patterns. A specific design of the discharge sluice system, including a double culvert and a pile row, has been developed by engineering company Witteveen+Bos and is examined in this research.

A specific discharge capacity is required to ensure sufficient flushing of the Spuikom. The discharge capacity of the sluice depends on the design of the system. A larger capacity is associated with higher resulting flow velocities and vice versa. Therefore, when designing the sluice, an optimal balance has to be found between acceptable flow velocities in the downstream area and the capacity of the discharge sluice. For this it is crucial to know which flow patterns arise. Part of this research is specifically about this Ostend case. More details on the Ostend case can be found in Chapter 3.

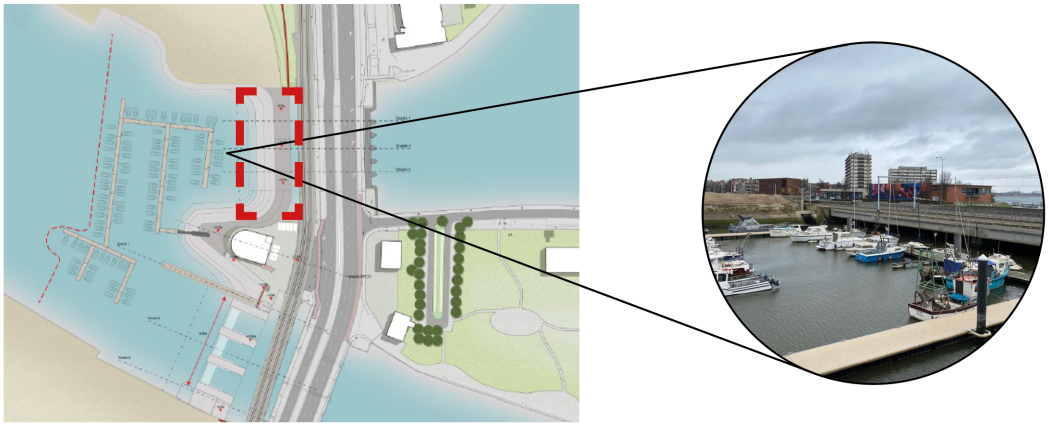

Figure 1.2: A map of the project area, adapted from Ridderinkhof et al. (2019).

1.2. Predicting nautical impact

It is clear that it is crucial to be able to predict the flow pattern downstream of a discharge sluice and thus the potential impact on nautical activities in the outflow area. The flow pattern can be determined

in different ways: with formulas from literature, by using a physical model or numerically. The simplest and least time consuming method is by using formulas from literature. This method is often used in the earlier phases of a project. It means that the downstream flow pattern is determined by using analytical equations and empirical coefficients. A major advantage of this is that a first estimate of the flow velocities can be made very quickly. A disadvantage is that the results are often not very accurate.

Results can also be obtained by setting up a scaled physical model of the sluice and measuring the flow velocities. This method requires much time and is in most cases very costly. However, the results are very accurate and are often used to verify the results of numerical models.

A third option is using a numerical model to determine the potential impact of a sluice on nautical activities in the outflow area. A numerical model is a widely used method to model flow phenomena, not just in the case of water but also for other purposes such as air flows around airplanes and oil through pipelines. The flow of a liquid or gas can be described by the Navier-Stokes equations, which consist of momentum equations for the different directions in the Cartesian reference frame and a continuity equation (Zijlema, 2020). There are different numerical approaches available to solve these complex equations.

1.3. Numerical approaches

Two numerical software programs are considered in this study. One uses the assumption that the horizontal length scale is of much higher order than the vertical length scale, which implies that the numerical model is based on the so-called shallow water equations (SWE) (Broomans, 2002). Another approach is to solve the simplified Navier-Stokes equations, the so-called Reynolds Averaged Navier-Stokes (RANS) equations. Delft3D-FLOW 4 (Deltares, 2021), hereinafter referred to as D3D, is a software package that is an example of the first approach. COMSOL Multiphysics 5.6 (COMSOL, 2019), hereinafter referred to as COMSOL, is an example of the second approach.

With D3D large areas can easily be modelled within relatively little computational time but much information about detailed flows around or through hydraulic structures is lost. On the other hand, with COMSOL it is possible to model the flow around hydraulic structures in much detail as the complete three-dimensional flow field is simulated. However, it takes a lot of computational time to model large areas and it is very computational extensive to include large-scale effects such as the tide or influx of salt water.

An example of a project in which COMSOL was used is the research by Erdbrink et al. (2014) on the reduction of cross-flow vibrations of underflow gates. Also physical experiments were done in this study. The reason why COMSOL was used here is because a lot of detail had to be obtained about the flow under a sluice gate. Another example of using a detailed numerical software program is the earlier mentioned project by Aziz et al. (2008). They used a numerical model similar to COMSOL in their research. This method was applicable since there were no large-scale effects present, such as the tide, in the outflow area of the stormwater discharge.

An example of using D3D is the earlier mentioned project by Dekker et al. (2009). This strategy was chosen because the area of interest was large and the outflow from the cooling water system was relatively simple. Simplifications and assumptions were made to mimick the cooling water outflow and the presence of a breakwater in front of the outflow opening.

Kranenburg et al. (2016) also applied a D3D model during their study on the effect of a discharge sluice on the flow field in the outflow area of the Krammersluizen complex. However, the outflow from the lock system appeared to be too complex to schematize with only assumptions and simplifications in D3D. They used a 1D model, Cormix (Jirka et al., 1996), to determine the near-field plume behaviour, whereas the D3D model was able to predict the far-field flow velocities. A coupling was made between the two models.

In the earlier mentioned study by Choi and Lee (2007) also a combination of two numerical models was used. In their research on wastewater outfalls they modelled the near-field mixing by a Lagrangian

plume model, JETLAG (Lee & Cheung, 1990), while the far-field transport was simulated by the Environmental Fluid Dynamics Code (EFDC) (EPA, 2021). The coupling was made by a so-called distributed entrainment sink approach. Sink terms were used to simulate the entrainment by the jet and source terms were included to mimick the main flow.

1.4. Problem definition

In some cases it can be crucial to know the potential impact of a discharge sluice on nautical activities in the outflow area. The Ostend case is an example of this. By knowing the potential impact on nautical activities in the marina, the engineers can decide to adapt the design of the sluice system, to adjust the marina configuration or even relocate the marina completely.

Applying simple formulas and rules of thumb from literature does not provide accurate results in the case of a discharge sluice such as the one in Ostend. The geometry of the discharge sluice system, including a pile row to reduce flow velocities, is too complex for this. Instead, it appears from similar projects in the past that numerical modelling is very suitable for solving these kinds of problems.

Different degrees of detail can be obtained when applying numerical models. COMSOL, an example of a detailed numerical model, is able to solve the complete three-dimensional flow field. Applying these types of models provides a lot of detail but for a case like the one in Ostend it requires a large amount of computational time.

The problem is that in a real project a time-efficient way to obtain results is always necessary. Therefore, a method must be found that requires less computational time but is still sufficiently accurate to predict the flow pattern downstream of a discharge sluice.

1.5. Objective and research questions

1.5.1. Research objective

The objective of this research is to find a numerical method that requires less computational time than modelling the entire problem with a detailed numerical model like COMSOL. The aim is that this method still gives accurate results in the case of determining the flow pattern downstream of a discharge sluice and the potential impact on nautical activities. For this it is investigated whether a coupled method of COMSOL and D3D can be used to accurately simulate the flow field downstream of a discharge sluice. Another option that is examined is using a D3D model in which the sluice outflow is schematized by means of the general discharge relation.

1.5.2. Research questions

The main research question of this work is based on the above-mentioned objective and is as follows:

“Can a coupled or schematized numerical method be used to accurately simulate the flow field downstream of a discharge sluice?

This main research question is sub-divided into three different parts:

1. How can a combination of a COMSOL and a D3D model be used to simulate the flow field and what does the coupling between the two models look like?
2. How can a D3D model with the sluice outflow being schematized by the general discharge relation be used to simulate the flow field?
3. How does the accuracy of the results obtained with both methods compare to the results obtained with the detailed numerical model COMSOL?

   Two other sub-questions are about the application of one of the methods to the Ostend case:

4. Which of the examined methods is most suitable to determine the impact of a discharge sluice on nautical activities in the marina of Ostend?
5. What impact does the planned discharge sluice in the port of Ostend have on nautical activities in the neighbouring marina?

1.6. Methodology

Step 1: Theoretical framework
A theoretical framework is offered to understand the relevant processes regarding a discharge sluice and the resulting jet. Attention is paid to the general functioning of a discharge sluice and the associated equations. Also, information regarding the numerical models that are used is presented. Furthermore, the current guidelines regarding marina design, that are used to determine the potential impact of the discharge sluice, are shortly pointed out.

Step 2: Applying two different methods and a baseline method to a simplified case
Two different numerical methods to predict the resulting flow field of a discharge sluice are examined. Due to a lack of measurement data, no validation of the results is possible. Therefore both methods are applied to a simplified case and the results are compared with a so-called baseline method. This baseline method consists of modelling the entire problem with a numerical model that simulates the complete three-dimensional flow field, COMSOL. The first examined method is a coupled method, called method COMSOL-D3D. The second option uses a D3D model in which the sluice outflow is schematized by means of the general discharge relation. This method is called method D3D. Also a prediction of the flow pattern using simple formulas and empirical coefficients from literature is made to check the accuracy of such a method.

Step 3: Choosing one method and applying this to the realistic Ostend case
One method is chosen to apply to the realistic Ostend case, in order to illustrate its functioning. First, a situation is examined in which the currents in the port are only caused by the outflow of the discharge sluice itself. Then, a situation is examined in which also a normative riverine discharge from the Noordede river / Ghent-Ostend channel is included. Both situations take into account water levels during spring tide.

Step 4: Determining the potential impact on the marina
After applying one method to the realistic Ostend case, the potential impact on the marina is determined. This is done by assessing the resulting flow fields on the basis of guidelines found in literature.

1.7. Thesis outline

This section consists of a reader's guide of this document.

- Chapter 2 - provides a theoretical framework in which knowledge is presented regarding a discharge sluice, the used numerical models and the plume behaviour. The chapter is concluded with the current guidelines on marina design.
- Chapter 3 - sketches the scope area and describes the water system in the port of Ostend. Additionally, system forcing and salinity dynamics are discussed.
- Chapter 4 - presents a detailed explanation of how each method is applied to the simplified case. Also, the simplified case itself is described.
- Chapter 5 - compares the results of each method after application to the simplified case with those of the baseline method. A discussion and conclusion on this comparison is given. Based on these results, one method is chosen to be applied to the Ostend case.
- Chapter 6 - gives an explanation of the Ostend model and the application of the chosen method.
- Chapter 7 - provides an illustration of the chosen method by applying it to the Ostend case. The potential impact on nautical activities in a neighbouring marina is assessed by determining whether the resulting flow velocities exceed predetermined limits.
- Chapter 8 - evaluates the results of the Ostend model. It is followed by a discussion on the main findings from this research. The chapter is concluded by a discussion on the limitations of the examined methods.
- Chapter 9 - gives a conclusion of this research. The research questions are answered and recommendations for further research are given.

2

Theoretical framework

First, in Section 2.1 general knowledge regarding a discharge sluice and its resulting plane turbulent wall jet is pointed out. Next, Section 2.2 continues with an elaboration on the most important characteristic of a hydraulic system through which water flows: the discharge coefficient μ. Then, information on the numerical models that are used in this research and their areas of application is given in Section 2.3. Section 2.4 deals with an important physical concept that potentially have big influence: flows generated by salinity differences. Another phenomenon that is important in this research, the Coanda effect, is discussed in Section 2.5. The guidelines regarding marina design that are used to assess the impact of the discharge sluice are discussed in Section 2.6, after which the chapter is concluded in Section 2.7.

2.1. Discharge sluice flow

A discharge sluice is intended to drain inland water and to reverse outside water. When the valves inside the culvert(s) are lifted a flow is generated by a difference in water level between both sides of the sluice. Water flows from the side with a higher water level to the side with a lower level. A definition sketch of this flow is given in Fig. 2.1. The thick dotted line indicates a pile row in front of the opening to reduce the flow velocities in the outflow area. In the Ostend case, the resulting flow is submerged as there is a layer of water present on top of the in- and outlet at any moment (Liu et al., 2015).

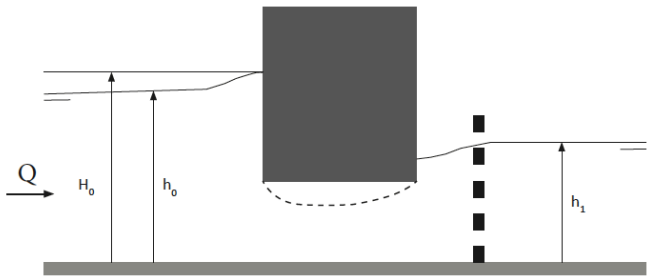

Figure 2.1: Definition sketch of a flow through a discharge sluice, a side view.

Figure 2.1 shows that the flow contracts at the point where it flows under the structure. The point at which the diameter of the stream is smallest is called the vena contracta (Battjes, 2002; Rajaratnam & Subramanya, 1967). The discharge Q is derived at this point and can be calculated by using the general discharge relation (Swamee, 1992), see Eq. (2.1). This relation is based on the conservation of energy between points 0 and 1. The flow should be spread over the entire width at points 0 and 1, in order to be able to use this conservation of energy. Moreover, there should be a free water surface at both sides of the sluice.

$$Q = \mu A \sqrt{2g(h_0 - h_1)} \tag{2.1}$$

in which,

μ = the discharge coefficient [-]
Q = discharge [m^3/s]
A = inlet flow surface [m^2]
g = acceleration due to gravity (= 9.81) [m/s^2]

Equation (2.1) can also be written in terms of pressure ($p = \rho gh$) (Thijsse, 1960):

$$Q = \mu A \sqrt{2\frac{p_0 - p_1}{\rho}} \tag{2.2}$$

in which,

p_0 = pressure upstream [Pa]
p_1 = pressure downstream [Pa]
ρ = fluid density [kg/m^3]

Bernoulli's Law
Bernoulli's law is an important flow-related law and is essential to understand the results that follow from the numerical models that are used in this work. The law states that an increase in the velocity of a liquid or gas is accompanied by a decrease in the pressure in that liquid or gas (Battjes, 2002). This is made clear by the following equation, in which the total energy head at elevation 1 is equal to the total energy head at elevation 2:

$$P_1 + \frac{1}{2}\rho v_1^2 + \rho g h_1 = P_2 + \frac{1}{2}\rho v_2^2 + \rho g h_2 \tag{2.3}$$

in which,

P_1 = pressure at elevation 1 [Pa]
v_1 = velocity at elevation 1 [m/s]
h_1 = height of elevation 1 [m]
P_2 = pressure at elevation 2 [Pa]
v_2 = velocity at elevation 2 [m/s]
h_2 = height of elevation 2 [m]

On the basis of Eq. (2.3) the various pressure values in a discharge sluice flow are explained. It can be expected that in the inflow to the culvert the pressure decreases sharply, from H_0 (Fig. 2.1) to a minimum value at the vena contracta. Thus, at the vena contracta the flow velocity has risen to a maximum value. Next, there are very large losses due to the outflow from the culvert, so the pressure drops even more. Without these losses, the pressure would rise again after the outflow, due to Bernoulli's law. Over the pile row the pressure eventually increases, due to the decelerating current and Bernoulli. However, due to the losses around the pile row this increase is not very large. The pressure variations in the rest of the downstream field are very small. This is in accordance with measurements in which the pressure variations across a jet are much smaller than those according to Bernoulli along a streamline (Battjes, 2002).

2.1.1. Resulting jet

This section describes the behaviour of a jet in the event that no pile row is present. The jet that results from a discharge sluice can be identified as a wall jet, as the opening is located at the bottom. The jet flows into a large body of water with a surplus velocity compared with the ambient fluid, which causes acceleration of the ambient fluid and deceleration of the jet itself (Schiereck & Verhagen, 2019). Momentum is exchanged in both the horizontal and vertical plane between the jet and the ambient fluid, causing eddies (i.e. turbulence) that are formed at the sides of the jet. A schematisation of a turbulent wall jet is presented in Fig. 2.2, in which the bottom is represented by the x-axis. A limiting surface water level is not present in this schematisation.

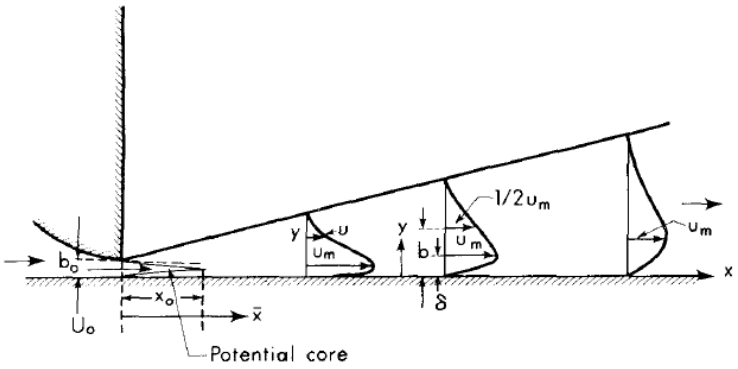

Figure 2.2: Schematisation of a plane turbulent wall jet, a side view (Rajatratnam, 1976).

The jet can be divided into two distinct regions: the flow development region and the fully developed flow region (Gessner & Jones, 1965). The flow development region is in Fig. 2.2 indicated by the 'potential core'. In this region there is still an area present which holds the same flow velocity U_0 as it was in the culvert, also indicated in Fig. 2.2. As can be seen, this area rapidly decreases in downstream direction and has a wedge shape. The potential core is bounded by two contracting shear layers that are developed as the jet enters the ambient fluid. In the region downstream of the point at which the two inward directed shear layers meet, the potential core has fully disappeared as the turbulence has penetrated to the jet axis. From this point on the jet is in its fully developed flow region (Imao et al., 2005; Rajatratnam, 1976). There are two other important layers. A wall boundary layer δ is developed at the bottom. Another layer is curved outwards (ascending black line), indicating the boundary of the free mixing region.

The flow velocity distribution over the depth at different distances from the culvert is also depicted in Fig. 2.2. The vertical velocity profile of a jet can be split up into three different sections: the top layer, the mixing layer where the velocity is close to maximum and the boundary layer (Barenblatt et al., 2005). At any point along the x-axis the flow velocity increases from zero at the bottom to a maximum U_m at the end of the so called boundary layer δ. It then decreases again to zero at a certain distance from the bottom.

2.1.2. Pile row

One could decide to place a pile row in front of the jet outlet, in order to reduce the resulting flow velocities. A pile row is able to diverge the flow and consequently the jet is spread over a larger width. In literature only formulas are found regarding the flow velocity reduction by pile rows in groynes at the sides of a river (van der Wal, 2000). These formulas are not applicable to a pile row in front of a discharge sluice.

2.2. Discharge coefficient

The discharge coefficient μ is an important characteristic of a hydraulic system through which water flows. It can be used to determine the discharge flowing through the system when the water level difference is known, as can be seen in Eq. (2.1). The loss coefficient ξ is directly related to the discharge coefficient and gives information about the amount of energy that is lost in a specific part of the system, due to inflow, outflow or friction. The loss coefficients of the individual parts can be summed up and in this way the total loss coefficient of the system is determined. The discharge coefficient μ is related to the loss coefficient ξ in the following way (Thijsse, 1960):

$$\mu = \frac{1}{\sqrt{\xi}} \tag{2.4}$$

Combining Eq. (2.2) and Eq. (2.4) results in an expression for the loss coefficient ξ (Thijsse, 1960):

$$\xi = \frac{(p_0 - p_1)\, 2A^2}{\rho Q^2} \tag{2.5}$$

in which,

p_0 = pressure at point 0, see Fig. 2.1 [Pa]
p_1 = pressure at point 1, see Fig. 2.1 [Pa]
A = sluice inlet flow surface [m^2]
Q = discharge through sluice system [m^3/s]
ρ = fluid density [kg/m^3]

For the considered discharge sluice system in the port of Ostend the loss coefficient ξ is made up of friction losses, in- and outflow losses and losses due to a pile row that is located in front of the outflow opening (Belaud et al., 2009). The distinct contributions to the total loss coefficient are quickly mentioned and a value for the discharge coefficient of the Ostend sluice system is calculated.

Friction losses
The energy losses due to the friction inside the culvert can be determined by multiplying the so-called resistance factor f by L/D, in which D is the diameter of the culvert (2.5 m) and L is the length of the culvert (10 m). The resistance factor f can be calculated by using the following expression (Genic et al., 2011):

$$f = 0.11\ (\frac{68}{Re} + (\epsilon/D_H))^{0.25} \tag{2.6}$$

in which,

Re = Reynolds number [-]
ε = the roughness height [m]
D_H = the hydraulic diameter [m]

For the considered case the Reynolds number is found to be in the order of $1 \cdot 10^7$, the roughness height 0.0025 m (Idel'chik, 1966) and the hydraulic diameter 2 m. This results in a resistance factor of 0.0207. Multiplying the resistance factor by L/D leads to a contribution to the loss coefficient of 0.0828.

$\xi_{friction}$ = 0.083

In- and outflow losses
From Idel'chik (1966) it follows that without any rounding of the inflow corners the contribution to the loss coefficient due to the inflow ξ_{in} is 0.5. For the outflow of the culvert with uniform cross-section into a much larger reservoir, the outflow loss depends on the velocity profile inside the culvert. With a uniform velocity profile inside the culvert, ξ_{out} equals 1 (Idel'chik, 1966). It is assumed that in the considered case the velocity profile inside the culvert is uniform, as the flow is very turbulent and the culvert is relatively long.

ξ_{in} = 0.500

ξ_{out} = 1.000

Losses due to the pile row
Around the pile row energy losses occur due to turbulent processes. However, these losses are small compared to the other parts of the discharge lock system. This is because the flow area between the piles is greater than the flow area of the culverts (respectively 18.96 and 11.25 m^2). The fact that the flow velocities decrease after the pile row is due to an energy loss but mainly due to the fact that the flow is spread over a greater width. The pile row thus acts as a diffuser. The loss coefficient of the pile row is therefore assumed to be negligible and consequently set to zero in the calculation of the discharge coefficient of the system.

$\xi_{pilerow}$ = 0.000*

Discharge coefficient of the system
In the table below the distinct contributions to the total loss coefficient are summed up and by using Eq. (2.7) the discharge coefficient of the sluice system is obtained.

Parameter	Value
$\xi_{friction}$	0.083
ξ_{in}	0.500
ξ_{out}	1.000
$\xi_{pilerow}$	0.000*
ξ_{total}	1.583
μ	0.794

Table 2.1: Distinct loss coefficients and the discharge coefficient of the system.

$$\mu = \frac{1}{\sqrt{\sum \xi + \sum f \frac{L}{D}}} \tag{2.7}$$

*Two COMSOL simulations were done to determine the exact loss coefficient of the pile row, one with a pile row and one without a pile row. The set-up of both models can be seen in Fig. 2.3. However, the analytical/empirical calculations are kept as simple as possible so the findings from the numerical models are not included in the analytical/empirical calculation of the discharge coefficient μ.

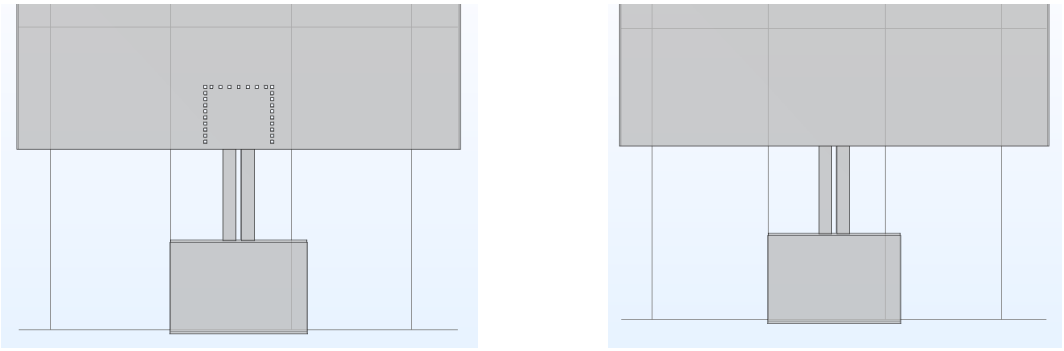

(a) COMSOL model geometry with pile row.

(b) COMSOL model geometry without pile row.

Figure 2.3: COMSOL model geometries.

The simulation with a pile row included resulted in a discharge coefficient value of 0.74. After application of Eq. (2.4), it followed that this value corresponds to a loss coefficient of 1.83. Doing a simulation without a pile row resulted in a discharge coefficient of 0.76. This value corresponds to a loss coefficient of 1.73. It can therefore be concluded that the pile row has a contribution to the loss coefficient of 1.83 - 1.73 = 0.1. This is different than the value assumed in the analytical/empirical calculation.

2.3. Numerical modelling

Models are often used to solve case like the one in the port of Ostend. A distinction can be made between numerical and physical models. Nowadays, researchers most often prefer to use the numerical ones, as they are very effective in terms of costs and effort. In contrast to physical models, pressure and flow velocity data can be obtained from every point of the model (Andersson et al., 2011). Geometrical shapes can easily be adjusted if necessary. The consequences of changes in the geometry and boundary conditions can quickly be identified. The results of the physical modelling are now often only used as a validation of the numerical models. In numerical models simplifications and assumptions are unavoidable in order to reduce the computational time of a simulation. It is very important to apply the

correct simplifications and assumptions, as it directly influences the success of the model outcomes. In this research, the methods that are examined use a COMSOL Multiphysics 5.6 (COMSOL) model (COMSOL, 2019) and a Delft3D-FLOW 4 (D3D) model (Deltares, 2021). In this section some general information on the used modelling programs is presented as well as their areas of application.

2.3.1. Comsol Multyphysics 5.6 (COMSOL)

COMSOL is a cross-platform finite element analysis, solver and multiphysics simulation software. It is intended to model flows in and around complex structures in great detail. Erdbrink et al. (2014), for example, used COMSOL to investigate new ways to reduce cross-flow vibrations of hydraulic gates with underflow. The software package contains a method for solving one-phase Newtonian fluids using incompressible Reynolds-averaged Navier-Stokes (RANS) equations in combination with a turbulence closure model. Courant stability is ensured with a strict maximum step of Δt = 0.02 s (Erdbrink et al., 2014). The Finite Element Method (FEM) is applied for spatial discretization. In this study the following equations are solved in COMSOL (COMSOL, 2019):

$$\rho\frac{\partial \mathbf{u}}{\partial t} + \rho(\mathbf{u}\cdot\nabla)\mathbf{u} = \nabla\cdot[-p\mathbf{l} + \mathbf{K}] + \mathbf{F} \tag{2.8}$$

$$\rho\nabla\cdot\mathbf{u} = 0 \tag{2.9}$$

in which,

- **u** = the velocity vector (u,v) [m/s]
- ρ = the density of water [kg/m^3]
- p = the water pressure [Pa]
- F = other forces that work on the system [N]

and,

$$\mathbf{K} = (\mu + \mu_T)\left(\nabla\mathbf{u} + (\nabla\mathbf{u})^{\mathsf{T}}\right) \tag{2.10}$$

in which,

- μ = the viscosity of water [Ns/m^2]
- μ_T = the turbulent viscosity to be computed through a turbulence closure model [Ns/m^2]

2.3.2. Delft3D-FLOW 4 (D3D)

D3D uses an alternating direction implicit method to solve the so-called shallow water equations (SWE). It is intended to determine large-scale morphological changes and currents. For example, a D3D model was used to predict the long-term morphological behaviour of the Sand Engine (Luijendijk et al., 2019; Luijendijk et al., 2017), which is a mega nourishment project at the Dutch north sea coast.

The SWE that are solved, also known as the Saint-Venant equations, are derived from integrating the Navier-Stokes equations over the depth under the Boussinesq and shallow water assumptions and consist of a continuity and 3D momentum equations (Zijlema, 2020):

$$\frac{\partial u}{\partial x} + \frac{\partial v}{\partial y} + \frac{\partial w}{\partial z} = 0 \tag{2.11}$$

$$\frac{\partial u}{\partial t} + u\frac{\partial u}{\partial x} + v\frac{\partial u}{\partial y} + w\frac{\partial u}{\partial z} = -g\frac{\partial h}{\partial x} + v_t^H\left[\frac{\partial^2 u}{\partial x^2} + \frac{\partial^2 u}{\partial y^2}\right] + \frac{\partial}{\partial z}\left(v_t^v\frac{\partial u}{\partial z}\right) \tag{2.12}$$

$$\frac{\partial v}{\partial t} + u\frac{\partial v}{\partial x} + v\frac{\partial v}{\partial y} + w\frac{\partial v}{\partial z} = -g\frac{\partial h}{\partial y} + v_t^H\left[\frac{\partial^2 v}{\partial x^2} + \frac{\partial^2 v}{\partial y^2}\right] + \frac{\partial}{\partial z}\left(v_t^v\frac{\partial v}{\partial z}\right) \tag{2.13}$$

$$\frac{\partial p}{\partial z} = -\rho g \tag{2.14}$$

An implicit numerical scheme is used in the D3D modelling so unconditional stability is obtained (Zijlema, 2020). However, inaccurate results can be obtained in the case of too large time steps. The Courant number is a good indication to check this and in the case of applying Delft3D-FLOW 4 this number should not be larger than 11 (Courant & Hilbert, 1962; Deltares, 2021).

$$c\frac{\Delta t}{\Delta x} < 11 \tag{2.15}$$

in which,

c = magnitude of the velocity [m/s]
Δt = time step [s]
Δx = spatial step [m]

2.3.3. COMSOL vs. D3D

In this subsection the main differences between the two modelling programs are clarified. A comparison, see Section 2.3.3, is made on the following points: the zone of application, the type of flow equations that are solved, how turbulence is modelled and how the grid is generated.

	COMSOL	**D3D**
Zone of application	Numerical modelling of all kinds of flows. Mainly intended for detailed simulation of complex flows. The grid solution is in the order of a few centimeters to a couple of meters.	Numerical modelling of sediment transport, waves, morphology and currents in shallow conditions. Mainly intended for large areas. The grid resolution is in the order of a few meters to hundreds of meters.
Flow equations	Incompressible Reynolds Averaged Navier-Stokes equations (RANS).	Shallow Water Equations.
Turbulence Modelling	RANS modelling with different options for the closure problem: k-ε, k-ω, LES and DES.	Separated treatment of the horizontal and vertical eddy viscosity. In horizontal sense a user-defined constant eddy viscosity can be used. In vertical sense a turbulence closure model is introduced (such as the k-ε closure model).
Grid generation	Flexible mesh, physically defined.	Horizontal: rectilinear or curvilinear, vertical: sigma-grid or z-grid approach (Delft3D-FLOW 4).

Table 2.2: A comparison between COMSOL and D3D.

2.3.4. Turbulence modelling

The development of a jet in an ambient fluid depends to a large extent on turbulence related phenomena. The Reynolds number is an indication of the turbulence intensity and gives the ratio between the advection (uL) and the viscous (ν) stresses (Battjes, 2002). A flow can be identified as being turbulent if the Reynolds number is larger than 4000. It is calculated for the flow through the considered discharge sluice (Uijttewaal, 2018):

$$Re = \frac{uL}{\nu} = \frac{2.5 \cdot 4}{1 \cdot 10^{-6}} = 1 \cdot 10^{7} \tag{2.16}$$

in which,

u = the flow velocity [m/s]
L = a characteristic linear dimension [m]
ν = the kinematic viscocity of the fluid [m^2/s]

There are different methods within numerical modelling to include turbulence effects. An overview of the different methods and more information regarding turbulence modelling are presented in Appendix A.

2.4. Density driven flows and flow stratification

The outflow area of the discharge sluice can have a different salinity rate than that of the incoming jet flow. The interaction between fresh and salt water has a significant effect on the development of the jet plume (van der Hout, 2020). In the case of a lower salinity rate in the outflow area the salter and heavier incoming jet tends to 'dive' under the fresh water body (Benjamin, 1968; Shin et al., 2004). Figure 2.4 shows a lock filling process with a salt and a fresh part. A so-called gravitationally driven flow is generated. Ultimately, the salty water stays in the bottom part, the fresher water in the upper part. The way in which salinity differences are taken into account in this research is discussed in Section 3.2.

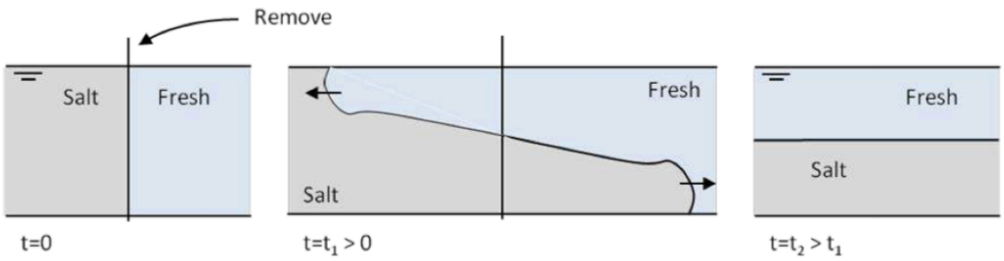

Figure 2.4: Lock filling process with two different densities (J. Pietrzak, 2017).

2.4.1. Flow stratification

A non depth-uniform flow field, better known as flow stratification, can occur in case of an outlet flow, in locks or in situations with large differences in temperature and/or salinity. Flow stratification influences the manoeuvring behaviour of a ship, as different flow velocities and flow directions are present over the water depth. In the case of a non-uniform flow field it is not possible to work with the depth averaged flow velocity, as it is not representative for the situation. The flow velocity in the top layers should then be taken into account, in order to determine the impact on vessels (van der Hout, 2011).

2.5. The Coanda effect

Lateral walls can also be expected in the outflow area of a discharge sluice, besides the bottom being present as a limiting boundary. An important phenomenon that can occur in the case of a jet and the presence of closely located lateral walls is the Coanda effect. The Coanda effect describes the tendency of a jet to deflect from its straight direction towards a lateral wall. This process is related to pressure gradients that are present normal to the jet. The influence of a nearby located lateral wall, considering a free turbulent jet, was investigated by Miozzi et al. (2010). The set-up of the experiments and the deflected jet is shown in Fig. 2.5.

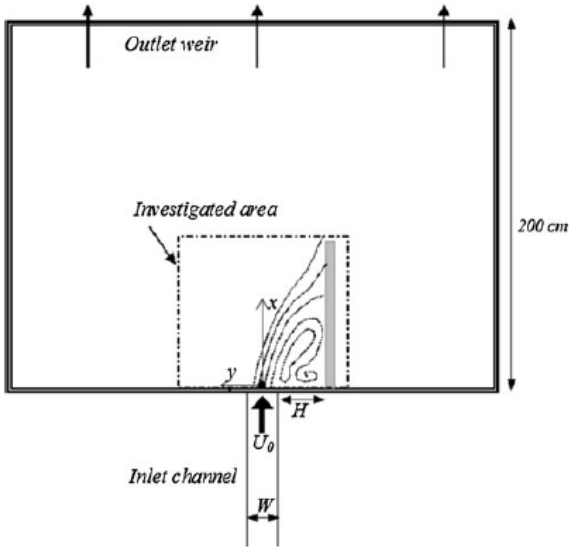

Figure 2.5: The setup of the Coanda Effect experiments (Miozzi et al., 2010).

The experiments showed that the presence of a lateral wall strongly deviates a jet from its straight direction to the wall itself. This effect can be explained by the presence of asymmetric pressure fields at the jet boundaries pushing the jet fluid towards the side where the wall is placed. This effect can beneficially be used in coastal situations. A flow from for example a sewer outlet can be deviated from its original path to a lateral wall to prevent the pollutants reaching certain locations. This Coanda effect might also be beneficially used in the port of Ostend to prevent hindrance to nautical activities.

2.6. Current guidelines marina design

The design of a marina is bounded by several guidelines and regulations. In this section the most relevant guidelines are pointed out.

2.6.1. Marina layout

A marina typically consists of an approach channel, fairways in between the floating pontoon structures, piers, slips and mooring piles (ASCE, 2012). The fairway width in between the floating structures should be between 1.50 and 1.75 times the longest slip length. Several guidelines regarding the approach channel of a marina are mentioned in PIANC (2017). In a perfect state, and considering ideal conditions, the approach channel width should be 1.3 times the largest vessel beam B.

2.6.2. Maximum flow velocities

According to Ridderinkhof et al. (2019), the maximum allowed current velocity inside the marina is 1 m/s in order to prevent damage to piles and floating structures. If the flow velocity is uniform over the depth, the depth-averaged flow velocity can be used. Otherwise only the flow velocities in the top layers should be taken into account. Considering the ship's navigability, a longitudinal current of 0.8 m/s is acceptable for recreational vessels provided there is at least 50 m up and downstream of the narrowing a straight fairway present (Rijkswaterstaat, 2020). Cross flow is permissible if $v_c \leq 0.3$ m/s and also the cross-flow field is not longer than 0.5 times the vessel length (Rijkswaterstaat, 2020). For small openings, such as pipes, with a diameter of the outflow opening $A < 0.2$ m^2, there is a cross flow up to 1 m/s permissible (Rijkswaterstaat, 2020).

2.7. Conclusion

In this chapter the most relevant processes in and around a discharge sluice found in literature are discussed. The flow through a discharge sluice is caused by a difference in water level between both sides. The discharge Q is related to the head difference, the discharge coefficient μ and the inlet surface A. The discharge coefficient is directly related to the loss coefficient ξ, which gives information about

the amount of energy that is lost in the system. The analytically/empirically found discharge coefficient value for the considered sluice system in the Ostend case is 0.79.

The jet that is generated by the discharge sluice can be identified as a submerged plane turbulent wall jet and is bounded by the bottom and a limiting water depth. Just past the opening the flow velocity is equal to the initial flow velocity U_0. This area is better known as the potential core. The flow velocity rapidly decreases in flow direction due to the momentum exchange with the ambient fluid and the emergence of eddies at the sides of the jet.

The flow pattern downstream of a discharge sluice can be predicted by the use of numerical models. Two examples are discussed: Delft3D-FLOW 4 (D3D) and COMSOL Multiphysics 5.6 (COMSOL). D3D is intended for predicting currents and morphological changes on a large scale, whereas COMSOL is intended to be used for detailed simulation of flow in and around complex structures.

In this study the potential impact on a marina is assessed by using guidelines. The following guidelines regarding cross and longitudinal currents inside marinas are found in literature:

- A cross current larger than 0.3 m/s inside the marina causes hindrance to manoeuvring vessels.
- A longitudinal current larger than 0.8 m/s inside the causes hindrance to manoeuvring vessels.
- A current larger than 1.0 m/s inside the marina causes damage to pontoon structures and moored vessels.

3

System analysis

Section 3.1 gives some historical background regarding the area of interest, the port of Ostend, and describes the water system. Section 3.2 proceeds to describe the saline characteristics of the system. The chapter is concluded by Section 3.3 in which the tidal signal that forces the system is elaborated.

3.1. The port of Ostend

The port of Ostend is located on the Belgian coast. It is the smallest Belgian coastal port and is mainly focused on the construction and maintenance of windmill parks in the North Sea. The port of Ostend used to be the largest Flemish port in terms of passenger transport, but this activity has declined sharply in recent years and has largely been converted to cargo transhipment. An important part of the total traffic consists of sand and gravel from the sea (Havencommissie, 2019).

The port of Ostend (Fig. 3.1) consists of a tidal port, where the sea flows freely, and a dock port, which is closed by locks (Inventaris, 2019). Furthermore, a big lake which is connected to the port basin, also known as 'The Spuikom', is part of the port area. This lake was created to prevent silting up of the port basin and the entrance channel. Nowadays this lake is only used for recreational purposes and it is connected to the port by means of bulkheads that can be opened and closed. In order to protect the hinterland against future sea level rise (Church et al., 2013), the entire dike ring in the port of Ostend is going to be enforced. The connections between the port basin and the Spuikom and the Noordede are part of this dike ring. Therefore the current bulkheads of the Spuikom are going to be replaced by a new discharge sluice located closely to the railway and traffic bridge (N34). A storm surge barrier is going to be constructed near the bridge over the Noordede River / Ghent-Ostend channel. The scope of this research is limited to a small part of the Spuikom and the outflow area of the proposed discharge sluice. An overview of the scope area is given in Fig. 3.1. Four distinct parts are identified: the 'RYCO', the port basin, the Noordede River and the Spuikom.

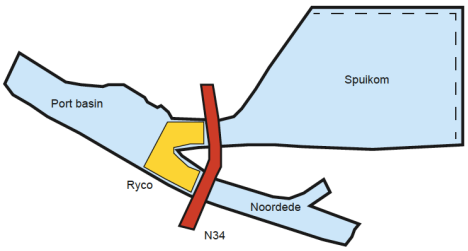

Figure 3.1: The scope area of this study.

3.1.1. The Royal Yachtclub Ostend (RYCO)
The RYCO, also known as the Royal Yacht Club Ostend, is the oldest yacht club in Belgium. The club building dates from 1906 and is a royal donation from Leopold II (Ryco, 2021). The marina contains berths for both motor and sailing boats. The berths can be reached by using floating pontoons structures and finger piers. Due to the construction of a movable storm surge barrier at the Noordede side and a discharge sluice at the Spuikom side, the functionality of the current marina may be impeded as a result of a too strong current from the Noordede river / Ghent-Ostend channel on the one hand and a strong current with possible foaming as a result of the discharge sluice on the other.

3.1.2. The port basin
The port basin offers shelter for fishing vessels and research vessels from local authorities and it offers the possibilities for supply and removal of raw materials. In addition, parts of offshore wind farms are shipped in and out via the port basin. The port basin is in open connection with the North Sea and the basin is therefore strongly influenced by the in- and outgoing tide. Normative conditions for the water levels are expected to occur during spring tide. The characteristics of the tidal signal are given in Section 3.3.

3.1.3. The Noordede River / Ghent-Ostend channel
The part of the river shown in the map is the last part of the tide bound Noordede river (the top branch on the bottom right of Fig. 3.1) before it flows into the port basin. The lower branch, the Ghent-Ostend channel, joins the river just upstream of the N34 bridge. The supplied water can be identified as fresh, PSU = 0.5 (Montagna et al., 2013). The Ghent-Ostend channel provides the largest share in the total discharge. According to Goossens and Moerkerke (2019), normative conditions for the currents in the marina occur during a maximum discharge from the channel of 100 m^3/s and a discharge of 10 m^3/s from the Noordede river. This occurs during low tide, for maximum 9 hours per tidal cycle, and only in the winter period. It is unclear how often this maximum riverine discharge occurs.

The lock complex upstream in the Ghent-Ostend channel prevents the influx of salt water during high water. In this way salinization of the underlying agricultural land is counteracted, the hinterland is protected against flooding and an attempt is made to aim for a constant level of +3.94 m TAW for inland navigation on the channel.

3.1.4. The Spuikom
This basin was developed about a hundred years ago to flush excess sediment from the port channel of Ostend. However, the Spuikom has never been used for this purpose. The currents generated in the first tests turned out to be far too powerful. The Spuikom thus developed into a popular site for oyster farmers, water sports enthusiasts, hiking recreationists, fishermen, birds and bird watchers, and a breeding ground for Belgian marine researchers (Vliz, 2021). The Spuikom is a shallow salt water body (PSU = 25-30) with an area of approximately 80 ha (Witteveen+Bos, 2019). The target water level of the Spuikom is +3.27 m TAW. The permissible variation of the water level is limited to ensure that water sports remain possible. The minimum allowable water level is +2.97 m TAW and the maximum water level is +3.37 m TAW. With the proposed discharge sluice the allowable water levels are maintained and a volume of water of 320.000 m^3 is exchanged per tidal cycle.

3.2. Salinity
A water body with density differences between incoming flow and the ambient fluid can result in a different plume development than without these differences (Section 2.4). It is therefore important to determine whether flows due to density differences play a significant role in the scope area. The Spuikom is an enclosed water basin without any fresh water supply. According to Vliz (2021), the water body has a strong salty character, with a salinity level varying between 25 and 30 PSU. The salinity levels in the port of Ostend are depicted in Fig. 3.3. Location C corresponds with the area just in front of the discharge sluice. It can be seen that, except for the winter months, the salinity level just in front of the discharge sluice varies between 20 and 30 PSU. It is therefore assumed that, for simulations of the period April-November, no density differences would have to be taken into account.

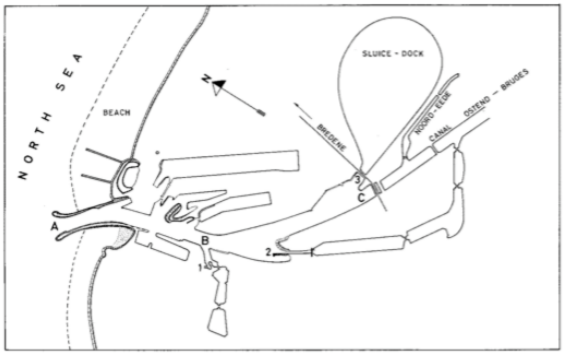

Figure 3.2: Sampling locations port of Ostend (Persoone & de Pauw, 1968).

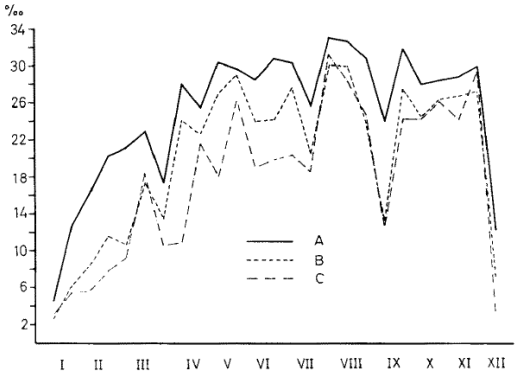

Figure 3.3: Salinity levels port of Ostend, x-axis: months, y-axis: salinity rate (Persoone & de Pauw, 1968).

During the winter months there is a significant inflow of fresh water into the system from the Noordede river / Ghent-Ostend channel (Witteveen+Bos, 2019). At low tide, the channel and the river discharge into the port basin and consequently the port of Ostend becomes brackish and stratified, with fresh layers at the top and salty layers at the bottom. It is assumed that when the sluice has started discharging after a few minutes the fresh water in front of the sluice system is flushed away by the outflow of the discharge sluice. Therefore no density differences have to be taken into account in the detailed COMSOL modelling. On the other hand, in the larger scale D3D model the inflow of fresh water and the consequential density differences flows should be included.

3.3. Tidal signal

Besides the riverine discharge, the marine forcing of the port of Ostend is dominated by the tidal signal. Water levels and velocities, i.e. the vector of water motion, are controlled by this signal (Bosboom & Stive, 2015). The port of Ostend experiences an asymmetrical semi-diurnal tide with a tidal period of approximately 12 hours and 25 minutes. The spring-neap tidal period amounts to 14.5 days. It is expected that normative conditions occur during spring tide. The tidal amplitudes and ranges during spring tide are shown in Table 3.1.

Mean High Water (MHW)	+4.72 m TAW
Mean Low Water (MLW)	+0.16 m TAW

Table 3.1: Tidal deflections of the water surface in the port of Ostend (AMDK, 2021).

3.4. The proposed discharge sluice

This section contains information regarding the design of the proposed discharge sluice connecting the Spuikom and the port of Ostend. The design is developed by the engineering consultancy firm Witteveen+Bos and fulfils the functional requirements imposed by local authorities. However, the design is still in the preliminary design phase and might therefore be adjusted later. The design as used in this study, depicted in Fig. 3.4, has the following characteristics:

- A culvert flow surface of 11.25 m^2. The surface is divided over two culverts, separated by a distance of 80 cm.
- Width culverts: 2.25 m.
- Height culverts: 2.5 m.
- Length culverts: 10 m.
- Bottom level culverts: -3.0 m TAW.
- A pile row is placed in front of the culverts to reduce resulting flow velocities.
- Bottom level pile row: -3.0 m TAW.
- Top level pile row: +4.0 m TAW.
- Distance pile row - outflow opening: 10 m.

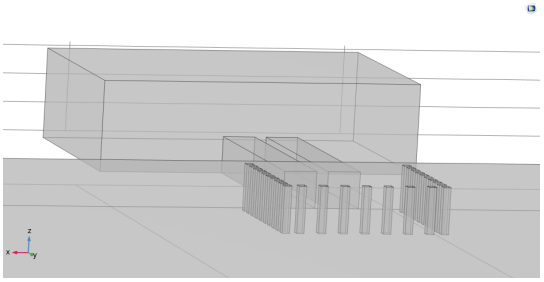

(a) Oblique view.

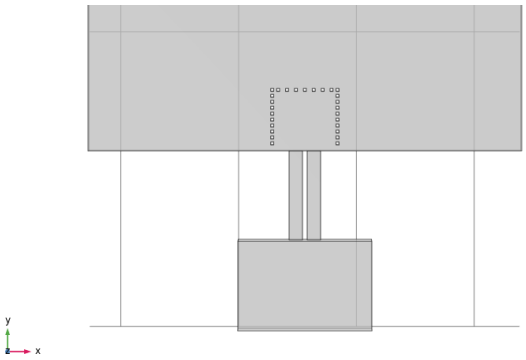

(b) Top view.

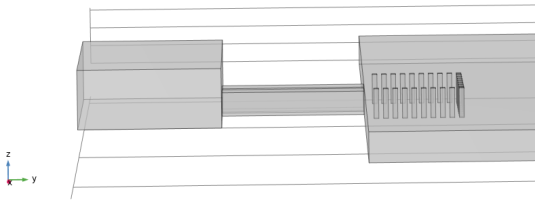

(c) Side view.

Figure 3.4: Geometry proposed discharge sluice, different views.

4

Set-up methods, simplified model

This chapter describes the set-up of the two examined methods and the baseline method. In the present study, together with the baseline method these two methods are applied to a simplified case to make a comparison between the results. First, the simplified case is described in Section 4.1. The set-up of the baseline method is presented in Section 4.2. Afterwards, a method that consists of a combination of a COMSOL and a D3D model is elaborated on in Section 4.3. Thirdly, a method that only uses a D3D model is explained in Section 4.4.

4.1. Simplified case

The methods are applied to a simplified case, in order to make a fair comparison between the methods. This case is based on the situation in the port of Ostend, but is much simpler. It includes the following features:

- A rectangular downstream water body with a length of 80 m and a width of 72 m, representing the marina.
- A discharge sluice with a pile row in front of it. The design is as presented in Chapter 3. The flow through the sluice is caused by a difference in water level between both sides of the sluice.
- The most extreme possible flow rate through the discharge sluice is taken into account.
- A flat bottom at -3 m TAW in the entire model area.
- A constant water level of +0.16 m TAW in the downstream area. This leads to a total depth of 3.16 m. Furthermore, a constant water level of +2.97 m TAW upstream of the discharge sluice, leading to a water depth of 5.97 m.
- A constant bottom roughness Manning coefficient of 0.035. This corresponds to a clayey soil (Marriott & Jayaratne, 2010).
- No density differences, incoming tide or varying water level.

4.2. Baseline method

Since no measurement data from the port of Ostend is available, validation of results following from the examined methods is not possible. Therefore, the results of both methods are compared to a method from which the results are expected to be closest to the truth, the baseline method. For this baseline method, the entire domain is modelled in COMSOL (COMSOL, 2019). As described in Chapter 2, COMSOL is able to simulate the flow around and through complex hydraulic systems in much detail. The complete three-dimensional flow field is simulated and it is therefore likely that the results of this method are sufficiently accurate.

The model includes a small part of the Spuikom, the culverts and the downstream outflow area. The constant water level at marina side is +0.16 m TAW, and at Spuikom side +2.97 m TAW. The geometry of the discharge sluice system is based on a design by Witteveen+Bos and follows from recommendations

made in Ridderinkhof et al. (2019). More details on this design can be found in Section 3.4. The design was made using Navisworks, a software application developed by Autodesk (Navisworks, 2021). For this research the design is imported using the AutoCAD import function in COMSOL. The elements of the design irrelevant to this study are deleted, resulting in the following geometry that is used during the simulations:

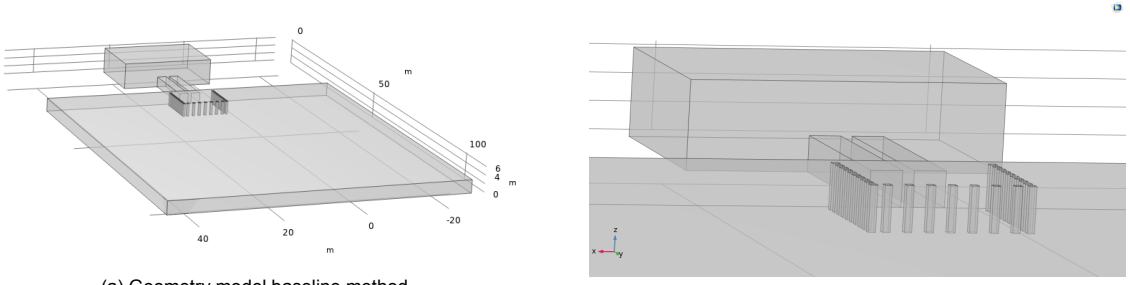

(a) Geometry model baseline method.

(b) Detailed pile row geometry.

Figure 4.1: The geometry that is used during the simulations with the baseline method.

4.2.1. Assumptions

Two important assumptions are taken into account in the COMSOL modelling: the type of flow regime and the rigid-lid approximation.

Flow regime

Knowledge about the flow regime in the culverts and the outflow area of the discharge sluice is important, as a so-called hydraulic jump could occur. This happens when there is a transition from a supercritical to a subcritical flow regime. In that case, this must be anticipated in the modelling. The Froude number is an important indicator of the flow regime and can be calculated for respectively the culverts and the outflow area (Chaudhry, 1993; Chow, 1959). In the Ostend case the culverts are always submerged and therefore a hydraulic jump can never arise in these, as a condition of a hydraulic jump is that there is a free water surface present (Battjes, 2002). On the other hand, in the outflow area of the sluice a hydraulic jump could potentially arise. Therefore the Froude number is calculated for this area, using the outflow flow velocity u, the gravitational acceleration g and the water depth inside the culvert h. The outflow flow velocity is determined by dividing the expected discharge (based on the water level difference) by the flow area (= 5.87 m/s).

$$Fr = \frac{u}{\sqrt{gh}} \approx \frac{5.87}{\sqrt{9.81 \cdot 2.5}} \approx 1.19 \tag{4.1}$$

A Froude number greater than 1 indicates supercritical flow, in which a hydraulic jump could arise. However, the Froude number is only slightly greater than 1 and there is still a minimum layer of 0.66 m water on top of the outflow opening (total water depth is 3.16 m) which suppresses this jump to happen. There is a small chance that a hydraulic jump occurs in this case. It is therefore not taken into account in the modelling.

The rigid-lid approximation

A well known simplification in the world of numerical flow modelling is the rigid-lid approximation (di Martino et al., 2001). A rigid-lid approach often leads to shorter computation times and is generally easier to deploy. In the case of a rigid-lid approach the water surface is fixed and no shear stresses are present at this boundary (Andersson et al., 2011). The use of a rigid-lid approach suppresses the actual surface deformation and introduces an error in the continuity equation (McSherry et al., 2017). In literature two conditions are described regarding the applicability of this approximation:

- The Froude number should be smaller than 0.3 (Fan et al., 2017).
- The surface deformations should be smaller than 10% of the water depth (Constantinescu et al., 2013).

The first condition is not met in the region from the outflow opening up to the pile row. The expected Froude number in this area exceeds this condition (0.7 - 1.05). It is expected that in the region downstream of the pile row the first condition is satisfied, as the flow velocities are lower here. Whether or not the second condition is met is more difficult to determine. In an acceleration zone of the flow, the change in water level is equal to the change in velocity head. In a deceleration zone, on the other hand, energy losses occur and the change in velocity head is no longer equal to the change in water level. In almost the entire domain the flow rate decreases relatively gradually and it is therefore assumed that the second condition is satisfied in these areas.

It is expected that for the flow around the pile row the second condition is not satisfied. The water is expected to be pushed up. As a result the resulting water level variation is expected to be greater than 10% of the water depth. Moreover, there is a strong accelerating flow through the pile row which is also expected to give relatively large surface deformations.

In short, according to the first condition a rigid-lid approach cannot be applied for the region from the outflow to the pile row as large errors would be introduced in the continuity equation. The second condition predicts errors introduced by the flow around the pile row.

However, this study does not focus on the area around the outflow and the pile row, but rather on the area at a significant distance from the pile row. It is assumed that the introduced errors do not significantly affect the downstream flow profiles at a distance of 40 m and further. Therefore a rigid-lid approximation is applied in this research.

4.2.2. Boundary conditions

COMSOL solves the Reynolds Averaged Navier-Stokes (RANS) equations. The numerical solution of these incompressible Navier-Stokes equations has a parabolic-elliptical shape. A flow velocity at the inflow boundary and a pressure condition at the outflow boundary is in that case prescribed. A well-posed problem is obtained in this way (COMSOL, 2019; Ferziger & Perić, 1996). An example of a project in which these boundary conditions are used is the study conducted by Erdbrink et al. (2014) on the influence of structure gates on a sluice gate flow. These boundary conditions physically ensure that water can flow freely through the outflow boundary, without the velocity being fixed.

The water level difference between both sides of the sluice, 2.81 m, that is modelled corresponds to a certain flow rate that passes through the system. This follows from the general discharge relation, Eq. (2.1). The imposed flow velocity on the inflow boundary (m/s) in the COMSOL model times the inflow area (m^2) determines this flow rate (m^3/s). A description of how this inflow velocity is obtained is presented in Section 4.2.5.

The upstream boundary is located 15 m upstream of the culverts' inflow. A sensitivity analysis is done to find the distance from the culvert inflow at which all the inflow effects are included. This analysis can be found in Appendix C. The width of the upstream boundary is also found in this way: 22.5 m. The downstream boundary is located at a distance of 80 m from the outflow opening so that the conditions for the simplified case are met. The top boundary is a rigid-lid that represents the water surface and its location corresponds with the simulated water levels.

At the walls a no-slip condition is applied. A no-slip wall is a wall where the fluid velocity relative to the wall velocity is zero (Rapp, 2017). An overview of the boundary conditions is presented in Fig. 4.2.

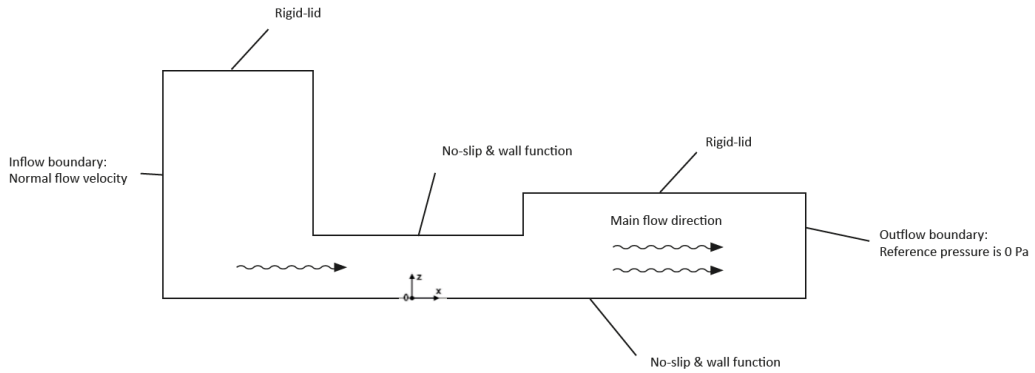

Figure 4.2: Boundary conditions of the COMSOL model that is used in the baseline method. Sketch is not to scale.

4.2.3. Grid design

The triangular grid that is used in this COMSOL model is created in a so called physics-controlled way. This means that the software itself builds a mesh based on the geometry that the user provides as an input. The user can choose a predefined mesh element size, ranging from extremely fine to extremely coarse. The mesh adapts itself to the current physics settings in the model. For example, in and around the sluice system the mesh is finer than in the downstream water body (COMSOL, 2019).

A sensitivity analysis with different mesh resolutions is carried out to determine the minimal mesh resolution for correct results. In this way computational time is saved. The analysis, further elaborated on in Appendix C, shows that the minimum grid category should be 'coarse' in the COMSOL simulations. In that case the smallest grid cell has a length of approximately 15 cm.

4.2.4. Other settings

Other physical and numerical settings regarding the COMSOL modelling are discussed in Appendix B.

4.2.5. Modelling process

The COMSOL modelling contains the following steps:

1. Setting up the geometry of the discharge sluice, including a pile row in front of the outflow opening.
2. Running a simulation with an initial guess of the inflow velocity (i.e. inflow discharge). Zero relative pressure is imposed at the outflow boundary.
3. Reading the resulting pressure difference between both sides of the discharge sluice system.
4. The discharge coefficient μ of the system is calculated using Eq. (2.2), in which the initial imposed discharge and the in the previous step determined pressure difference are filled in. A value of 0.74 is found.
5. The inflow discharge that corresponds to the simulated water level can now be calculated using Eq. (2.1) and the in the previous step calculated discharge coefficient.
6. A final simulation is done with the calculated inflow discharge (i.e. inflow velocity) imposed at the inflow boundary.

4.3. Method COMSOL - D3D: A modelling train consisting of a COMSOL and a D3D model

Method COMSOL - D3D consists of two different model software programs: COMSOL and D3D. The idea is that the first region including the discharge sluice and the pile row is modelled in COMSOL. Afterwards, a coupling is made between COMSOL and D3D. As a result, the outflow area of the sluice can be modelled in D3D. A schematization of method COMSOL-D3D can be seen in Fig. 4.3.

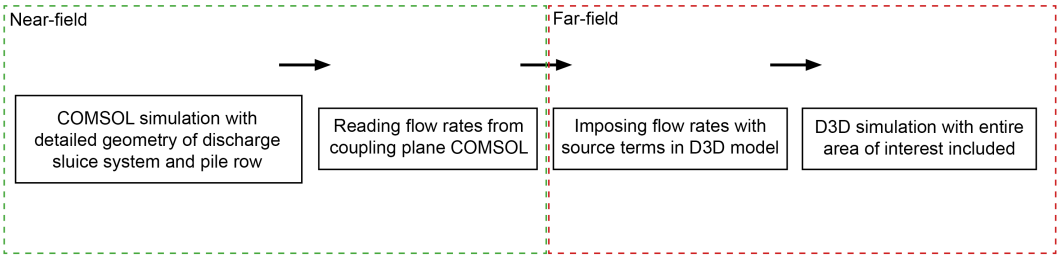

Figure 4.3: Schematisation method COMSOL - D3D.

This section is split up into three different parts: the COMSOL modelling (Section 4.3.1), the coupling between the COMSOL and D3D modelling (Section 4.3.2) and the D3D modelling (Section 4.3.3).

4.3.1. COMSOL

For the COMSOL domain of this method exactly the same simplifications, assumptions, boundary conditions, modelling process and grid choice apply as for the baseline method. The discharge coefficient μ is thus determined in the same way as in the baseline method. The length of the downstream domain, however, is shorter. This length is chosen so that there are no more turbulent effects due to the pile row present at the outflow boundary. The geometry of the COMSOL domain is depicted in Fig. 4.4.

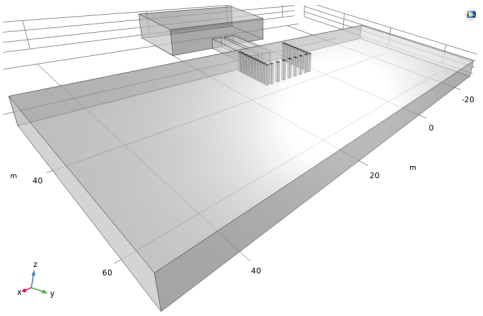

Figure 4.4: Geometry COMSOL domain, method COMSOL-D3D.

4.3.2. Coupling COMSOL and D3D

The coupling strategy between the models is based on research projects by Choi and Lee (2007) and Kranenburg et al. (2016). In these projects, a combination of sink and source terms was used to mimick a jet outflow.

The intention is to use as much information as possible from the detailed COMSOL model to mimick the jet in the D3D model. After the COMSOL simulation has been finished, a part of the outflow boundary at which water flows out of the model is chosen as the 'coupling plane'. The cross-section is located far enough from the pile row so that it is not affected by its turbulence effects. The coupling plane is split up into an output grid which corresponds to the grid in D3D. The plane has ten horizontal grid cells of 2 m wide and ten vertical grid cells. The height of each grid cell is equal and is 0.316 m. An illustration of the used output grid on the outflow boundary is presented in Fig. 4.5.

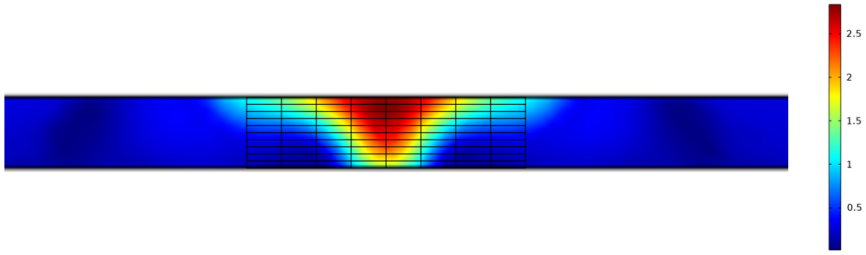

Figure 4.5: The output grid of the coupling plane, corresponding with the one in D3D, that is copied on the outflow boundary of the COMSOL model.

From the rectangles that are visible in Fig. 4.5 the discharge flowing through is obtained by integrating the flow velocity over the cell surface. In the post-processing part in COMSOL an integration order can be chosen (COMSOL, 2019). This is the order of the polynomial used to fit the point distribution of values that are integrated. An integration order of 30 is used in this research. In this way the integration is done as accurately as possible. One hundred different discharge values are obtained in this way. These values are used as an input for the so-called source terms in D3D.

Source terms
At the corresponding location in D3D source terms are attached to the corresponding grid cells, ten in horizontal and ten in vertical direction. With a source term water is discharged from a cell. In total there are 100 source terms included in the D3D model. The discharge values obtained from COMSOL are assigned to these source terms. Also a 90 degree direction is assigned to the source terms, which corresponds to the direction of the jet. In this study it is assumed that the jet leaves the outflow plane perpendicularly. Lastly, a v-magnitude, a flow velocity, is specified per cell. It adds momentum to the source term. The v-magnitude is calculated by dividing the discharge over the surface of the grid cell.

The total discharge of all the source terms should equal the total discharge that flows through the plane in the direction of the jet. It is a summation of the discharge flowing through the culvert and the amount of water that is entrained by the jet, Eq. (4.2). The entrainment of surrounding water by a jet is a well-known phenomenon and is described by Choi and Lee (2007) in their research on a wastewater outflow and the dilution of polluted discharge.

$$Q_{\text{source}} = Q_{\text{sluice}} + Q_{\text{entrained}} \tag{4.2}$$

Sink terms
As described by Turan et al. (2007) and Choi and Lee (2007), a jet flowing through an ambient fluid entrains surrounding water. Kranenburg et al. (2016) have tried to mimick this effect by adding sink terms just behind the source terms. In that study an estimate of the amount of entrained water was done. Instead of placing the sink terms directly behind the source terms, Choi and Lee (2007) placed sink terms along the trajectory of the jet to mimick the entrainment. This method is called the Distributed Entrainment Sink Approach (DESA). In this way you get a more realistic return current as you place the sink terms at the place where water is actually drawn in.

In this work the amount of water that is entrained by the jet in the first 40 m can accurately be determined by reading the amount of water that flows back through the entire outflow boundary. The entrainment phenomenon is mimicked in D3D by placing negative discharge terms, i.e. sink terms, along the jet's trajectory. The total amount of water flowing back is uniformly distributed over these sink terms. This is done uniformly because the suction along the jet is comparable at every point.

When modelling the jet in this way, it must be prevented that the source and sink terms conflict, i.e. water that directly flows back from the source to the sink terms. 'Thin dams', the thick black lines in Fig. 4.6, are placed directly behind the source terms to prevent this flow to occur. An overview of the thin dams and the combination of sink and source terms in D3D is given in Fig. 4.6.

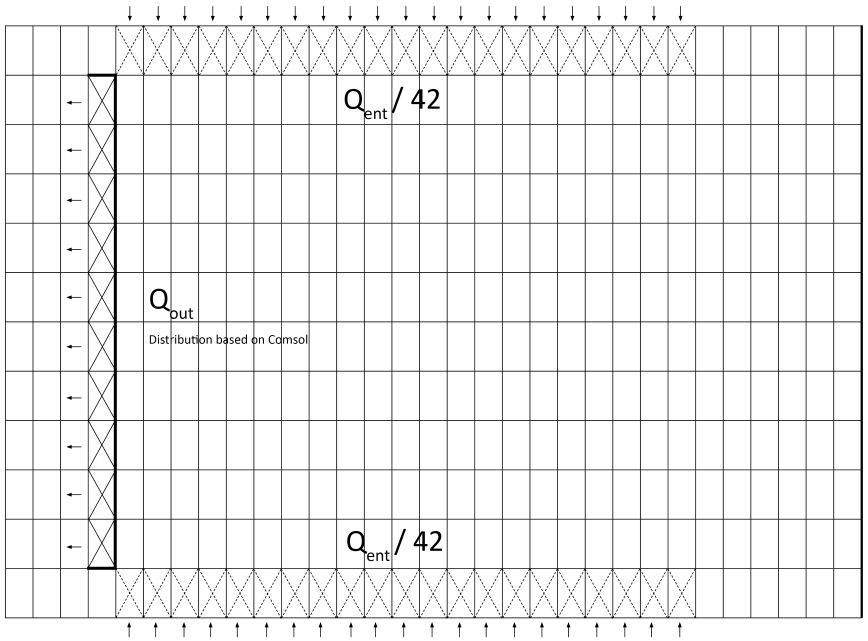

Figure 4.6: A combination of sink and source terms in D3D, left: the source terms, top and bottom: the sink terms.

4.3.3. D3D

The last step of this method consists of a D3D simulation with the previous described sink and source terms attached to 100 grid cells. The D3D model that is used consists of a rectangular body of water with three land boundaries and one open boundary, at the sea side. The bottom is flat, has a Manning roughness of 0.035 and is located at a depth of -3 m TAW. There is constant water level of +0.16 m TAW present. The difference with the baseline COMSOL model is that the model is many times longer, 2010 versus 80 m. This is because the model crashes in D3D if the water level boundary is too close to the jet outflow. This will not happen if it is placed far away enough. In that case the water level change at the outflow boundary caused by the jet is negligible.

Boundary conditions

The only open boundary is the one that is perpendicular to the jet and represents the sea. This boundary is located 2010 m downstream of the outflow opening. It is a water level boundary with a constant value of +0.16 m TAW.

Grid design

The grid that is used is rectangular and contains grid cells with a width of 2 m and a length of 1.5 m. These dimensions are based on a sensitivity analysis. The details can be found in Appendix C.

4.4. Method D3D: Delft3D-FLOW 4 with fixed source terms and porous plate

Method D3D only uses a D3D model. The set-up, the boundary conditions and the grid for this model are exactly the same as for the D3D model that is used in method COMSOL - D3D. However, the discharge sluice is not mimicked by a combination of sink and source terms. Instead, source terms are placed at the location which corresponds to the culverts' outflow openings. These terms are added to ten grid cells, divided over two columns. Because the outlet openings are located at the bottom, it is decided to use the bottom five grid cells of the two columns.

The total discharge value that is assigned to the source terms is calculated using the general discharge relation Eq. (2.1). The discharge coefficient μ in this relation is not calculated by using COMSOL (as in the baseline method and method COMSOL-D3D) but in an analytical/empirical way. This is done

so that this method only consists of one type of numerical model. The complete calculation of the discharge coefficient can be found in Section 2.2.

The discharge, in total 65.99 m^3/s, is uniformly distributed over the ten source terms. Also a direction and a momentum per source term are imposed. Two small thin dams are included in the model to mimick the sides of the pile row (thick black lines in Fig. 4.7).

The front of the pile row and its diffusing character is mimicked by adding a so-called porous plate to the model (dashed line in Fig. 4.7). A porous plate is an option in D3D that represents a partially transparent structure. It extends into the flow along one of the grid directions. In the vertical direction it covers some or all layers but its thickness is much smaller than the grid size in the direction normal to the porous plate (Deltares, 2021). An energy loss coefficient c_{loss} is assigned to the porous plate, which determines the porosity of the structure. A formula for bridge piers, which are similar in structure, is used to determine this loss coefficient (Deltares, 2021), see Eq. (4.3).

$$C_{loss} = \frac{NC_{drag}d_{pile}}{2\Delta y}\left(\frac{A_{tot}}{A_{eff}}\right)^2 = 0.5544 \tag{4.3}$$

in which,

N = the number of piles [-], 9
C_{drag} = the drag coefficient of a squared pile [-], 1.05
d_{pile} = the diameter of a pile [m], 0.5
Δy = the cross sectional length [m], 11.5
A_{tot} = the total cross sectional area [m^2], 36.34
A_{eff} = the effective wet cross sectional area [m^2], 22.12

This value differs from the value that follows from the COMSOL simulations with and without a pile row in Section 2.2. Further research will therefore have to be done into the exact value of the loss coefficient of the pile row. For the schematization of the pile row in method D3D, the value of Eq. (4.3) is used.

An overview of the set-up is presented in Fig. 4.7. The big crosses indicate the location of the source terms in horizontal sense, the smaller crosses the location in a vertical sense.

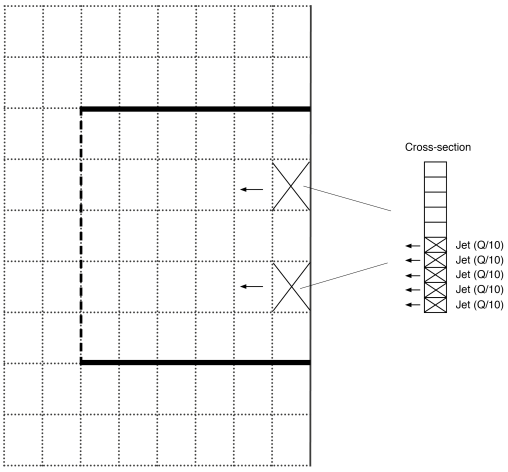

Figure 4.7: Source terms and thin dams method D3D, top view.

4.4.1. Other settings

Other physical and numerical settings regarding the D3D modelling are discussed in Appendix B.

5

Comparison of methods

In this chapter the methods described in the previous chapter are applied to a simplified case. In Section 5.1 and Section 5.2 the results following from each method are compared to the results obtained with the baseline method. Furthermore, in Section 5.3 a prediction of the downstream flow pattern is made using formulas and coefficients from literature. This chapter is concluded in Section 5.4 with a discussion and conclusion on the comparison of the methods.

5.1. Method COMSOL - D3D versus baseline method

In method COMSOL - D3D two different numerical modelling software programs are used, COMSOL and D3D. The resulting jets in the first 80 m that are obtained from the baseline method and method COMSOL - D3D are shown below each other (Fig. 5.1). Note that in the figure resulting from method COMSOL - D3D there is no jet present between the outflow opening and the coupling plane. This is the COMSOL domain of this method and therefore not shown in this image.

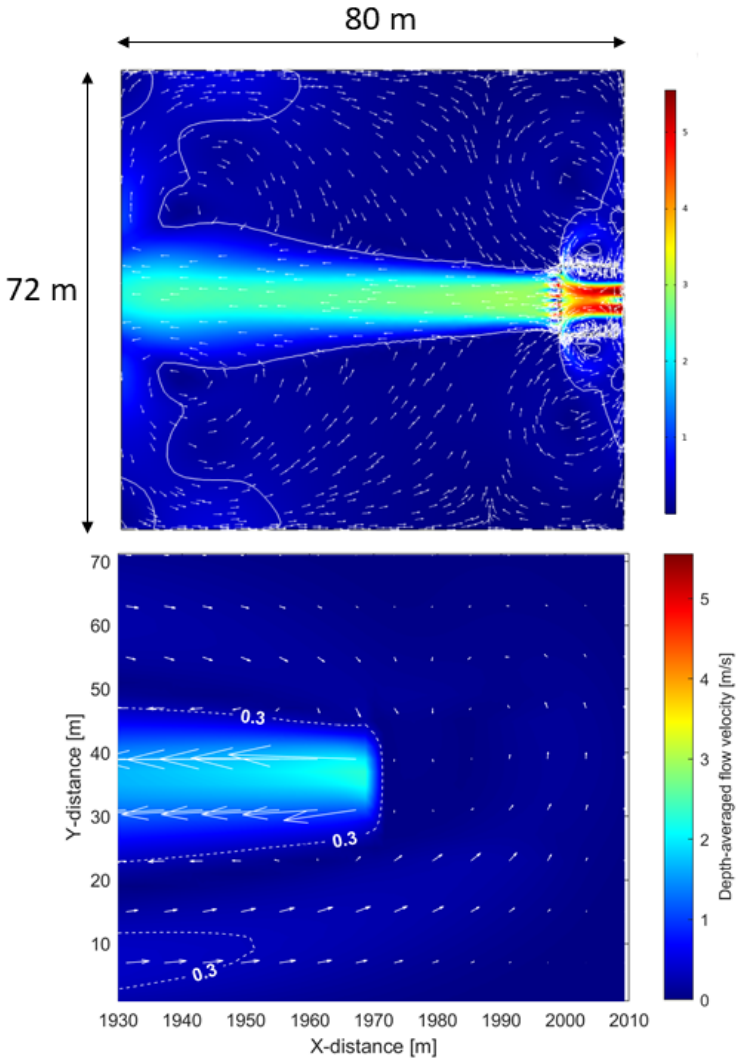

Figure 5.1: Comparison of the jets obtained with the baseline method (top) and method COMSOL - D3D (bottom).

It can be seen in Fig. 5.1 that both jets have the same direction. However, the width of the jet between the 0.3 m/s contour lines of method COMSOL - D3D is greater after coupling than the width of the baseline method jet between the 0.3 m/s contour lines at the corresponding location. Furthermore, it is noticeable that in general the depth-averaged flow velocity is smaller in method COMSOL - D3D and the jet also decreases in power faster. A more detailed comparison is made by plotting the vertical distribution of the flow velocity at four locations, 1, 2, 3 and 4. These four locations are distributed as follows:

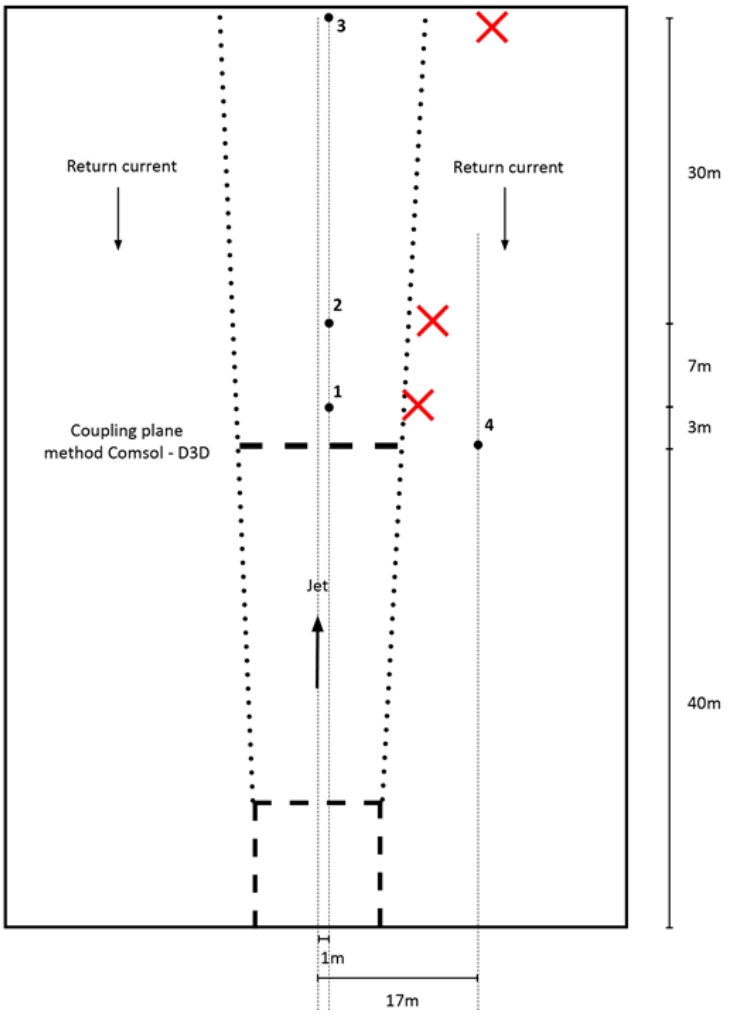

Figure 5.2: Distribution of the locations 1, 2, 3 and 4, the red crosses indicate the comparison points for method D3D.

In Fig. 5.3 a comparison is made of the vertical distribution of the horizontal flow velocity at the four above mentioned locations. A positive flow velocity means a flow in the direction of the jet, a negative flow velocity indicates a flow in opposite direction, i.e. a return current.

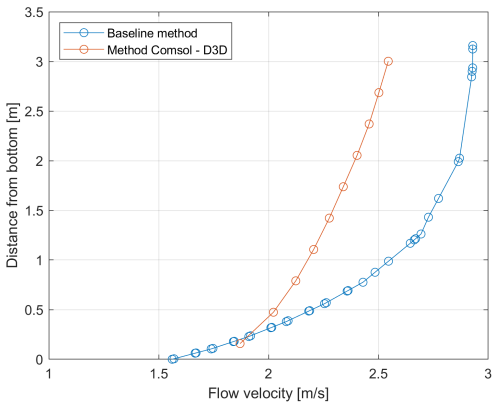

(a) Comparison horizontal velocities at location 1.

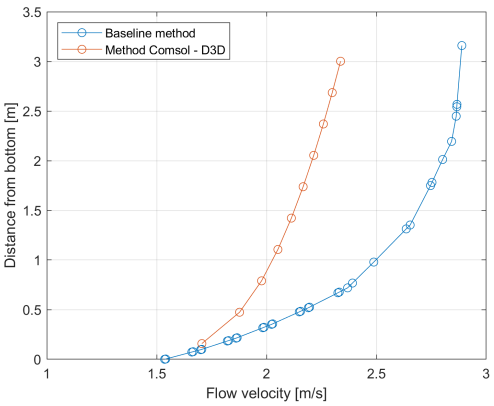

(b) Comparison horizontal velocities at location 2.

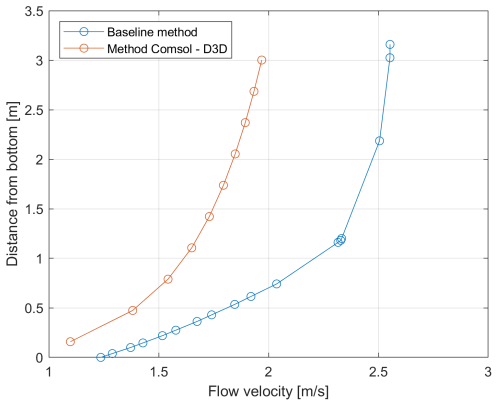

(c) Comparison horizontal velocities at location 3.

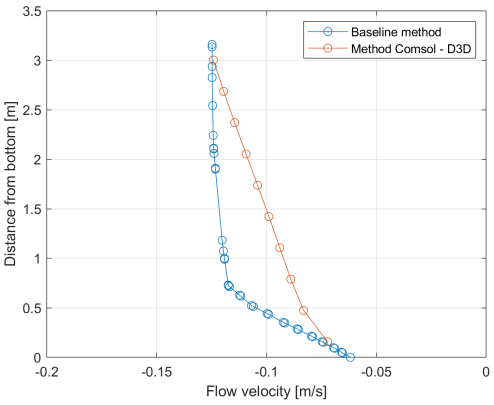

(d) Comparison horizontal velocities at location 4.

Figure 5.3: Comparison of flow velocities baseline method and method COMSOL - D3D at four different locations.

From the above figures it becomes clear that at each location, comparing the flow velocity graphs of the two methods, the shapes are comparable. At location 1, 2 and 3 all the profiles are leaning towards a logarithmic profile, which occurs in the case of an uniform open channel flow (Battjes, 2002). However, there is a clear difference in magnitude of the flow velocities between the methods. At location 1 there is a difference up to 14.5% in horizontal flow velocity, at location 2 a difference up to 23.5% and at location 3 a difference up to 29.5%. The reasons behind this are further discussed in Section 5.4.

A comparison is also made of the cross-sectional horizontal distribution of the depth-averaged flow velocity in Fig. 5.4. This is done for three different horizontal distances from the outlet opening, at 43, 50 and 80 m. Note that the magnitude of the flow velocities has an absolute value. The big bump in the middle is the main jet in which water flows away from the opening, the two small bumps on the sides indicate the return flow.

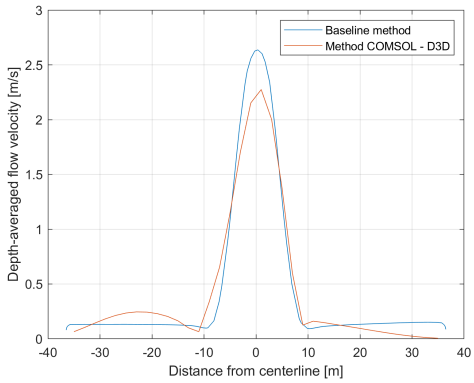

(a) Comparison horizontal distribution flow velocity at x = 43 m.

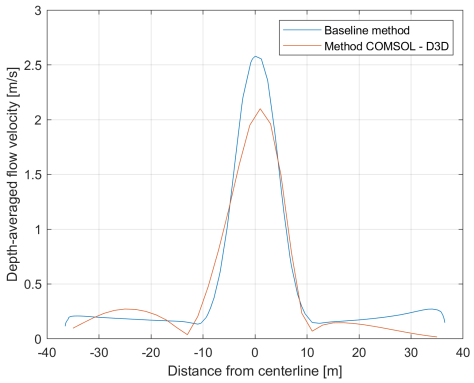

(b) Comparison horizontal distribution flow velocity at x = 50 m.

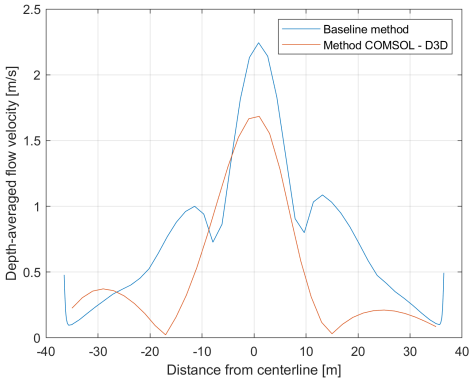

(c) Comparison horizontal distribution flow velocity at x = 80 m.

Figure 5.4: Comparison of horizontal distribution flow velocity at three different distances from outflow opening, method COMSOL-D3D and baseline method.

As expected, again an underestimation of the flow velocities in method COMSOL-D3D can be seen. In addition, a large difference in the magnitude of the return current is visible at a distance of 80 m.

5.2. Method D3D versus baseline method

Method D3D only uses a D3D model. The outflow from the sluice is mimicked by adding source terms to the bottom five grid cells at two locations. These locations correspond with the locations of the culverts' outflow openings. The amount of imposed discharge is based on the general discharge relation in which the discharge coefficient is determined in an analytical/empirical way (Section 2.2). Again, the depth-averaged flow pattern is compared to the one obtained with the baseline method (Fig. 5.5).

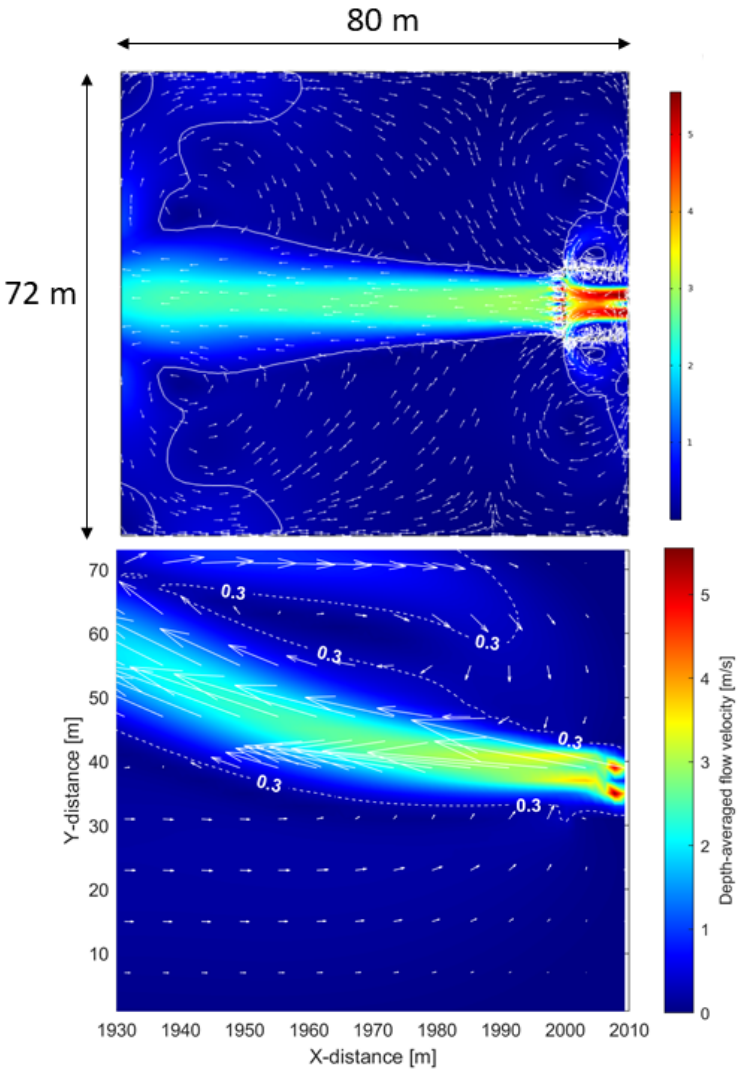

Figure 5.5: Comparison of the jets obtained with baseline method (top) and method D3D (bottom).

It is clear from Fig. 5.5 that the power of the jet is comparable but there is a large difference in the direction of the jet. The jet computed with method D3D is strongly deflected towards the northern quay. As a result, the flow pattern in the entire area is very different. The upward deflection of the jet may be caused by the Coanda effect. This effect is explained in Section 2.5. The reason why this does happen with method D3D and not with the baseline method is potentially because the length of the D3D model is necessarily many times larger than the model used in the baseline method, respectively 2010 and 80 m. A discussion on this potential Coanda effect can be found in Section 5.4. When comparing the different methods it has no further reason to look at the direction of the jet. Therefore, the focus is only on the magnitude and vertical distribution of the flow velocities at the centerline of both jets. It is decided to take the vertical flow profiles at fixed x - distances from the outlet opening at the centerline of the jet, at 43, 50 and 80 m, indicated by the red crosses in Fig. 5.2. These profiles are compared to the profiles obtained with the baseline method at location 1, 2 and 3, see Fig. 5.6.

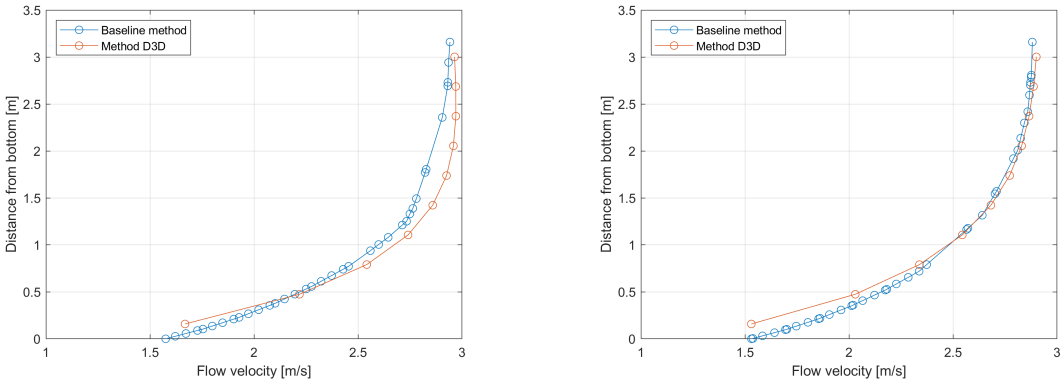

(a) Comparison horizontal velocities at x = 43 m.

(b) Comparison horizontal velocities at x = 50 m.

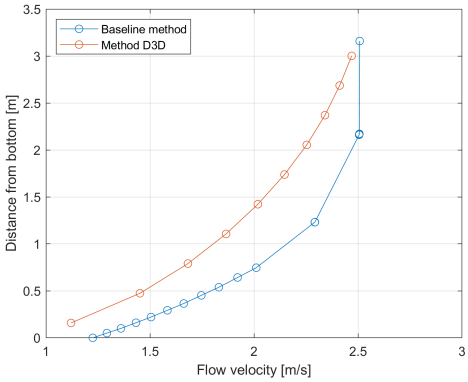

(c) Comparison horizontal velocities at x = 80 m.

Figure 5.6: Comparison of flow velocities baseline method and method D3D at three different locations

Figure 5.6 shows that both the shapes and the magnitudes of the flow velocity profiles are very similar. Only at a distance of 80 m from the outlet opening there is a small difference in flow velocity, an average difference of 8.5%. Also a comparison is made of the cross-sectional horizontal distribution of the depth-averaged flow velocity at three different distances from the outflow opening, see Fig. 5.7.

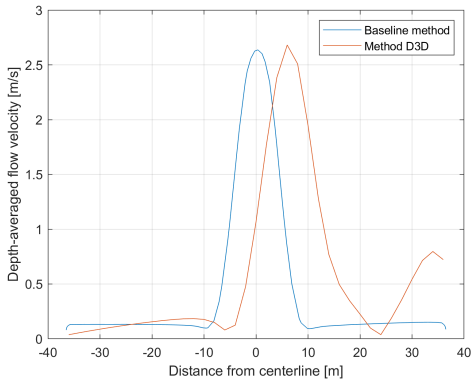

(a) Comparison horizontal distribution flow velocity at x = 43 m.

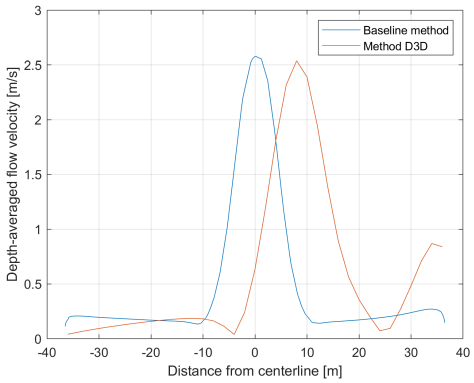

(b) Comparison horizontal distribution flow velocity at x = 50 m.

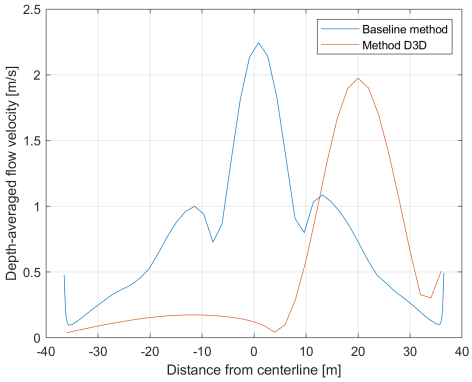

(c) Comparison horizontal distribution flow velocity at x = 80 m.

Figure 5.7: Comparison of horizontal distribution flow velocity at three different distances from outflow opening, method D3D and baseline method.

In the figures above it can be clearly seen that the magnitude of the flow velocities corresponds (maximum difference of 12.5%), but that the jets differ greatly in direction.

5.3. Prediction flow patterns by means of formulas from literature

A prediction of the flow patterns by means of formulas from literature is made, in order to demonstrate that it is difficult to determine the flow through a discharge sluice system with a complex geometry in this way. In this method, hereinafter reffered to as the literature method, formulations and simplifications as found in the literature (Section 2.1) are used to determine the resulting flow field downstream of the discharge sluice in the simplified case. First, the discharge Q that flows through the two culverts of the discharge sluice is calculated. It is calculated using Eq. (5.1), in which the discharge coefficient is used that is determined analytically/empirically, see Section 2.2 (= 0.79):

$$Q = \mu \cdot A \cdot \sqrt{2 \cdot g \cdot (h_0 - h_1)} = 0.79 \cdot 11.25 \cdot \sqrt{2 \cdot 9.81 \cdot (2.97 - 0.16)} = 65.99\ m^3/s \qquad (5.1)$$

This value, 65.99 m^3/s, slightly differs from the value that is found in the COMSOL simulation, 64.96 m^3/s. This difference is caused by a difference in the value of the discharge coefficient μ.

It is assumed that at the moment the jets exit the culverts, the flow velocity is uniformly distributed over the culverts' openings. As the jets get further away from these openings, they become wider and higher. A horizontal widening of 1:20 at both sides of both jets is taken into account (Rijkswaterstaat, 2000). With this widening, the jets meet in the middle after 8 m and from that point they continue as one jet. The vertical widening is based on the fact that after a distance L_0 the flow is spread over the entire water depth. L_0 is equal to 8 times the downstream water depth, in accordance with the design manual for locks (Rijkswaterstaat, 2000). The total water depth is 3.16 m so L_0 is 25.28 m. The initial height of the jet equals the height of the culvert, 2.5 m, so a total height of (3.16 - 2.5) must be overcome

in 25.28 m. This results in a vertical widening of 0.0261 m per meter. In the upper part of the water column where the jet is not yet present there is a current in the other direction, the so-called return current. Also at the sides of the jet there is a return current present. Two illustrations, one from the side, one from above, are presented to clarify the above.

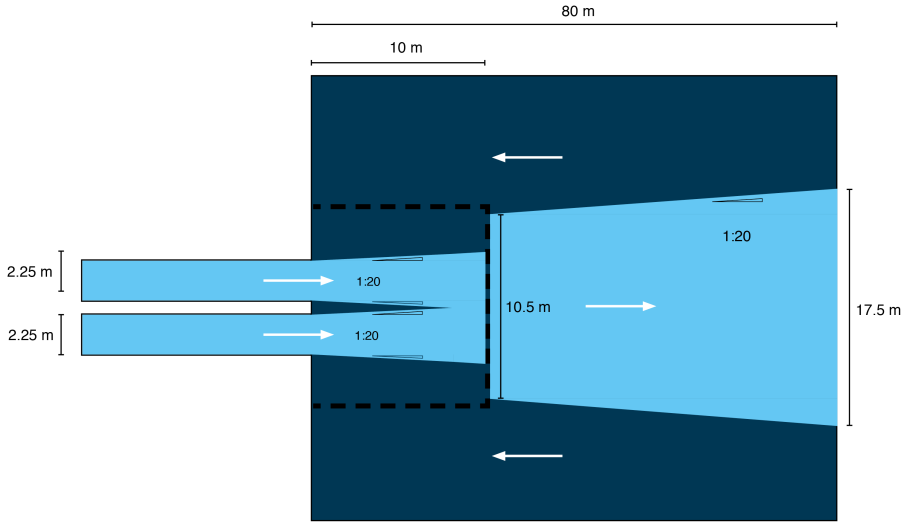

Figure 5.8: Flow pattern from above as assumed in literature method, figure is not to scale.

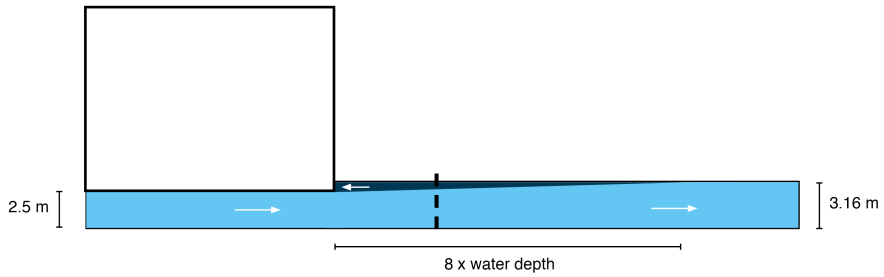

Figure 5.9: Flow pattern from the side as assumed in literature method, figure is not to scale.

It is assumed that in the first stage, from the outflow opening to the pile row, the flow velocity remains uniformly distributed over the flow area of the jet. This means that the velocity at any point is found by dividing the total flow rate by the total flow area. The formula for calculating the flow area for the first 8 m $A_{0\text{-}8}$ differs from that for the last 2 m because after 8 m both jets join each other:

$$A_{0-8} = (W_{culvert} + \Delta_H \cdot N_{sides} \cdot x) \cdot (H_{culvert} + \Delta_V \cdot x) = (4.5 + 1/20 \cdot 4 \cdot x) \cdot (2.5 + 0.0261 \cdot x) \quad (5.2)$$

After 8 m the total jet width equals 6.1 m and the jet height is 2.7068 m. The flow area in the last two meters $A_{9\text{-}10}$ to the pile row is described by the following formula:

$$A_{9-10} = (W_{culvert} + \Delta_H \cdot N_{sides} \cdot x) \cdot (H_{culvert} + \Delta_V \cdot x) = (6.1 + 1/20 \cdot 2 \cdot x) \cdot (2.7068 + 0.0261 \cdot x) \quad (5.3)$$

The flow velocity, uniformly distributed over the flow area can now be calculated by dividing the total discharge Q (= 65.99) by the flow area. It is plotted against the distance from the outflow opening for the first ten meters:

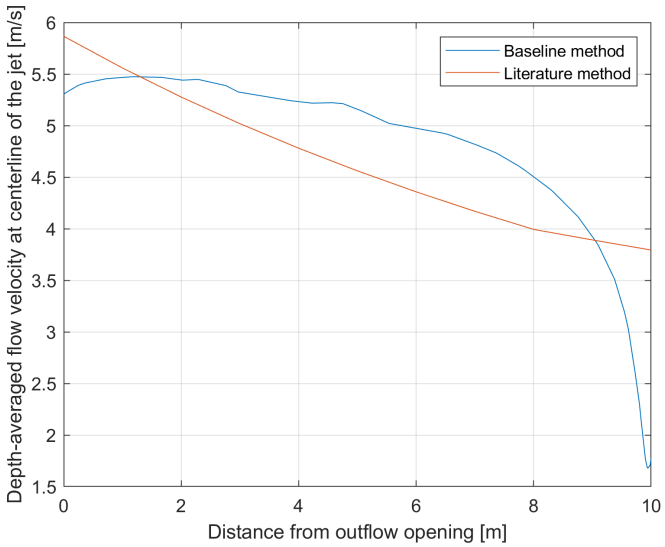

Figure 5.10: Flow velocity against the distance from the the outflow opening.

From Fig. 5.10 it follows that by using formulas from literature a good first estimate of the depth-averaged flow velocity in the first two meters can be made. However, the development of the jet velocity with distance from the outflow opening is hard to predict. After ten meters a significant difference can be seen between the two flow velocities. This is due to the decelerating effect of the pile row, which is not included in this part of the method.

It is expected that the pile row has an effect on the development of the jet. The next part is about the horizontal spread due to the pile row. As can be seen in Fig. 5.8, it is assumed that, due to the spreading effect of the pile row, the jet becomes as wide as the flow area of the pile row, 10.5 m. This is done because no applicable formulas were found in the literature about the effect of a pile row on a jet. Downstream of the pile row it is assumed that the distribution in the horizontal sense is no longer uniform but follows a certain Gaussian-like curve (Schiereck & Verhagen, 2019):

$$u(y) = u_m \cdot exp(-0.693 \cdot (y/b)^2) \tag{5.4}$$

Normally this formula is applied in case of a jet without a pile row. U_m is the maximum flow velocity (at the centerline), y is the distance from the centerline and b is 0.1 times the distance from the outflow opening. In this method the values for U_m and b are adapted such that the width of the curve corresponds with the assumed width of the jet. The jet starts with a width of 10.5 m and has a grow rate of 1/20 at both sides. Since the width of a Gaussian curve is infinitely large, the curve width in this case is the distance between the points where the flow velocity is 0.05 m/s. Also, the area under the curve times the water depth at that point must correspond to the total discharge. This is done for four distances from the outflow opening, respectively 10, 25, 50 and 80 m. The figures below show the distribution of the depth-averaged flow velocity in a horizontal sense at the above-mentioned distances and makes a comparison with the profiles obtained with the baseline method:

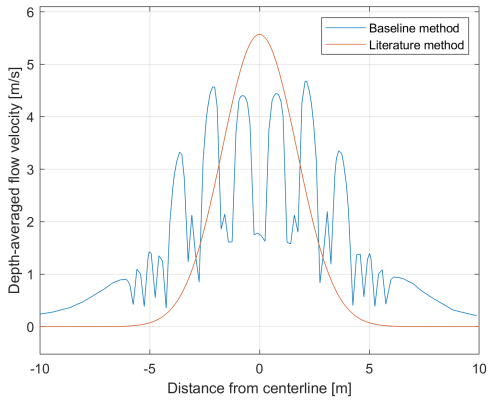

(a) Comparison horizontal distribution flow velocity at x = 10 m.

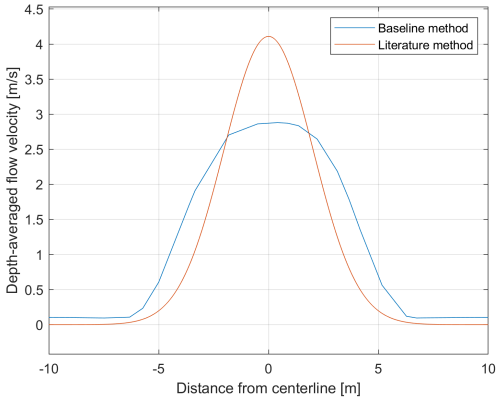

(b) Comparison horizontal distribution flow velocity at x = 25 m.

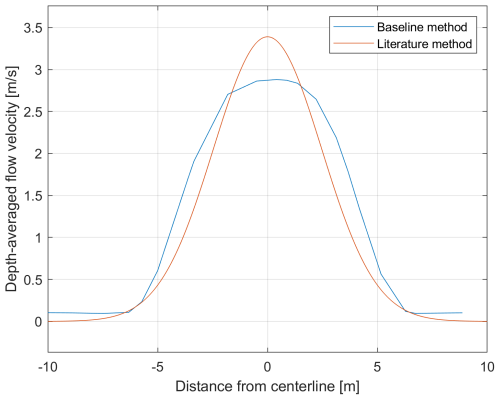

(c) Comparison horizontal distribution flow velocity at x = 50 m.

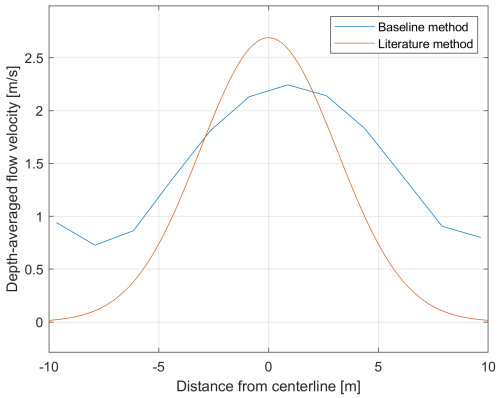

(d) Comparison horizontal distribution flow velocity at x = 80 m.

Figure 5.11: Comparison of horizontal distribution flow velocity baseline method and literature method at four different distances from the outflow opening.

The comparison at x = 10 m shows a strongly fluctuating profile for the baseline method. This is due to the fact that this location is just downstream of the pile row. The other figures show that the literature method overestimates the depth-averaged flow velocity. The reason for this is that with the method used to include the effect of the pile row, the jet appears to be less wide than it actually is. Therefore, to meet the total flow rate, the flow velocity is higher. Another striking point is that after 80 m according to the baseline method the jet deviates slightly from the center. This is potentially due to the Coanda effect. This effect cannot be included in the literature method and therefore not visible.

Vertically speaking, it is assumed that the pile row has no influence on the jet, as can be seen in Fig. 5.9. The jet widening in the vertical sense continues with the same ratio as before the pile row. However, when the jet reaches the water surface, 25.28 m after the outflow opening, the vertical distribution of the flow velocity is assumed to have a standard logarithmic profile. The formulas describing a logarithmic flow profile assume an equilibrium between the bottom shear stress and the flow velocity. However, there is no equilibrium in the considered case as the flow is largely dominated by the jet. Therefore the earlier described formulas cannot be used. The profile is approximated by the use of Eq. (5.5) (Battjes, 2002):

$$u(z) = u_{max} \cdot (z/h)^{1/3} \tag{5.5}$$

in which,

z = distance from the bottom [m]
h = total water depth [m], 3.16

The vertical distribution of the horizontal flow velocity is determined for three different distances from the outflow opening, respectively 25, 50 and 80 m. For the three distances the distribution is determined for the center of the jet. The depth-averaged flow velocity is known for these locations and follows from Fig. 5.11. For each location, u_{max} is chosen such that the average flow velocity equals the value that follows from Fig. 5.11. In this way the following figures are obtained, showing the vertical distribution of the horizontal flow velocity at the center of the model at three different distances:

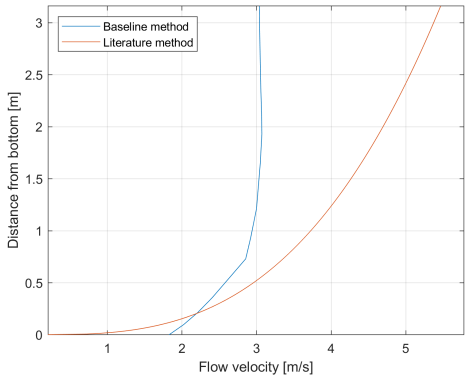

(a) Comparison vertical distribution at x = 25 m.

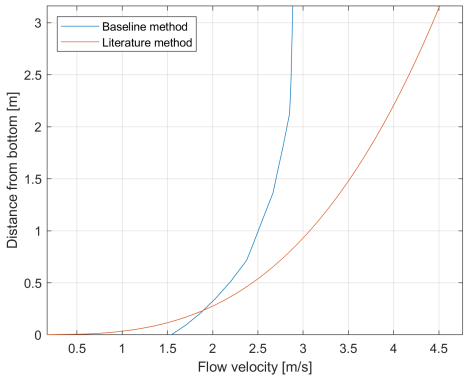

(b) Comparison vertical distribution at x = 50 m.

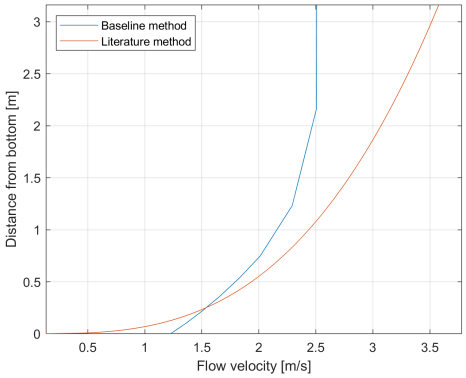

(c) Comparison vertical distribution at x = 80 m.

Figure 5.12: Comparison of vertical distribution flow velocity baseline method and the literature method at three different distances from the outflow opening.

As expected, at each distance from the outflow opening the literature method again overestimates the horizontal flow velocities compared to the velocities that follow from the baseline method.

5.4. Discussion and conclusion comparison of methods

This section provides a discussion and conclusion on the results that follow from the comparison between the results obtained with the baseline method and the methods COMSOL-D3D and D3D. Furthermore, the results obtained with a method that uses formulas and coefficients from literature are discussed.

5.4.1. Baseline method

Due to a lack of measurement data, no validation of the results is possible. Therefore a baseline method is adopted to compare the results of the considered methods with. The results following from the baseline method are assumed to be the closest to the truth, since in this method the complete three-dimensional flow field is simulated in COMSOL.

The results show that at a certain distance from the outflow opening the baseline method predicts a completely different direction of the jet than in method D3D. The deflection visible in the results of method D3D may be assigned to the so-called Coanda effect (see Section 2.5). The fact that this effect can be seen in method D3D and not in the baseline method is potentially because the model domain in this method is many times longer than in the baseline method. This is based on theory, but cannot be proven numerically as validation data is lacking. Due to a greater model length the deflection of the jet is stronger. If the COMSOL model domain in the baseline method was longer, this effect may also be visible. More details on this can be found in Section 8.3. As a result, in the comparison between the results of each method and those of the baseline method, only the magnitudes of the flow velocities are considered and not the direction of the jet.

It can be said with more certainty that the flow pattern in the direct vicinity of the discharge sluice where the flow is highly three-dimensional can be simulated well with the baseline method. The flow through the construction and around the piles is simulated with great detail as the complete three-dimensional flow field is taken into account. In this area the potential Coanda effect does not yet play a role.

5.4.2. Method COMSOL - D3D vs. baseline

Applying method COMSOL-D3D method requires less computational time than the baseline method, since a significantly smaller part needs to be simulated in the detailed model. There are also differences in the results. In Section 5.1 it is shown that method COMSOL - D3D gives a different flow pattern than computed with the baseline method. The magnitude of the flow velocities does not fully correspond. Using method COMSOL - D3D gives an underestimation of the flow velocities along the centerline, up to a maximum difference of nearly 30% at 40 m downstream of the coupling plane. An overestimation of the flow velocities at the sides of the jet is visible. Apparently the coupling between the models is not working properly. This is due to the following reasons:

- In a horizontal sense, after coupling, D3D redistributes the flow rate itself. It is not exactly clear why D3D does this. The program does not seem to handle the way the flow rates are imposed. Because of this different flow velocities arise in the first cells after the source terms than imposed. If, for example, the two outermost cells of the coupling plane are considered (see Fig. 5.13), an overestimation of the flow velocities can be seen in the first cells downstream of the coupling compared to what is imposed. The redistribution by D3D thus leads to an underestimation of the velocities in the middle and an overestimation at the outer sides.
- Also a vertical flow velocity is seen in the first cell after coupling (Fig. 5.14) which does not match what is seen in the baseline method.

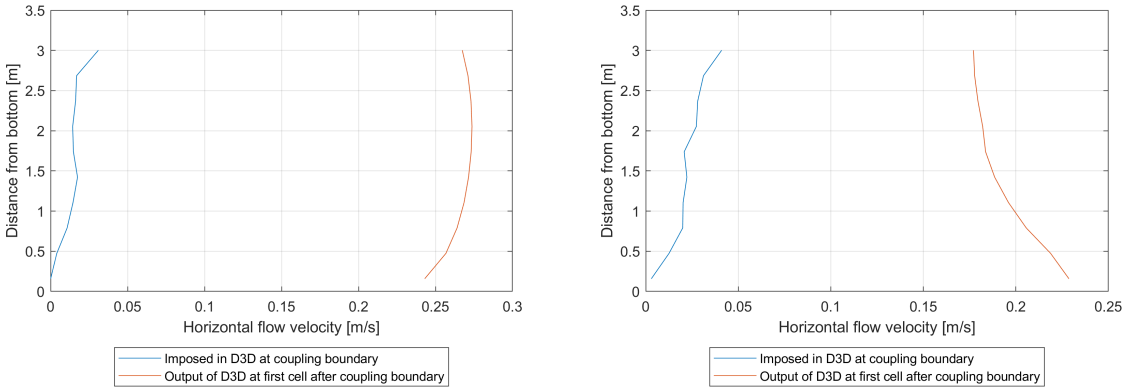

(a) Vertical distribution horizontal flow velocity at first cell after coupling, right side of the jet, seen from the outflow opening.

(b) Vertical distribution horizontal flow velocity at first cell after coupling, left side of the jet, seen from the outflow opening.

Figure 5.13: Horizontal flow velocity distribution at first cell after coupling, sides of the jet.

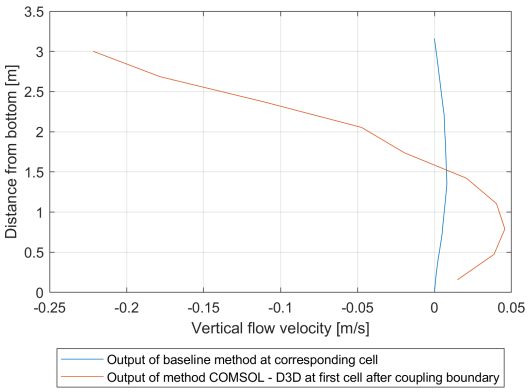

Figure 5.14: Vertical distribution vertical flow velocity at first cell after coupling, centerline jet.

5.4.3. Method D3D vs. baseline

Method D3D requires very little computational time compared to the baseline method because only a coarse model is used. In terms of results, the two methods are not far from each other. Method D3D produces a flow pattern, in terms of flow magnitude, that is significantly closer to that of the baseline method than method COMSOL-D3D. The reason for this is that the thin dams ensure that the jet is introduced gradually into the model and consequently there is no incorrect redistribution of the flow rates. Moreover, the discharge coefficient μ that is determined in an empirical way and used in this method almost matches the μ from the baseline method, respectively 0.79 and 0.74. This ensures that the imposed discharge is almost equal in both methods. As already mentioned, the big difference in the results is the fact that the jet in method D3D deviates strongly to the northern quay, while this effect is hardly visible in the results of the baseline method. However, this effect is not taken into account in the comparison of the results.

In both methods, method COMSOL - D3D and method D3D, it can be seen that the power of the jet decreases faster in the D3D domain than in the COMSOL domain. This is because different equations are solved in the models and turbulence is taken into account in a different way.

5.4.4. Method formulas from literature

It turns out to be very difficult to accurately predict flow pattern downstream of two culverts and a pile row. In literature a number of formulas are found that deal with the downstream development of jet

flow velocities. However, little is said about the effect of a pile row and the presence of two culverts. In this study an attempt was made to make an estimate of the flow pattern using modified existing jet formulas and rules of thumb. The calculated flow velocities downstream of the pile row appeared to much higher than those computed with the baseline method. This is due to the fact that in this method the calculated width of the jet in the center was smaller than that in the baseline method. On the other hand, it is expected that the flow velocities in the culverts themselves can be well calculated using formulas from the literature, since many formulas regarding a pipe flow can be found in literature.

5.4.5. Conclusion

Two methods and a literature method are applied in this chapter to determine the flow pattern for a simplified case in which a sluice discharges into a rectangular water body, with a fixed water level and without density differences being present. The results of each method are compared to the results obtained with a baseline method. As expected, the literature method is not applicable in the case of predicting the flow pattern downstream of a discharge sluice that includes a pile row and two culverts. It would have been different if the geometry of the discharge sluice was simpler.

In the figures below, the cross-sectional horizontal distributions of the flow rates of the baseline method and methods COMSOL-D3D and D3D at three different distances from the outflow opening are plotted in the same figures. It can be concluded that method COMSOL - D3D gives an underestimation of the flow velocities compared to the results of the baseline method. This is because in the way the coupling is done, the flow rates are wrongly distributed over the width. An improvement of this coupling is found (see Section 8.5).

Method D3D presents comparable results as obtained with the baseline method. There is only a big difference in the direction of the jet. However, it is decided to not compare the results on the basis of the direction as it is unclear which direction is correct. It is decided in this study to continue with method D3D, due to the fact that the results of method D3D are closer to those of the baseline method in terms of velocity magnitude in this case. Moreover, this method is easier and faster to use.

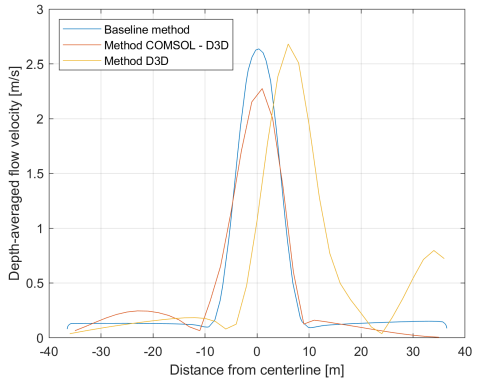

(a) Comparison horizontal distribution flow velocity at x = 43 m.

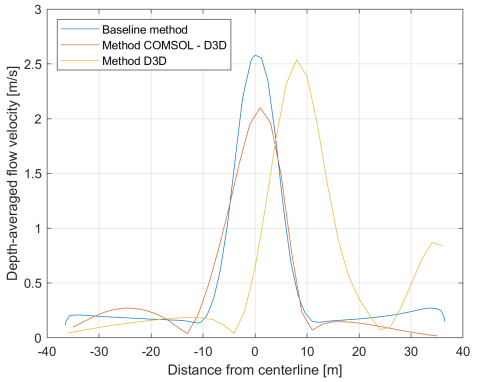

(b) Comparison horizontal distribution flow velocity at x = 50 m.

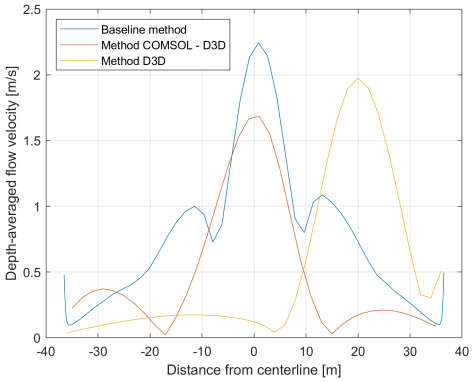

(c) Comparison horizontal distribution flow velocity at x = 80 m.

Figure 5.15: Comparison of horizontal distribution flow velocity at three different distances from outflow opening, method COMSOL-D3D, method D3D and baseline method.

6

Model set-up, Ostend model

This chapter elaborates on how the chosen method, method D3D, is applied to situation in the port of Ostend. First it is explained how the model of the port of Ostend is obtained (Section 6.1) and then how method D3D is applied (Section 6.2).

6.1. Port of Ostend model

The model that is used is a Delft3D-FLOW 4 model. The domain consists of the entire port of Ostend and a part of the north sea. A tide-varying water level and density differences are taken into account. The model is largely based on an already existing model of HIC (2021). How the model in this research is obtained and how the boundary conditions are determined is discussed below.

In 2004 a numerical hydraulic model for the port of Ostend was developed by the consortium Technum - IMDC - Alkyon, commissioned by the Flemish Government. Hereinafter this model is referred to as the 'Mother model'. This model fits into the CSM - ZUNO - Coastal Strip model train of Rijkswaterstaat (Fig. 6.1) and contains a three times higher resolution than the Coastal Strip model.

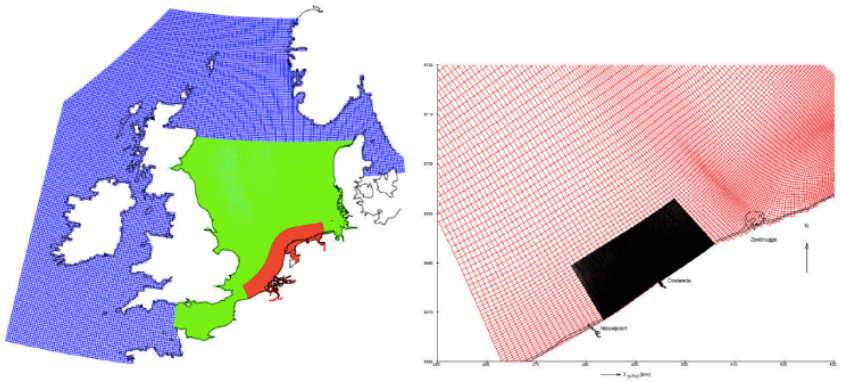

Figure 6.1: Connection of the Ostend model with the CSM - ZUNO - Coastal Strip model train. CSM: blue. ZUNO: green. Coastal Strip: red. Ostend Mother model: black. (Dujardin et al., 2017).

The boundary conditions of each model in Fig. 6.1 are obtained by using a so-called nesting method. More details on nesting can be found in the Delft3D User Manual (Deltares, 2021). The bathymetry is generated on the basis of depth data from existing models. In the Mother model local refinement was applied by the Waterbouwkundig Laboratorium (WL), resulting in the so-called Ostend 'Daughter' model. This model is nested in the Mother model (Fig. 6.2) by means of time series on the lateral and seaward boundaries. On the seaward boundary this is a Riemann time series, on the lateral boundaries a time series of the current is used. The period that is simulated extends from March 17, 2013 to April

17, 2013. This period was selected because tides in this period appear to correspond best with average spring tide, middle and neap tide (Witteveen+Bos, 2019).

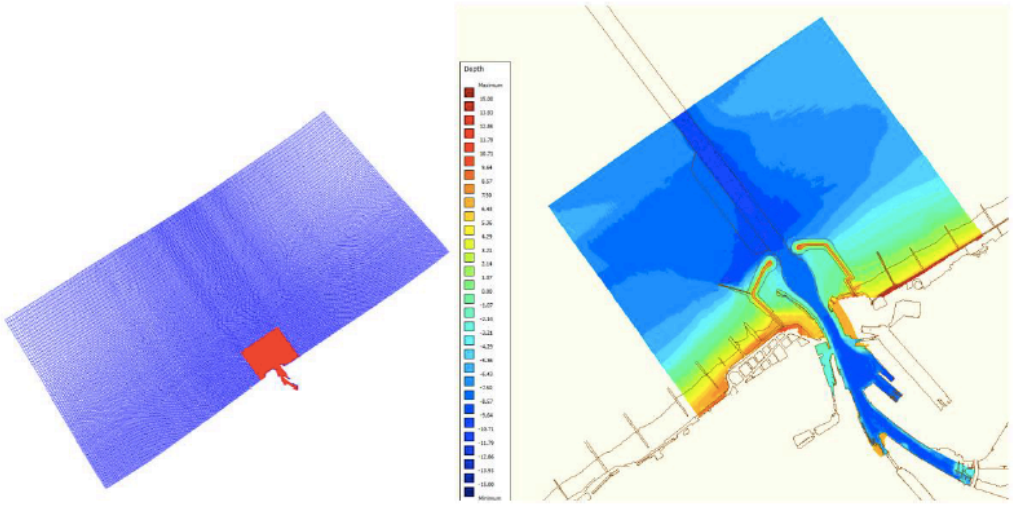

Figure 6.2: Left: Ostend Mother model (blue) and Daughter model (red). Right: Bathymetry Daughter model. (Witteveen+Bos, 2019).

Before this research was executed the Mother and Daughter model had been run with a single vertical layer and without salinity taken into account. In order to obtain representative salinity boundary conditions for the Daughter model, for this research one run with the Mother model is executed. Observation points are placed on the locations such that they correspond with the location of the boundaries of the Daughter model. In this Mother model run salinity boundary conditions derived from the Coastal Strip are imposed. After the spin-up is resolved an average salinity value of 23 PSU is found at the observation points.

Then, a local grid refinement in the area around the intended discharge sluice is done in the Daughter model, resulting in the so-called 'Granddaughter' model (Fig. 6.3). The ratio of the grid resolution between both models is 1:6. The bathymetry is obtained by triangular interpolation of the existing bathymetry data. The bathymetry in front of the discharge sluice is adapted to the bathymetry that is taken into account by Goossens and Moerkerke (2019), see (Fig. 6.4).

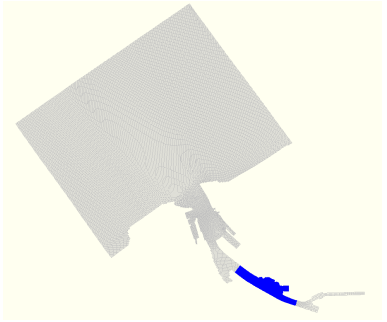

Figure 6.3: Grey: Daughter model. Blue: Granddaughter model.

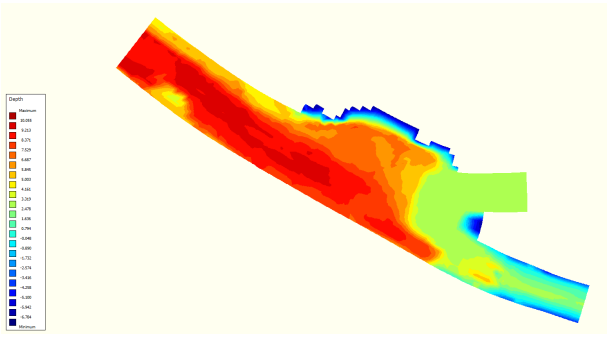

Figure 6.4: Bathymetry of the Granddaughter model.

The boundary conditions of the Granddaughter model are obtained by nesting the model into the Daughter model. A simulation with the Daughter model, using ten vertical layers and including salinity, is done using the boundary conditions during spring tide, occurring during the period April 07, 2013 - April 12, 2013, as it is expected that this would give the normative conditions for the current velocities in the marina. A run is done with an upstream discharge of 110 m^3/s from the Noordede River / Ghent-Ostend channel being present during low tide. This is the maximum discharge flow rate described by

Goossens and Moerkerke (2019). It is unclear what the exact return period of this discharge is. The imposed salinity value at the boundaries is 23 PSU, the initial water level 0.5 m and the initial salinity level 23 PSU. After the spin-up has been resolved, the boundary conditions for the Granddaughter model can be read. These conditions consist of a total discharge time series at the upstream boundary and a water level time series at the downstream boundary. A validation of why the granddaughter model can be used instead of the Daughter model is presented in Appendix D.

6.2. Applying method D3D to the Ostend case

Instead of applying the method to a simplified stationary situation, method D3D is now applied to a case in which there is a varying water level and thus a varying resulting discharge from the sluice. The set-up of this model that represents the Ostend case is presented in Fig. 6.5. Not only the water level inside the marina but also the Spuikom water level varies in time. The magnitude of the discharge follows from the difference between the Spuikom and the marina. In this research the focus is on the potential impact on the nautical activities in the marina in the port of Ostend and therefore only the flow from the Spuikom towards the marina is taken into account. This occurs when the tide-varying water level at the marina side drops below the water level at the Spuikom side. It is assumed that the discharge stops when the water level at the marina side is at its lowest point. At that time complete flushing of the Spuikom has been reached. This process takes about three hours. It is also assumed that the water level in the Spuikom decreases linearly over this period, from +3.27 m TAW to +2.97 m TAW.

First, five days, April 07, 2013 - April 12, 2013, are simulated without any application of method D3D. So this is as if there is no discharge sluice in the area present. The simulation is done to determine the water levels in the marina without outflow from the discharge sluice. To avoid spin up effects, the focus is only on the last two days, the 10th and 11th of April 2013. These two days contain four tidal cycles and thus four moments at which the water level at marina side drops below the water level at Spuikom side. The method D3D is applied in the same way as for the simplified case: with source terms attached to the bottom five cells at two locations and a porous plate, mimicking the discharge sluice. Since a sigma-layer system is used, this causes the total height of the five grid cells to vary with the water depth, from 1.58 m to 3.14 m. As a result, the total height of the grid cells does not always correspond to the real height of the culverts.

The magnitude of the imposed discharge depends on the difference between the Spuikom and marina water level and follows from the general discharge relation. The water levels in the marina are known are known from the initial simulation without the discharge sluice included. Afterwards the difference between the water level in the Spuikom and in the marina is calculated every ten minutes. By knowing the difference between water levels of the Spuikom and the marina the resulting discharge that should be imposed can be calculated every ten minutes. The total discharge is equally divided over the ten source terms. With the calculated discharges a time series is set up for each source term. The time series include the right moment in time, the imposed discharge, the flow velocity, the flow direction and a salinity rate of 20 PSU.

Two situations are simulated using the Ostend model, one with a discharge from the Noordede River / Ghent-Ostend channel taken into account during these two simulated days and one without. A situation without riverine discharge is simulated by setting the upstream total discharge boundary conditions to zero. In this way, on the one hand, it is examined how much impact the discharge sluice and maximum riverine discharge together have on the nautical activities in the marina. On the other hand, the potential impact of the discharge sluice itself is determined.

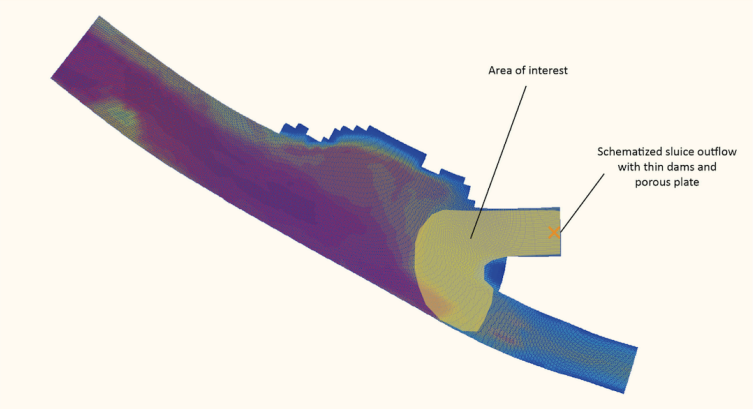

Figure 6.5: Set-up of the Ostend model.

7

Potential impact on the nautical activities in the marina

Based on the findings in Chapter 5, it is decided to use method D3D to determine the potential impact of the discharge sluice on nautical activities in the marina in the port of Ostend. In this way an illustration of the application of the method is given. First, a situation without the riverine discharge from the Noordede river / Ghent-Ostend channel is presented in Section 7.1. In this way, only the impact on nautical activities caused by the discharge sluice itself is examined. A situation with a normative discharge from the Noordede river / Ghent-Ostend channel included is examined in Section 7.2. The resulting flow patterns are examined on the basis of guidelines from Rijkswaterstaat (Rijkswaterstaat, 2020). For both situations the depth-averaged flow velocities as well as the flow velocities in the top layer, representing the top 0.316 m of the water column, are looked into.

7.1. Situation without discharge from the Noordede River / Ghent-Ostend channel

The impact on nautical activities in the marina is examined for the part of the tidal cycle at which water flows from the Spuikom to the marina. This occurs when the water level at the marina side drops below the Spuikom water level. According to the guidelines (Rijkswaterstaat, 2020), the cross flow velocity may not exceed 0.3 m/s for small vessels. In Fig. 7.1 the area at which the depth-averaged flow velocity is higher than this value is indicated for three different time steps: 15, 90 and 180 minutes. The corresponding water levels in the marina are visible in the attached graph. The number of minutes indicates the time that has elapsed after the water level in the marina drops below the level of the Spuikom (dashed black line). The existing pontoon structures are indicated in grey.

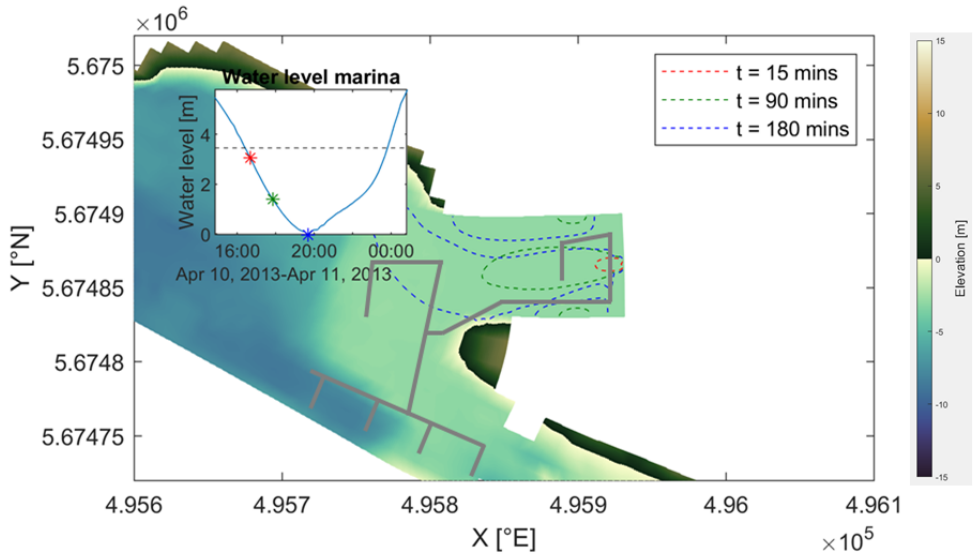

Figure 7.1: The impact on the marina in the port of Ostend, depth-averaged, 0.3 m/s contour lines, without riverine discharge.

It can be seen that 90 minutes after the start of the outflow, a large part of the northern side of the marina is in the area with a depth-averaged flow velocity greater than 0.3 m/s. After 180 minutes the entire northern side of the marina is in this area. According to the guidelines (Rijkswaterstaat, 2020), the cross-sectional flow in this area is then too strong to perform manoeuvres.

Since the flow velocity is not equal in the entire vertical column, it is useful to look at the flow velocity at specific layers. For the vessels entering this marina, with an average draft of half a meter, the flow velocity in the upper layers has more impact than that in the lower layers. This is also mentioned by van der Hout (2011) in his research to stratified flow fields. A similar image is therefore made as Fig. 7.1 but with only the flow velocities in the top layer taken into account, representing the top 0.316 m of the water column. Again the area with a flow velocity greater than 0.3 m/s is indicated with contour lines for three time steps.

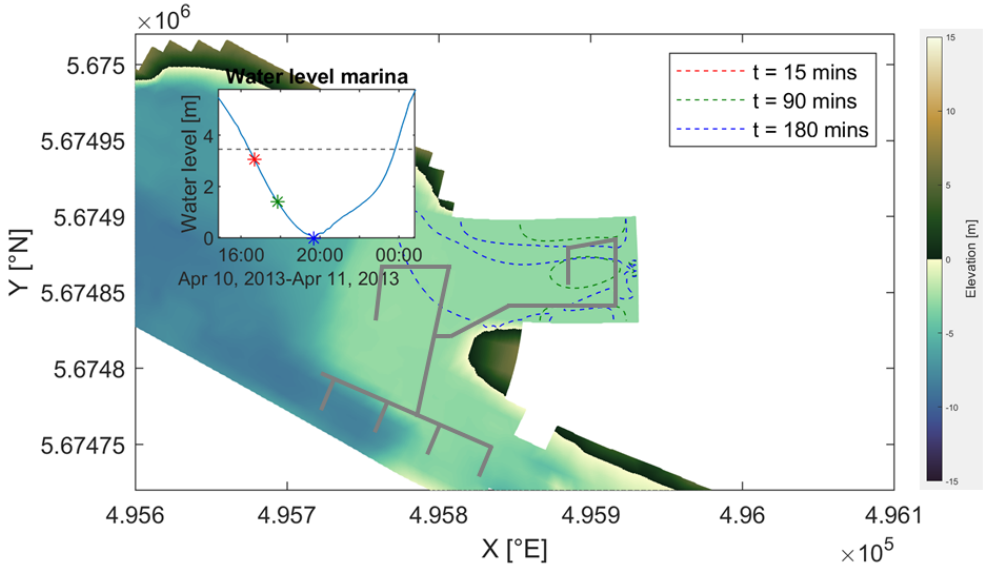

Figure 7.2: The impact on the marina in the port of Ostend, top layer, 0.3 m/s contour lines, without riverine discharge.

A similar flow pattern as in Fig. 7.1 can be seen in Fig. 7.2. The difference is that after 90 minutes a smaller part of the marina is covered by the area with a flow velocity greater than 0.3 m/s. This figure again shows that the sluice outflow has a major impact on the flow velocities in the marina and that it potentially causes hindrance to incoming and outgoing vessels.

The guidelines also refer to a maximum permitted flow velocity in the longitudinal direction, namely 0.8 m/s. An image, Fig. 7.3, is therefore made with the area that contains a flow velocity greater than 0.8 m/s indicated by contour lines.

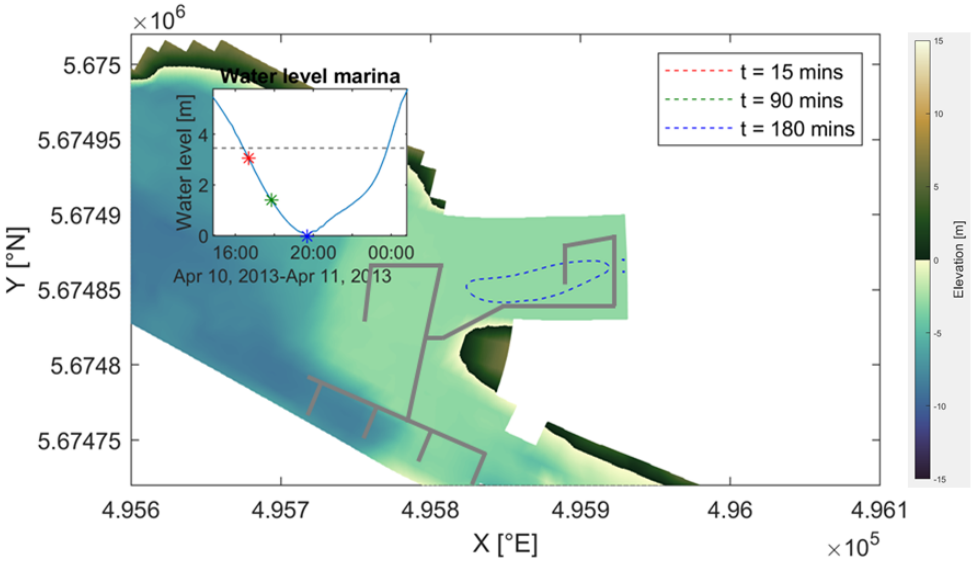

Figure 7.3: The impact on the marina in the port of Ostend, top layer, 0.8 m/s contour lines, without riverine discharge.

As expected, the area with a flow velocity greater than 0.8 m/s is smaller than the area with a flow velocity greater than 0.3 m/s. It can be seen in Fig. 7.3 that after 180 minutes a small part of the marina is covered by the area with a flow velocity greater than 0.8 m/s. Since this area is not yet visible after 90 minutes, it can be expected that this area will start to form somewhere between 90 and 180 minutes after the start of the outflow.

7.2. Situation with discharge from the Noordede River / Ghent-Ostend channel

The same images as in Section 7.1 are made for a situation with a maximum riverine discharge from the Noordede river included. According to Goossens and Moerkerke (2019), this discharge is 110 m^3/s. It is unknown what the return period of this maximum discharge is.

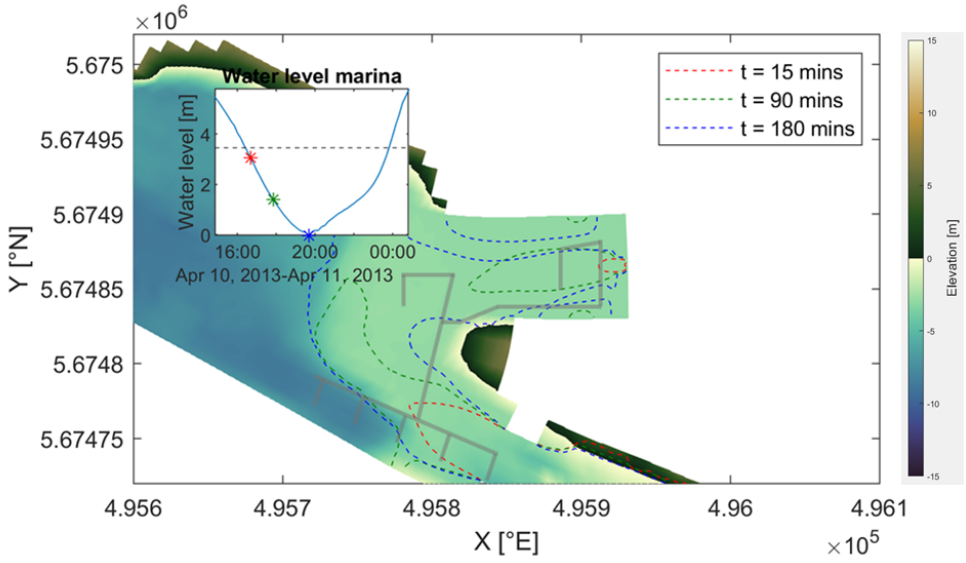

Figure 7.4: The impact on the marina in the port of Ostend, depth-averaged, 0.3 m/s contour lines, with riverine discharge.

The southern part of the marina (bottom part) is particularly affected by the outflow from the Noordede river. It can be seen in Fig. 7.4 that at the considered riverine flow rate already at the first time step a small part of the marina is covered by the area with a depth-averaged flow velocity greater than 0.3 m/s. After 90 minutes almost the entire southern part of the marina is covered by the area with a depth-averaged flow velocity greater than 0.3 m/s. The northern part of the marina (top) is mostly affected by the outflow of the discharge sluice. Just as in Fig. 7.1, it can be seen that already 15 minutes after the moment the water level at the marina side drops below the Spuikom level, the right-most part of the marina is starting to experience hindrance from the discharge sluice. The area with a depth-averaged flow velocity greater than 0.3 m/s grows in time and after 180 minutes it covers the entire marina.

Next, an image is shown with only the flow velocities in the top layer and contour lines that indicate the area with a flow velocity greater than 0.3 m/s. This image is again a result of the situation in which a maximum riverine discharge is taken into account.

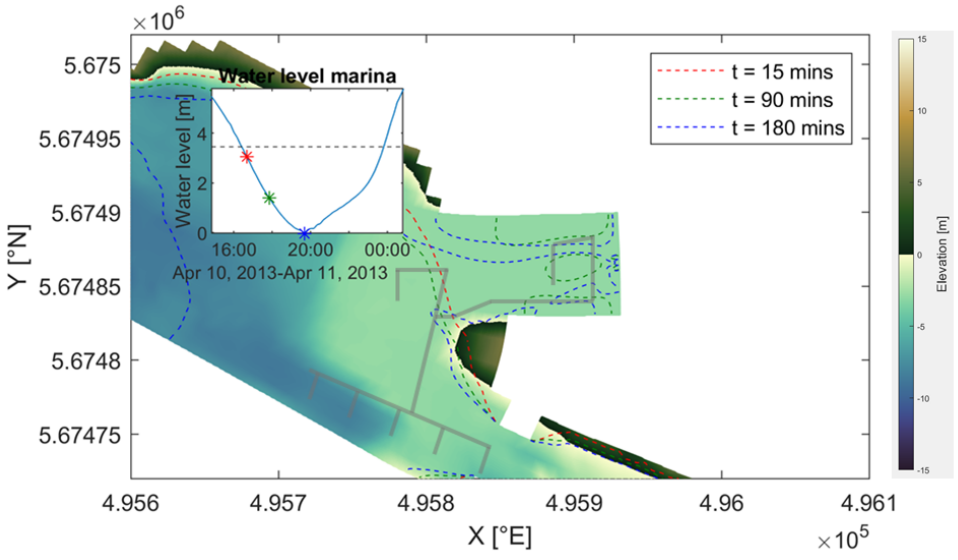

Figure 7.5: The impact on the marina in the port of Ostend, top layer, 0.3 m/s contour lines, with riverine discharge.

From Fig. 7.5 it follows that the size of the area in which the flow velocity in the top layer is greater than 0.3 m/s is largely dominated by the riverine discharge from the Noordede river / Ghent-Ostend channel. At the moment that the water level of the marina drops below that of the Spuikom, a large part of the area consists of a top layer with a flow velocity greater than 0.3 m/s. Only the part into which the sluice discharges contains a lower velocity at that moment. This quickly changes as the water level in the marina drops further. After 90 minutes, also the top layer of 75% of the northern part of the marina contains a flow velocity greater than 0.3 m/s. After 180 minutes, the entire marina contains a velocity greater than 0.3 m/s in the top layer.

The same image is made with 0.8 m/s contour lines.

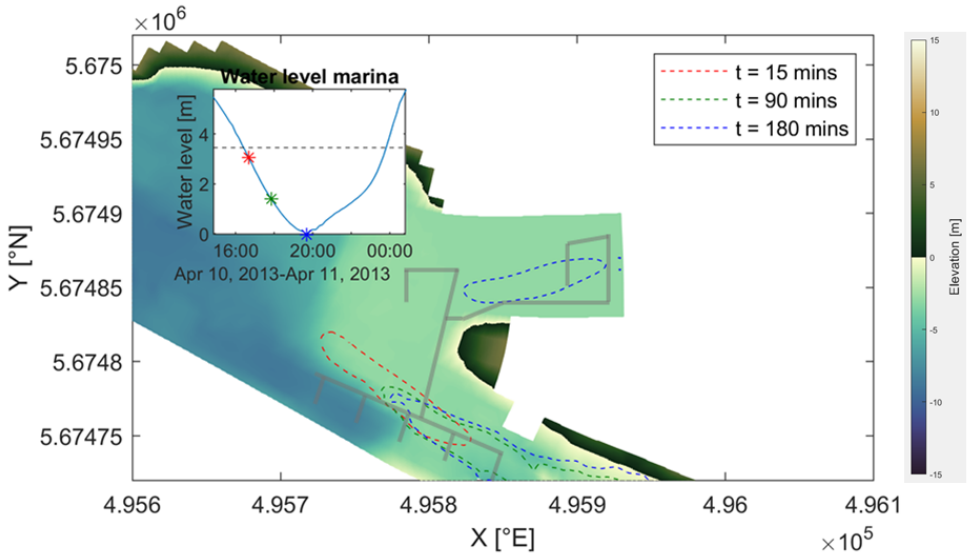

Figure 7.6: The impact on the marina in the port of Ostend, top layer, 0.8 m/s contour lines, with riverine discharge.

In Fig. 7.6, again it can be seen that the influence of the discharge sluice itself is only visible at the 180-minute time step. The southern part of the marina is mostly affected by the outflow from the Noordede river / Ghent-Ostend channel. It is striking that the riverine discharge already causes an exceedance of 0.8 m/s in a large part of the port at the first time step. Strangely enough this area is smaller during the last two time steps. This can be explained by the fact that the river outflow initially has greater flow velocities at the top of the water column but the depth-averaged flow velocity at this first step is lower than at the last two steps.

7.3. Conclusion

From the images in which no riverine discharge is taken into account it can be concluded that the outflow of discharge sluice itself potentially causes hindrance to nautical activities in the marina. This only concerns the northern part of the marina. Considering the situation in which the riverine discharge is added it becomes clear that the southern side of the marina is completely dominated by current velocities caused by this riverine discharge. The guidelines regarding maximum allowed flow velocities are also exceeded here. It must be noted that only extreme conditions are considered and that these conditions occur not very often. Based on the examined flow patterns in this chapter, it will have to be considered in further research whether the marina needs to be moved or whether mitigating measures can be applied to reduce the flow rates.

8

Discussion

This chapter provides a discussion on the results obtained after applying method D3D to the Ostend case (Section 8.1), discusses inaccuracies of the baseline method in Section 8.2, reflects on three important findings from this study (Section 8.3, Section 8.4 & Section 8.5) and presents the limitations of method COMSOL-D3D and method D3D (Section 8.6). The results following from the comparison between the considered methods and the baseline method after application to a simplified case are already discussed in Section 5.4.

8.1. Discussion results Ostend model

In this study it was decided, as an illustration of the method, to apply method D3D to the Ostend case, in which also a varying water level and density differences were included. It is expected that the obtained flow patterns do not fully correspond to reality. This has a few reasons:

- The existing D3D model that was used in this work, developed by Waterbouwkundig Laboratorium, gives the correct water level values at low water but overestimates the water levels at high water. The model gives high water level values of more than +6 m TAW, while in reality it is about +4.7 m TAW. As a result, the difference between high and low water is greater. Because the duration of the tide remains the same, the graph of the water level trend is steeper. As a result, the duration from the moment that the water level drops below that of the Spuikom to the lowest water level moment is shorter. Since in this study it was assumed that discharge takes place until the lowest water level, this duration is therefore shorter.
- In this model it was assumed that water is only discharged from the Spuikom into the marina and not the other way around. The discharge of water from the marina into the Spuikom takes place during high water in the marina and would cause a suction towards the discharge sluice. This effect was not examined in the present study.
- The effect of wind and waves was not taken into account in this model. Although these two factors are expected to have little influence, they can be added to the model in future studies.
- The potential interaction between the flow and pontoon structures and moored vessels was also not taken into account in this model. It may be that these are positioned so that they block the resulting jet and therefore have a significant influence on the resulting flow pattern in the entire marina. In further studies this potential effect should be taken into account.

8.2. Inaccuracies baseline method

In this study no measurement data of the flow velocities or water levels in the port of Ostend was available. Consequently the results obtained with method COMSOL-D3D and method D3D could not be validated using real data. Therefore the methods have been applied to a simplified case and a baseline method was adopted to compare the results with. It was assumed that the flow patterns obtained with this baseline method are very close to the flow patterns that would occur in reality. This assumption is valid since in the baseline method the complete three-dimensional flow field is simulated.

During this study, however, it has become clear that the results obtained with this baseline method are likely to be less accurate than expected. This has a few reasons.

Firstly, for the COMSOL modelling it was assumed that the flow through the discharge sluice has a subcritical character in both the culverts and the outflow area. In this way no hydraulic jump can occur. Because in this case the culverts are always submerged, it can be said with certainty that a hydraulic jump will never arise in the culverts themselves. However, for the downstream water body there is uncertainty about this. A hydraulic jump could occur in the outflow area of the discharge sluice. This depends on the amount of discharge flowing through the culverts and the downstream water level condition. Further research should be done to find out if a hydraulic jump would occur in the case of high discharges. If so, the COMSOL simulation would not be valid anymore due to its rigid-lid approximation and the fact that only one phase is modelled. Instead, two-phase modelling should be applied in that case.

Secondly, in the COMSOL model a rigid-lid approximation was adopted. There are two conditions that dictate when this approximation can be used. The Froude number should be lower than 0.3 and the surface deformations should not exceed 10% of the water depth. During the discharge process by the sluice, the flow velocities in the area between the outflow opening and the pile row are between 4 and 5 m/s. This means that, according to the first condition, the rigid-lid approach could not be used here. The rigid-lid suppresses the actual deformations and introduces an error in the continuity equation, leading to overestimations or underestimations of the bulk velocity in the zones where the rigid-lid is, respectively, lower or higher than the real water level (Ramos et al., 2019).

The fact that the water is pushed up against the pile row is also not taken into account by the rigid-lid approach. In this way the second condition is not met. This also causes an error in the continuity equation. In the region downstream of the pile row, the flow velocities are lower and, according to the literature, a rigid-lid approach could be used here. The question is how much influence the errors generated in the first meters have on the final parameters that were read from COMSOL at a distance of 40 m and further from the outflow opening. In this study it was assumed that this influence is negligible. A two-phase model should be drawn up in a subsequent study to see how much the results would differ.

A third inaccuracy of the baseline method, the fact that the physics that causes the Coanda effect is potentially not correctly simulated, is discussed in Section 8.3.

In conclusion, the flow pattern obtained with the baseline method most likely deviates slightly from reality. However, a comparison between this method and methods COMSOL-D3D and D3D on the magnitude and the vertical distribution of the flow velocities is still valid since of all methods in this study the results of the baseline method are expected to be the most accurate.

8.3. Coanda effect

From the comparison between the flow pattern obtained with the baseline method and method D3D it has become clear that there is a large difference in the jet direction. This may be due to the presence of the so-called Coanda effect, elaborated on in Section 2.5. This effect is more visible in the flow pattern of method D3D because the model domain is many times longer than that of the baseline method. This assumption is based on theory but cannot be proven using the numerical model as validation data is missing. From this observation it can be concluded that if the physics causing the Coanda effect is to be simulated correctly, the length of the model in the baseline method should be longer. In this study, therefore, the direction of the jet was not taken into account in the comparison of the methods.

It is unclear what the exact model length should be to correctly simulate the physics with the baseline method. In addition to a model that is long enough also the geometry should correspond exactly to reality. Even a small asymmetry in the geometry can cause the jet to deflect left or right.

Also for the COMSOL part of method COMSOL-D3D the physics that causes the Coanda effect must be simulated correctly. However, this method is based on a COMSOL model that is as small as possible, so that little computational time is required. It is therefore undesirable to make the COMSOL model so long that the physics is simulated correctly. Instead, it is advised to make the coupling between the two models in the area before the point where the jet starts to deviate from the center but downstream of the area in which three-dimensional flows caused by the pile row are present. In this study this is at a distance of about 10-15 m downstream of the pile row. In this way the coupling is already made before the Coanda effect starts to play a role in the direction of the jet.

8.4. Discharge coefficient

The discharge coefficient μ is an important parameter that has a large influence on the amount of water that flows through a discharge sluice. It gives information about the resistance of the entire system and is directly linked to the total energy loss that occurs in the system. In the methods that are examined in this study this coefficient was determined in two ways. In the baseline method and in method COMSOL-D3D the discharge coefficient was determined using the resulting pressure difference from a test run in COMSOL. A value of 0.74 was found. In method D3D and the literature method the discharge coefficient was calculated with formulas from literature. A value of 0.79 was found.

In the calculation of the coefficient using formulas from literature, no energy losses due to the pile row were assumed. This assumption appeared to be not completely valid as COMSOL simulations showed that the pile row actually has a contribution of 0.1 to the total loss coefficient. A COMSOL simulation with and without a pile row was done to demonstrate this. The fact that the pile row has relatively little influence on the total loss coefficient and thus on the discharge capacity of the system is because the flow area between the piles is larger than the flow area of the culverts. The flow therefore experiences no great resistance from the pile row, but is only spread over a greater width. The pile row can thus be regarded as a diffuser rather than an energy reducer. This diffusing property of the pile row was simulated in method D3D with a porous plate and in the literature method with the assumption that the flow is spread over the entire pile row width.

There is a small difference between the calculated discharge coefficients (0.74 vs. 0.79). This can be explained by the fact that the formulas used for the empirically/analytically determined μ are based on specific experiments. The boundary conditions of these specific experiments most likely deviate from the boundary conditions in the COMSOL model. Moreover, no contribution from the pile row to the total loss coefficient was taken into account, while this does affect the loss coefficient. A difference between the analytically/empirically determined discharge coefficient and the value obtained with COMSOL can therefore be expected.

8.5. Improvement coupling COMSOL-D3D

After it turned out that the coupling between COMSOL and D3D did not work in the way it was done, a number of ways were tried to make the coupling still work:

1. It was checked whether it works better if a full logarithmic profile is imposed. The idea is that the shallow water equations in D3D can handle this better since no vertical corrections have to be made to arrive at a perfect flow profile. It appeared that also here a horizontal redistribution of the flow rates takes place in the first cells after coupling.
2. Afterwards a refinement of the grid was tried. The width of the cells in these simulations was 1 m instead of 2 m. This also turned out to not have a positive effect on the coupling.
3. Finally, it was tried in D3D to prevent the horizontal redistribution. This method consisted of applying thin dams on both sides of the cells with the source terms in the D3D model, in the longitudinal direction of the jet with a length of two grid cells. The set-up can be seen in Fig. 8.1. The idea behind this is that the flow is 'guided' for a longer distance and therefore it is introduced

more gradually. This turned out to largely prevent an incorrect horizontal redistribution and thus to have a positive effect on the coupling. The results using method COMSOL - D3D combined with these thin dams are shown in Appendix E. At location 1, 43 m from outflow opening, the difference in flow velocity between this method and the baseline method is maximum 6% (for comparison: 14.5% with the initial method), maximum 9% at location 2, 50 m from the outflow opening (23.5% with initial method), and maximum 13 % at location 3, 80 m from the outflow opening (29.5% with initial method).

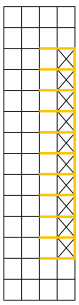

Figure 8.1: Set-up method COMSOL - D3D with extra thin dams (yellow), grid cells with source terms are indicated with a cross.

8.6. Limitations methods COMSOL-D3D and D3D

In this section the main limitations of methods COMSOL-D3D and D3D are summed up.

8.6.1. Limitations method COMSOL - D3D

- The limitations for the baseline method, described in Section 8.2, also apply to the COMSOL part of method COMSOL - D3D.
- The outflow boundary must consist of a single jet that flows out of the model, in order to ensure a good coupling between the COMSOL results and the D3D model. In the remaining part of the outflow boundary, water should flow back into the model, also known as the return currents. If, for example due to the pile row, the jet is split into several small jets, it is very hard to apply method COMSOL - D3D. In that case source terms would have to be placed across the entire width of the cross section to include all jets. Simulating the return current using sink terms then becomes complicated. In the case of multiple jets on the outflow boundary, it is therefore advised to impose the entire flow velocity boundary from COMSOL in D3D.
- The coupling between COMSOL and D3D is established by extracting the flow rates per corresponding cell from COMSOL and imposing them as a source term in D3D. In D3D only a magnitude and a direction can be assigned to the source terms. This means that turbulence effects cannot be transferred via the coupling. Details about this are therefore lost and in this way the coupling is limited.
- In this study it was assumed that the direction of the jet is perpendicular to the outflow plane of the model. Consequently the imposed direction for the source terms in D3D is exactly 90 degrees. However, it is expected that this is not always exactly perpendicular and therefore it can be seen as a limitation of this method.

8.6.2. Limitations method D3D

- A porous plate with a loss coefficient was added to the D3D model, in order to mimick the effects of a pile row in D3D. This simplification simulated the diffusing and energy reducing effect of the pile row. In this research it worked to use a formula that is intended for bridge piers to determine the loss coefficient for the porous plate but it is questionable whether this works for all types of pile rows.
- In this method source terms were attached to the bottom five grid cells at two locations that correspond to the culverts' openings. Due to the fact that in this research for the D3D model a sigma-grid system was used and the water level varies in time, the height of the grid cells also varies. This also varies the height of the grid cells out of which water flows. For the part considered in this research this height varies between 0.316 (at low water) and 0.637 m (at the moment the marina water level drops below the Spuikom water level). The height of a cell influences the outflow surface and thus the outflow velocity. The culvert height is in fact 2.5 m. This means that at the beginning of the considered part of the tidal cycle the total grid cell height is larger than the actual height of the culvert, 3.2 m. This results in an underestimation of the flow velocities. As the water level drops, the total height of the five grid cells drops until it is 1.58 m at its lowest point. This height is lower than the actual height of the culvert opening. This results in an overestimation of the flow velocities. In subsequent studies a z-grid should be applied to ensure the same grid cell height over time.

9

Conclusions and recommendations

This chapter presents the main conclusions of this work in Section 9.1, and gives recommendations for further research in Section 9.2.

9.1. Conclusions

The main conclusions of this research are discussed on the basis of answers to the research questions that are presented in Chapter 1. First, the sub research questions are answered. This is followed by an answer to the main research question.

- **How can a combination of a COMSOL and a D3D model be used to simulate the flow field and what does the coupling between the two models look like?**

  From this study it has become clear that there is much potential in using a combination of a COMSOL and a D3D model to determine the flow pattern downstream of a discharge sluice. The coupling was established by reading the flow rates from a specific cross-sectional plane in the COMSOL output and imposing them on corresponding cells in D3D. These flow rates were imposed by means of source terms and the return current was mimicked by adding so-called sink terms to the grid cells that correspond to the sides of the jet.

- **How can a D3D model with the sluice outflow being schematized by the general discharge relation be used to simulate the flow field?**

  In this study also the possibility was examined to determine the downstream flow pattern with a D3D model in which the sluice outflow was schematized by the general discharge relation. The flow rate, based on the discharge relation, was imposed using ten source terms at the corresponding locations of the culverts' openings. The discharge coefficient in this discharge relation was determined by using formulas from literature. A so-called porous plate was included to simulate the effect of the pile row. This has worked successfully in this study, but future research will have to show whether this applies to all types of pile rows.

- **How does the accuracy of the results obtained with both methods compare to the results obtained with the detailed numerical model COMSOL?**

  For a simplified case, the flow fields resulting from methods COMSOL-D3D and D3D were compared to the flow field resulting from a so-called baseline method. The domain in the simplified case is small enough so that the baseline method was applicable. Moreover, it considered stationary conditions. Applying the methods to a simplified case allowed a comparison between the accuracy of the results.

In the way the coupling was done in this research, method COMSOL - D3D showed an underestimation of the flow velocities at the centerline of the jet compared to the baseline method. This is due to the fact that D3D incorrectly redistributes the flow rates itself in a horizontal sense after the flow rates have been imposed. It resulted in an underestimation of the flow rates along the centerline of the jet, while an overestimation on the sides was visible. Also a vertical flow in the first cells after coupling could be seen in the results of this method that did not correspond to what was seen in the results of the baseline method. It was found that by adding thin dams to the sides of the grid cells with the source terms, the flow rate can be brought into the model more gradually. This has led to results that have a better correspondence with the results obtained with the baseline method. The maximum difference in flow velocity over the vertical at a distance of 3 m after coupling was 6%. At a distance of 40 m after coupling this maximum difference was 13%.

The method in which the sluice outflow was schematized by using the general discharge relation, method D3D, showed jet velocity magnitudes that have a large correspondence with the results from the baseline method. At a distance of 43 and 50 m from the outflow opening the difference in horizontal flow velocity was on average 1-2%. The average difference at a distance of 80 m was 8.5%. The analytically/empirically determined discharge coefficient μ corresponded well to the μ found in the COMSOL simulation (0.79 vs. 0.74). This is in large part an explanation of why the results of method D3D and the baseline method are so close to each other. It is expected that this is the case when the μ is easy to calculate with formulas from literature. For more complex geometries, including irregularities inside the culverts and in/outflow roundings, it is expected that a COMSOL model should be set up to determine the discharge coefficient μ.

In short, method COMSOL - D3D showed a flow pattern that contained large differences compared to the one obtained with the baseline method. This is due to the fact that the coupling between the models did not function. However, there is a lot of potential in this method and there is a way to make this coupling better. If thin dams are added to the sides of the grid cells where the source terms are located, the discharge is imposed into the D3D model in a more gradual way. This turned out to largely prevent an incorrect horizontal redistribution and thus to have a positive effect on the coupling. More details on this improvement can be found in Section 8.5.

The results obtained with method D3D, in terms of velocity magnitudes, appeared to be much closer to the results of the baseline method. This is largely due to the fact that the analytically/empirically determined μ corresponds to the μ from COMSOL and that the thin dams prevent an incorrect redistribution of the flow rates. This changes when the geometry becomes more complex. As a result, the μ would become difficult to determine analytically/empirically.

- **Which of the examined methods is most suitable to determine the impact of a discharge sluice on nautical activities in the marina of Ostend?**

  This research showed that of the examined methods, method D3D provided in this case results that have the greatest correspondence with those from the baseline method. In addition, method D3D required the least computational time. Therefore, method D3D was used in the research into the impact of a discharge sluice on nautical activities in the marina in the port of Ostend.

- **What impact does the planned discharge sluice in the port of Ostend have on nautical activities in the neighbouring marina?**

  The impact of the discharge sluice on the marina in the port of Ostend was determined using method D3D. It turned out that the outflow from the discharge sluice causes hindrance to the neighbouring marina. Considering an 0.3 m/s limit, 90 minutes after the flow from the discharge sluice has started, half of the northern part of the marina is unnavigable. After 180 minutes this applies to the entire northern part. The southern part is not affected by the sluice outflow. Also a situation is simulated in which a maximum flow out of the Noordede river / Ghent-Ostend channel (= 110 m^3/s) was taken into account. In this case it turned out that the entire marina is hindered by

flow velocities that exceed the guidelines from Rijkswaterstaat. However, the situation with this maximum riverine discharge does not happen very often. Based on the examined flow patterns, the marina will either have to be relocated or measures will have to be taken to reduce the flow velocities.

The main research question:

Can a coupled or schematized numerical method be used to accurately simulate the flow field downstream of a discharge sluice?

Yes, both a coupled and a schematized numerical method can be, in certain conditions, used to accurately simulate the flow field downstream of a discharge sluice. In addition, it was found that both considered methods require significantly less computational time than a method in which the entire area of interest is modelled using a model that simulates the complete three-dimensional flow field.

The coupled method (including extra thin dams), method COMSOL-D3D, showed a flow pattern that has a great correspondence with the one obtained with the baseline method. It was shown that it is important to bring the flow rate gradually in the D3D model, in order for this coupling to work properly. This can be achieved by adding thin dams to the sides of the grid cells that include the source terms. Furthermore, the coupling should be made in the area before the predicted point at which the jet starts to deviate from the center but downstream of the area in which three-dimensional flows caused by the pile row are present. In this way the coupling is already made before the potential Coanda effect starts to play a role in the direction of the jet.

The schematized method, method D3D, in which the sluice outflow is schematized by means of the general discharge relation, also showed results that have a great correspondence with those from the baseline method. However, it is expected that this would not be the case in every situation. In the case the discharge coefficient μ cannot be determined accurately in an analytical/empirical way, this method is expected to show different results than obtained with the baseline method. It is expected that the discharge coefficient can no longer be accurately determined when the geometry of the system becomes more complex. An example of this is when partially closed valves or other irregularities inside the culverts are added. Furthermore, the effect of the pile should be simulated by a simplification in D3D. In this study this was possible by using a porous plate but further studies should determine if this applies to all types of pile rows.

As expected, determining the flow pattern by using formulas from literature appeared to be not possible for a case like the one in Ostend. Due to the presence of two culverts and a pile row formulas from literature could only be applied to determine the flow velocities inside the culverts themselves. The results of this literature method in the area downstream of the outflow opening differed greatly from those obtained with the baseline method. It is expected that applying this method to determine the flow pattern downstream of a discharge sluice would only be possible if the system consists of one culvert and in case there is no pile row present. Existing jet equations from literature can then be applied.

Below is an advice for which method is most suitable for a specific part of the discharge sluice domain:

- If one is interested in the flow velocity inside the culverts, it is advised to determine this with formulas from literature.
- If one is interested in the flow in the first meters downstream of the culverts or the flow around the pile row, for example for designing the bottom protection, it is recommended to model the situation completely in COMSOL or a model similar to COMSOL. If the Froude number downstream of the outflow opening is greater than 0.3 here the advice is to apply two-phase modelling.
- If one is interested in the area downstream of the pile row in which the turbulence effects from the pile row have disappeared and there is a straight jet present there are two options:
  - The entire situation is modelled with D3D and the discharge sluice and pile row are mimicked in a schematized way. This is possible when the geometry of the system is simple enough to accurately determine the discharge coefficient in an analytical/empirical way. Furthermore,

the diffusing effect of the pile row should correctly be included in the D3D model. It was possible to accurately determine the effect of the pile row on the flow in this study with a schematized porous plate in D3D. Further research must show whether this applies to all types of pile rows. If both conditions are met, it is advised to use this method in that case because accurate results are obtained in a relatively simple and fast way.

– The discharge sluice, the pile row and a part downstream of the pile row are modelled in COMSOL and a coupling is made with a D3D model. It is advised to use this method when the geometry of the system is complex and the discharge coefficient cannot be easily determined analytically/empirically.

9.2. Recommendations for further research

The recommendations for further research can be divided into different categories: recommendations regarding the baseline method, method COMSOL-D3D, method D3D, the literature method and regarding the realistic Ostend model.

9.2.1. Recommendations regarding the baseline method

- Due to the fact that the model in the baseline method is relatively short, the physics that causes the Coanda effect was not simulated. A subsequent study will therefore have to investigate how long the model domain should be to correctly simulate this physics. Also the exact geometry as it would be in reality should be taken into account. This potentially has large influence on the Coanda effect.
- The COMSOL modelling in this research was done using a rigid-lid approximation. This was done because it makes the modelling easier and because it was assumed that the errors caused by this approach do not have a major impact on the parameters that are ultimately extracted from the model output. It was nevertheless found that in a relatively large area, from the outflow opening to the pile row, the requirements for a rigid-lid approach are not met. A study in which two-phase modelling is applied should be done and a comparison with the results of a rigid-lid approach should be made. In this way it can be said to what extent the errors caused by the rigid-lid approach affect the downstream flow profiles.
- It was assumed that the outflow of the discharge sluice in the first tens of meters ensures complete flushing of the water that is present before opening the valves. Therefore no density differences were assumed for the COMSOL modelling. For the sake of completeness, however, it is good to include these density differences in subsequent studies and to see to what extent it influences the results.

9.2.2. Recommendations regarding method COMSOL - D3D

- This research has shown that the COMSOL - D3D method has the potential to be used in similar projects as the Ostend case. The coupling based on reading flow rates from a COMSOL model and imposing them in D3D has shown similar results as obtained with a computational more expensive method. In future studies it is the challenge to pass on more information with the coupling, not only flow rates but also, for example, turbulence effects. At the moment it is not yet possible to impose these kinds of effects on a boundary in D3D but perhaps this can be implemented or there are other large-scale models in which this is possible.
- It is important to correctly simulate the physics that causes the Coanda effect. Since the COMSOL domain would have to be very long to simulate this physics correctly and the intention is to find a computational time efficient method it is advised to couple in the area before the jet starts deflecting, if the jet deflects at all. For this, research must be done whether the jet deflects and, if so, from which point downstream of a discharge sluice it starts to deviate from the center. It is also important that at this point the three-dimensional flows resulting from the pile row are no longer present, as these effects cannot be passed in a coupling.

9.2.3. Recommendations regarding method D3D

- The biggest challenge with method D3D is to correctly include the effects of a pile row. In this study this was done by placing a porous plate with a certain loss coefficient. This loss coefficient was calculated by using a formula that is originally intended for bridge piers. This is purely a simplification. More research needs to be done whether a pile row in D3D can be simplified with the help of a porous plate or whether that just happened to work in this study.

9.2.4. Recommendations regarding the literature method

- After application of the literature method, it turned out that it is very difficult to predict the effect of the pile row on the development of the jet. In the case of a pile row and a double culvert, there are no applicable formulas in literature to determine the downstream flow pattern. It is therefore advised to determine this effect using a numerical or a physical model and to encompass it with a number of empirical formulas. As a result, in comparable projects a first assumption regarding the resulting flow velocities can be made more quickly.

9.2.5. Recommendations regarding the realistic Ostend D3D model

- The D3D model used in the research into the potential impact of the discharge sluice on the marina simulates wrong water levels in the marina of Ostend. For this research, which mainly concerned a comparison between methods, it has no major consequences, but in subsequent studies on the impact on the entire area it is important to get the water levels correct. For this, the boundary conditions of the Mother model must be adjusted in such a way that the water levels in the port of Ostend correspond to reality.
- No validation is done of, for example, water levels or current velocities in the final D3D model that is used. First a measurement campaign will have to be started in the port of Ostend to validate this D3D model.
- In the final D3D modelling only a flow through the discharge sluice from the Spuikom to the marina is taken into account. In reality, the same amount of water flows the other way. This flow in other direction creates a suction of water from the marina and this can also potentially cause hindrance to nautical activities in the marina. For example, if vessels are too close to the culverts, they can be sucked towards the discharge sluice and get stuck. The flow in the other direction, which occurs when the water level in the marina is higher than in the Spuikom, must therefore also be included in subsequent studies. However, it is expected that the flow rates in the RYCO will be considerably lower when the Spuikom is filled than when it is emptied.
- Only extreme conditions are considered in the D3D modelling. Water levels during spring tide and a maximum riverine discharge are taken into account. In order to get an idea of the flow pattern in the downstream port throughout the year, other boundary conditions will also have to be considered. A normal discharge from the Noordede river / Ghent-Ostend channel and a normal tide, for example, should be simulated.

A

Turbulence modelling

The flow resulting from a discharge sluice outlet has a strong turbulent character, which means that the fluid contains many chaotic changes in pressure and flow velocity. Vorticity, which is the tendency of a fluid to rotate, has an important role in these processes (K. Pietrzak, 2013; Talstra, 2011). In the case of a turbulent flow, energy is being transferred within the fluid, from large-scale turbulent structures to small-scale turbulent by the breaking vortices. The created vortices break up into smaller parts due to their instability. The smaller vortices again break up into even smaller pieces. This process continues to the smallest scale: the Kolmogorov scale (Uijttewaal, 2018). For civil engineering applications it is often not necessary to describe the smallest turbulence scales in the numerical models. These small fluctuations are therefore averaged. First the basic Navier-Stokes equations are presented to explain how this averaging works. The continuity equation is as follows and implies a divergence free velocity field:

$$\frac{\partial u_i}{\partial x_i} = 0 \tag{A.1}$$

Conservation of momentum results in the following momentum equation:

$$\frac{\partial u_i}{\partial t} + \frac{\partial u_i u_j}{\partial x_j} = -\frac{1}{\rho}\frac{\partial p}{\partial x_i} + \frac{\partial}{\partial x_j}\left(v\frac{\partial u_i}{\partial x_j}\right) \tag{A.2}$$

The Reynolds number appears to be the only remaining parameter if equation Eq. (A.2) is considered in dimensionless form. This is done by using a characteristic velocity U and length scale L. Applying Reynolds averaging means that the mean motion is resolved and the turbulent fluctuations are ignored (Andersson et al., 2011). A separation is made into an ensemble averaged component (overlined) and a fluctuating component (prime) for the velocity vector and the pressure, also known as the Reynolds decomposition. Averaging in time could potentially lead to interpretation problems when the mean flow varies in time so ensemble averaging is used. An ensemble is a number of realizations of the flow under comparable conditions (Westin & Henkes, 1988).

$$u = \bar{u} + u' \tag{A.3}$$

$$p = \bar{p} + p' \tag{A.4}$$

Substitution of Eq. (A.3) and Eq. (A.4) into the momentum equation Eq. (A.2) and ensemble averaging of the different terms leads to the Reynolds equation Eq. (A.5). Different terms fall out of the equations, using the Reynolds conditions: $\bar{u'} = 0$ and $\bar{\bar{u}} = \bar{u}$.

$$\frac{\partial \rho \bar{u}_i}{\partial t} + \frac{\partial \rho \bar{u}_i \bar{u}_j}{\partial x_j} + \frac{\partial \rho \overline{u_i' u_j'}}{\partial x_j} = -\frac{\partial \bar{p}}{\partial x_i} + \mu \frac{\partial^2 \bar{u}_i}{\partial x_j^2} \tag{A.5}$$

The Reynolds condition $\bar{u'} = 0$ causes the fluctuating parts to disappear from the equation, except the non-zero product of the velocity fluctuations $\rho\overline{u_i' u_j'}$, also known as the Reynolds stress tensor. It

consists of nine elements: normal stresses and shear stresses. This Reynolds stress tensor introduces new unknown variables, for which additional expressions should be found (Westin & Henkes, 1988). Due to the symmetry of the stress tensor, six independent stresses should be described. Neglecting the three normal stresses leads to three unknown shear stresses. Many turbulence models have been introduced to give approximations of these stresses (e.g. k-ε, k-ω, RNG) (Alfonsi, 2009; Lesser et al., 2004). From experimental and numerical results it appeared that a k-ε model gave the best results for the prediction of the flow velocity in the case of a sluice gate flow (Akoz et al., 2009).

In COMSOL the turbulent viscosity parameter μ_T is computed trough one of the turbulence closure models. Several turbulence models are available, including various k-ε models, k-ω models, a Reynolds stress model (RSM), Detached Eddy Simulation (DES) and Large Eddy Simulation (LES) (COMSOL, 2019). In D3D a turbulence closure model is applied to calculate the vertical eddy viscosity v_t^v. Four different options are available within D3D: A user-defined constant vertical eddy viscosity, the Algebraic Eddy viscosity closure Model (AEM), the k-L turbulence closure model and the k-ε turbulence closure model. These models give a relation between the turbulent kinetic energy k, the dissipation rate ε, the mixing length l_m and the vertical eddy viscosity v_t^v (Deltares, 2021).

B

Model specifications

B.1. COMSOL

This paragraph treats physical and numerical settings of the used COMSOL models. The consulted literature provides justification for these settings.

B.1.1. Physical settings

It is assumed that the vertical turbulent activities are negligible compared to those in the horizontal (L » d). Turbulence production (k) and dissipation (ε) terms can therefore be described in non-conservative form. The coupled pair of PDE's are solved by a k-ε turbulence closure model (COMSOL, 2019). More details regarding turbulence modelling can be found in Appendix A.

Gravity is not included in the COMSOL model, in order to save computational time. This assumption can be made due to the fact that only one phase is modelled, the fluid is incompressible and there are no density differences present. If gravity would be included, a body force ρg that works on the entire model is added to Eq. (2.8). Excluding the gravity has no influence on the flow velocity development (COMSOL, 2019). The following governing equations are solved in COMSOL, of which the bottom four equations are part of the k-ε closure model.

$$
\begin{aligned}
&\rho\frac{\partial \mathbf{u}}{\partial t} + \rho(\mathbf{u}\cdot\nabla)\mathbf{u} = \nabla\cdot[-p\mathbf{l} + \mathbf{K}] + \mathbf{F}\\
&\rho\nabla\cdot\mathbf{u} = 0\\
&\mathbf{K} = (\mu + \mu_T)\left(\nabla\mathbf{u} + (\nabla\mathbf{u})^{\mathsf{T}}\right)\\
&\rho\frac{\partial k}{\partial t} + \rho(\mathbf{u}\cdot\nabla)k = \nabla\cdot\left[\left(\mu + \frac{\mu_T}{\sigma_k}\right)\nabla k\right] + P_k - \rho\epsilon\\
&\rho\frac{\partial \epsilon}{\partial t} + \rho(\mathbf{u}\cdot\nabla)\epsilon = \nabla\cdot\left[\left(\mu + \frac{\mu_T}{\sigma_\varepsilon}\right)\nabla\epsilon\right] + C_{\epsilon 1}\frac{\epsilon}{k}P_k - C_{\varepsilon 2}\rho\frac{\epsilon^2}{k}, \quad \epsilon = \mathrm{ep}\\
&\mu_T = \rho C_\mu\frac{k^2}{\epsilon}\\
&P_k = \mu_T\left[\nabla\mathbf{u} : \left(\nabla\mathbf{u} + (\nabla\mathbf{u})^T\right)\right]
\end{aligned}
\tag{B.1}
$$

The roughness values of the bottom of the outflow area and the culverts were determined using Eq. (B.2) and typical Manning values for concrete and clay (Chow, 1959; Marriott & Jayaratne, 2010). Other physical parameters were based on COMSOL (2019) and Jørgensen (2000).

$$n \approx 0.038 \cdot (k_s)^{1/6} \tag{B.2}$$

in which,

- n = the manning coefficient [-]
- k_s = equivalent sand roughness height [m]

Symbol	Parameter	Unit	Global	Source
μ	Dynamic viscosity	Pa · s	$8.90 \cdot 10^{-4}$	Jørgensen (2000)
ρ	Density	kg/m^3	1000	Jørgensen (2000)
k_{seq}	Equivalent sand roughness height concrete	m	$1.0 \cdot 10^{-3}$	Marriott and Jayaratne (2010)
k_{seq}	Equivalent sand roughness height clay	m	0.61	Marriott and Jayaratne (2010)
T	Temperature	K	293.15	COMSOL (2019)
I_T	Turbulent intensity	[-]	0.05	COMSOL (2019)
L_T	Turbulence length scale	m	Geometry based	COMSOL (2019)

Table B.1: Physical parameters COMSOL model.

B.1.2. Numerical settings

In COMSOL the underlying finite element method for discretization is the Galerkin method (COMSOL, 2019; Fletcher, 1984). The so-called Péclet number Pe determines the stability of the resulting numerical problem (Shires, 2021). It relates the convective and diffusive effects and should be larger than one:

$$Pe = \frac{\beta h}{2c} > 1 \tag{B.3}$$

in which,

Pe = the Péclet number [-]
β = convective velocity vector [m/s]
c = the diffusion coefficient [m^2/s]
h = the mesh element size [m]

It follows from Eq. (B.3) that either large convective or small diffusive activity leads to a Péclet number larger than 1, thus instability. Besides, there is also an important role for the mesh element size. The smaller the mesh element size, the smaller the element Péclet number. As long as the diffusion coefficient c is larger than zero, there is a mesh resolution at which the discretization is stable. By refining the mesh spurious oscillations can then be removed. Instead, stabilization methods which add artificial diffusion are used (Zijlema, 2020). In COMSOL all transport interfaces, including turbulent flow, automatically use stabilization. So-called consistent stabilization is used by default since this method works well for most applications. Details regarding the stabilization methods in COMSOL can be found in the COMSOL user manual (COMSOL, 2019). In the COMSOL simulations that are done in this research stabilization is guaranteed by applying streamline and crosswind diffusion (COMSOL, 2019).

The order computational elements with which the velocity and the pressure is resolved can be indicated in COMSOL. In Pm + Pn the order with which the velocity is resolved is indicated with an 'm', while the order with which the pressure is resolved is indicated with an 'n'. P1 + P1 therefore means first order, i.e. linear, elements for both the velocity and pressure components. Less computational power is required for linear elements than for higher-order elements. It is also less likely that spurious oscillations are introduced, thereby improving the numerical stability. A P1 + P1 discretization can save computational time but streamline stabilization of the Navier-Stokes equations is required. Streamline stabilization is the default option in the turbulent flow interface (COMSOL, 2019).

B.2. D3D

This paragraph treats physical and numerical settings of the used D3D models: the Granddaughter model (OGD) and the simplified D3D model. The consulted literature provides justification for these settings.

B.2.1. Physical settings

The turbulence production term (k) and the dissipation term ε are again solved by a k-ε turbulence closure model. The exchange of lateral momentum is affected by the magnitude of the horizontal eddy viscosity v_h (Uittenbogaard et al., 2005). Difficulties arise in that v_h has no direct physical basis and is a function of both local flow parameters and flow history (Blazek, 2015). A higher v_h denotes more conversion of kinetic (advective) energy in to potential energy through dissipation by turbulence. In the models v_h is taken as 1.0 and 0.1 m^2/s, in line with findings from Dujardin et al. (2017).

As no density differences are included in the simplified model, diffusion is only present in the OGD model. Vertical diffusion is solved here by the k-ε model. Horizontal diffusion is assigned a value of 10 m^2/s. This is based on an advice to use a diffusivity that is ten times greater than the viscosity. The manning coefficient for the OGD model is obtained from the Daughter model (Dujardin et al., 2017) and equals 0.016 for the entire area. The Manning coefficient for the simplified model equals the bottom roughness value in the COMSOL model.

Symbol	Parameter	Unit	Simplified	OGD	Source
v_h	Horizontal eddy viscosity	m^2/s	0.1	1	Deltares (2021)
D_h	Horizontal eddy diffusivity	m^2/s	-	10	Deltares (2021)
n	Manning coefficient	$m^{1/3}s$	0.035	0.016	Dujardin et al. (2017)

Table B.2: Physical parameters D3D models.

The vertical profile is divided into different computational layers, following the sigma coordinate approach.

B.2.2. Numerical settings

The timestep (∆t) in both models is defined at 0.005 minutes, i.e. 0.3 seconds. This value has been chosen so that, on the one hand, the simulation time is kept as low as possible, but the Courant stability criterion is still met. For numerical stability the Courant number should remain below 1 (Deltares, 2021). This is shown by the following calculation of the Courant number:

$$\frac{\Delta t}{\Delta x} = \frac{0.3}{1.5} = 0.2 \tag{B.4}$$

The other numerical settings are default values (Deltares, 2021).

Numerical constant	Value	unit
Timestep (∆t)	0.005	min.
No. of σ-layers	10	-
Threshold depth	0.1	m
Smoothing time	60	min.

Table B.3: Numerical constants applied for D3D models.

C

Sensitivity analysis

Several sensitivity analyses are performed in this study. One is used to determine the most suitable grid size in the COMSOL modelling (Appendix C.1), one to determine the length and width of the upstream part in COMSOL (Appendix C.1.2) and one to determine the most optimal grid size in the D3D model (Appendix C.2).

C.1. Sensitivity analyses COMSOL modelling

C.1.1. Grid size

The mesh in the COMSOL model is a so-called physics-controlled mesh (COMSOL, 2019). As a user you choose an element size for the mesh from 'Extremely Coarse' to 'Extremely Fine'. COMSOL then automatically creates a mesh based on the geometry. Four different element sizes are examined in this sensitivity analysis: 'Normal', 'Coarse', 'Coarser' and 'Extra Coarse'. The goal is to find the grid size that still gives accurate results but minimizes computational time. The horizontal distributions of the flow velocity at 1 meter from the bottom at different distances (43, 50 and 80 meters) from the outflow opening are compared to each other. The y-axis in this case is a cross-section of the model, perpendicular to the direction of the jet. Furthermore, the vertical distributions of the flow velocity in the middle of the model at different distances (43, 50 and 80 meters) are compared. First, a comparison at a distance of 43 meters presented, then at 50 meters and last at 80 meters from the outflow opening.

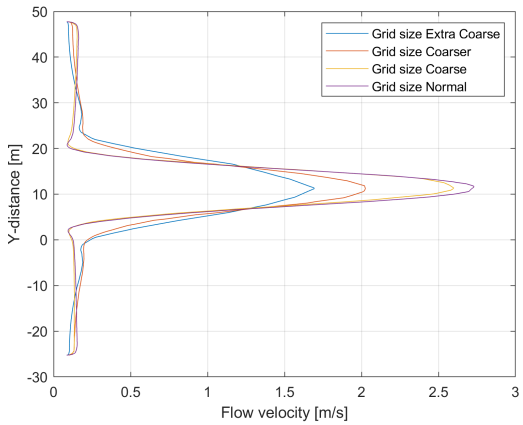

Figure C.1: Comparison horizontal distributions at x = 43 m, different grid sizes.

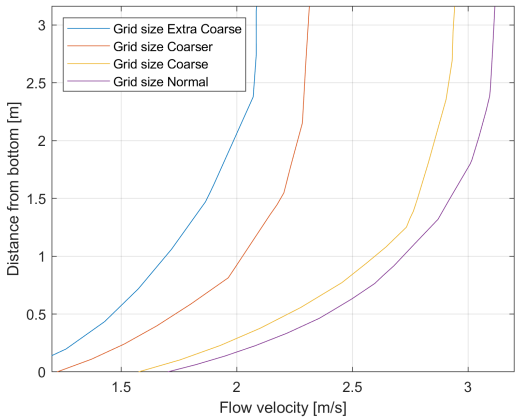

Figure C.2: Comparison vertical distributions at x = 43 m, different grid sizes.

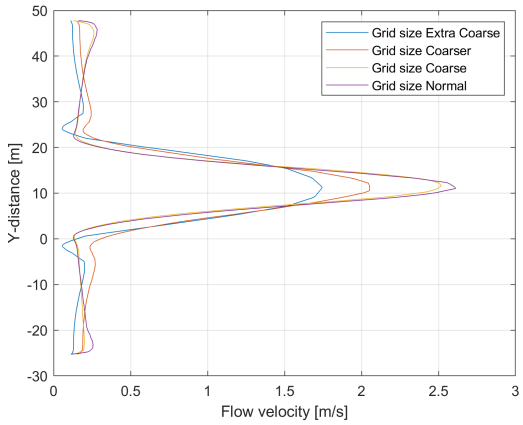

Figure C.3: Comparison horizontal distributions at x = 50 m, different grid sizes.

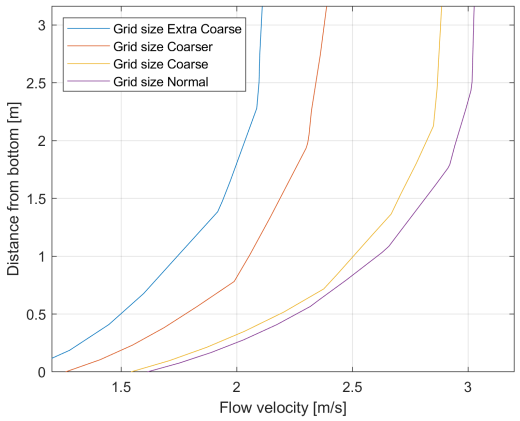

Figure C.4: Comparison vertical distributions at x = 50 m, different grid sizes.

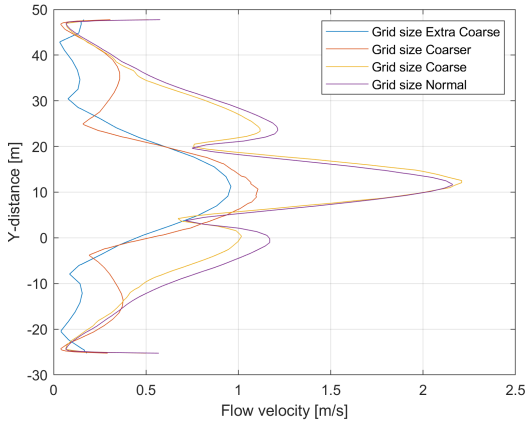

Figure C.5: Comparison horizontal distributions at x = 80 m, different grid sizes.

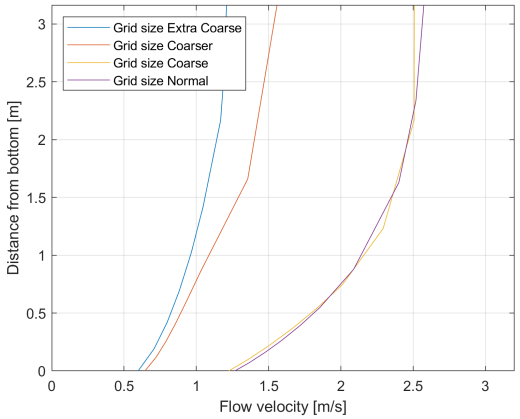

Figure C.6: Comparison vertical distributions at x = 80 m, different grid sizes.

In the figures above it can be seen that the differences in flow profiles between grid sizes 'Coarse' and 'Normal' are maximum 8%. The differences with the flow profiles of the other two grid sizes are much greater. It is therefore assumed that grid size 'Coarse' is the most optimal choice in terms of accuracy and computational time.

C.1.2. Length and width upstream water body

Simulations are done with an upstream domain twice as long and twice as wide, in order to determine the influence of the width of the inflow boundary and the length of the upstream domain. The 'normal' dimensions of the upstream part are 10 m long and 22.5 m wide. Again the horizontal and vertical flow profiles at three different distances from the outflow opening are compared.

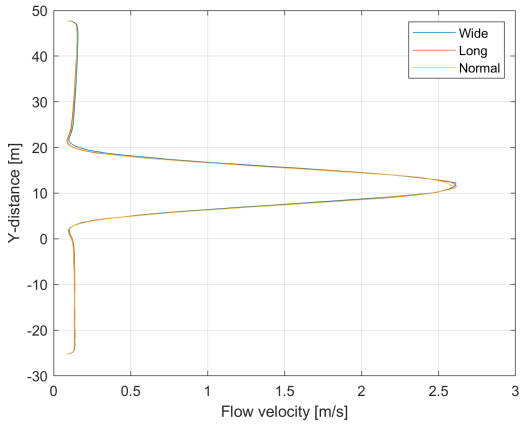

Figure C.7: Comparison horizontal distributions at x = 43 m, different width and length upstream water body.

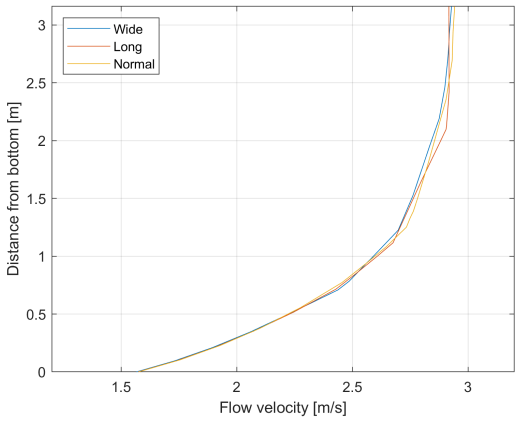

Figure C.8: Comparison vertical distributions at x = 43 m, different width and length upstream water body.

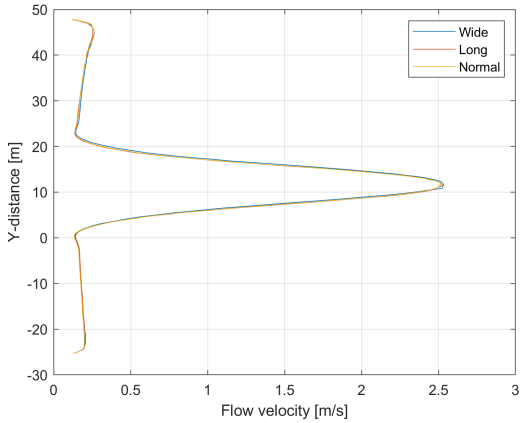

Figure C.9: Comparison horizontal distributions at x = 50 m, different width and length upstream water body.

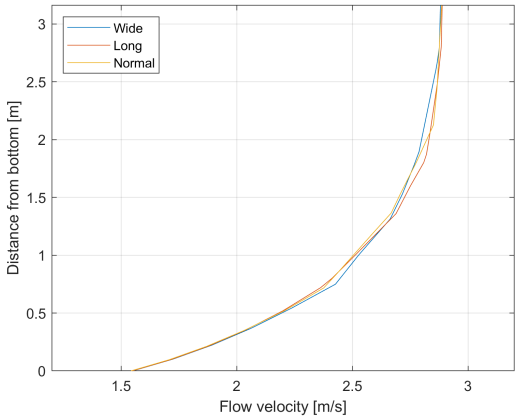

Figure C.10: Comparison vertical distributions at x = 50 m, different width and length upstream water body.

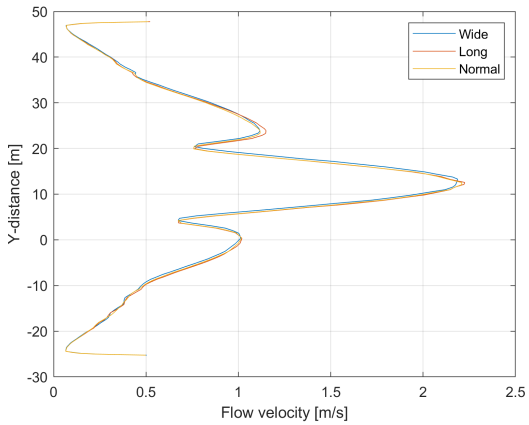

Figure C.11: Comparison horizontal distributions at x = 80 m, different width and length upstream water body.

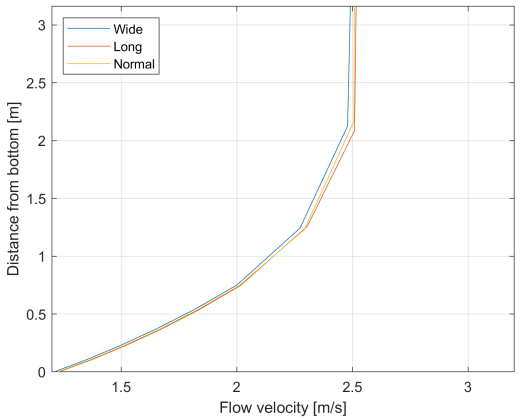

Figure C.12: Comparison vertical distributions at x = 80 m, different width and length upstream water body.

Based on the above figures it is determined that to a certain extent widening or lengthening the upstream domain in COMSOL has no influence on the downstream flow pattern. All the inflow effects are included in the case of the 'normal' dimensions.

C.2. Sensitivity analysis D3D modelling

A simplified D3D model is set up to vary with different parameters such as the grid size, the viscosity, the roughness, the amount of vertical layers and loss coefficient of a porous plate. A jet is caused by source terms that are added to a few grid cells. The width of the jet corresponds with the width of the jet in the Ostend case. Simulations with a grid size of respectively 1, 2 and 4 m are done. The 0.3 m/s jet for the three different classes can be found in Fig. C.13. In the background, indicated by colours, the jet obtained with the smallest grid size is shown. The dashed line indicates the 2m grid size jet, the dotted line the 4m grid size jet. It is observed that by using a 2 m grid cell size the bending in the jet can still be simulated, with a 4 m grid cell size this is more difficult. Moreover, the smallest ships that moor in a marina have a length of several meters. A grid cell size of four meters would skip a lot of detail. Therefore it is decided to do the D3D model simulations with a grid cell size of two meters.

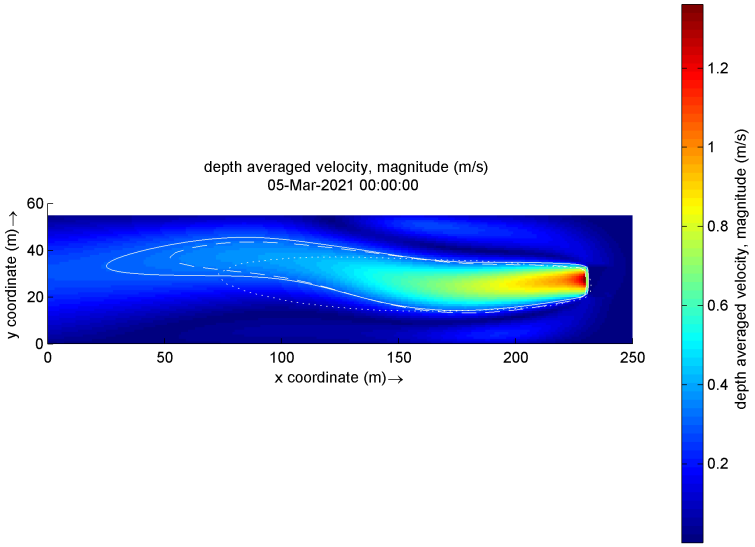

Figure C.13: Jets in D3D with different grid sizes.

D

Validation Granddaughter model

A comparison was made between the water levels and depth-averaged flow velocities at corresponding locations in the Daughter and the Granddaughter model. This validates that the granddaughter model can be used.

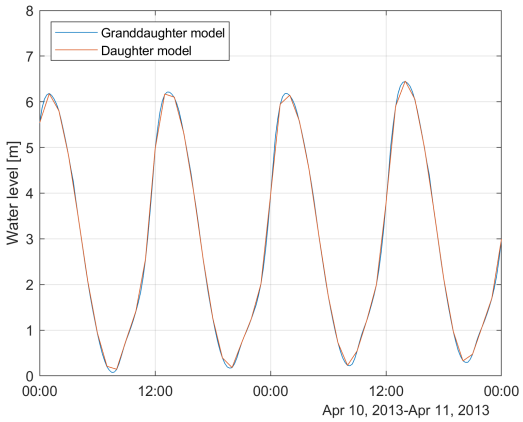

Figure D.1: Comparison of water levels at corresponding location in Daughter and Granddaughter model.

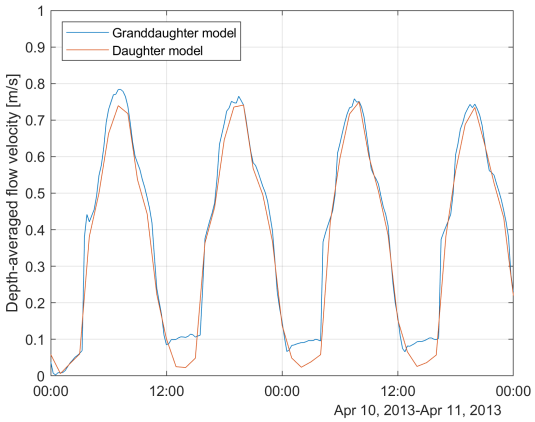

Figure D.2: Comparison of depth-averaged flow velocities at corresponding location in Daughter and Granddaughter model.

E

Results extra simulation ’thin dam method’

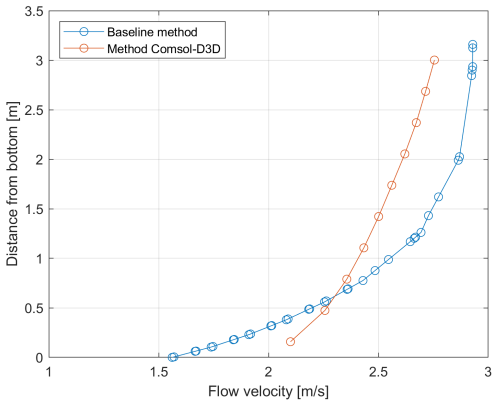

(a) Comparison horizontal velocities at location 1, thin dam method.

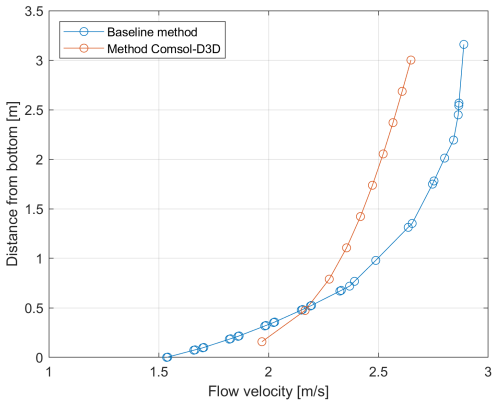

(b) Comparison horizontal velocities at location 2, thin dam method.

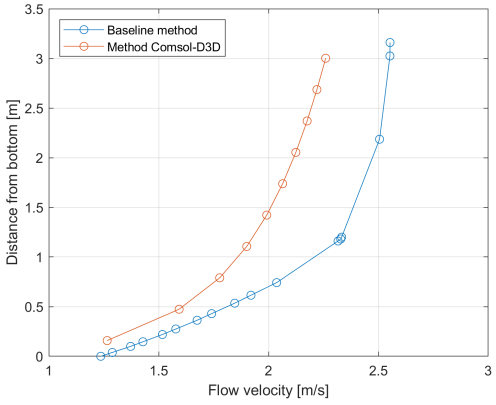

(c) Comparison horizontal velocities at location 3, thin dam method.

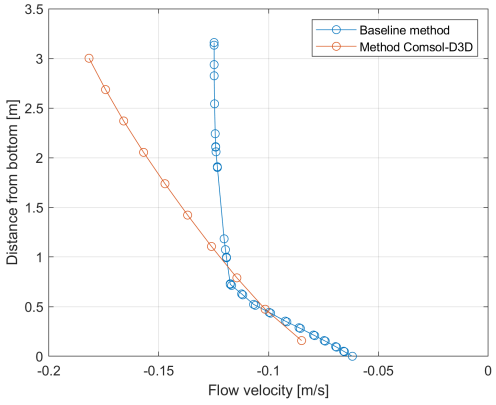

(d) Comparison horizontal velocities at location 4, thin dam method.

Figure E.1: Comparison of flow velocities baseline method and method Comsol - D3D at four different locations, thin dam method.

Bibliography

Akoz, S., Oner, A. A., & Kirkgöz, M. S. (2009). Experimental and numerical modeling of a sluice gate flow. *Journal of Hydraulic Research 47*, *47*(2), 167–176. https://doi.org/10.3826/jhr.2009.3349

Alfonsi, G. (2009). Reynolds-Averaged Navier-Stokes Equations for Turbulence Modeling. *Applied Mechanics Reviews*, *62*(4). https://doi.org/10.1115/1.3124648

AMDK. (2021). Overzicht van de tijwaarnemingen langs de Belgische kust - Periode 2001-2010 voor NIEUWPOORT, OOSTENDE EN ZEEBRUGGE. https://www.afdelingkust.be/sites/default/files/atoms/files/10-jarig20overzicht20_getij.pdf.

Andersson, B., Andersson, R., Håkansson, L., Mortensen, M., Sudiyo, R., & van Wachem, B. (2011). *Computational fluid dynamics for engineers*. Cambridge University Press.

ASCE. (2012). *Planning and design guidelines for small craft harbors*. Task Committee on Marinas 2020.

Aziz, T. N., Raiford, J. P., & Khan, A. A. (2008). Numerical Simulation of Turbulent Jets. *Engineering Applications of Computational Fluid Mechanics*, *2*(2), 234–243. https://doi.org/10.1080/19942060.2008.11015224

Barenblatt, G., Chorin, A., & Prostokishin, V. (2005). The turbulent wall jet: A triple-layered structure and incomplete similarity. *PNAS*, *102*(25).

Battjes, J. A. (2002). Vloeistofmechanica TU Delft - lecture notes.

Belaud, G., Cassan, L., & Baume, J.-P. (2009). Calculation of Contraction Coefficient under Sluice Gates and Application to Discharge Measurement. *Journal of Hydraulic Engineering*, *135*(12), 1086–1091. https://doi.org/10.1061/(ASCE)HY.1943-7900.0000122

Benjamin, T. B. (1968). Gravity currents and related phenomena. *Journal Fluid Mechanics*, *31*, 209–248.

Blazek, J. (2015). *Computational Fluid Dynamics: Principles and Applications (Third Edition)*. Butterworth-Heinemann.

Bosboom, J., & Stive, M. (2015). *Coastal Dynamics I*. Delft Academic Press.

Broomans, P. (2002). Numerical Accuracy in Solutions of the Shallow-Water Equations - MSc Thesis.

Chaudhry, M. H. (1993). *Open-channel flow*. Prentice Hall.

Choi, K. W., & Lee, J. H. W. (2007). Distributed Entrainment Sink Approach for Modeling Mixing and Transport in the Intermediate Field. *Journal of Hydraulic Engineering*. https://doi.org/10.1061/(ASCE)0733-9429(2007)133:7(804)

Chow, V. T. (1959). *Open-channel hydraulics*. McGraw-Hill.

Church, J. A., Clark, P. U., Cazenave, A., Gregory, J. M., Jevrejeva, S., Levermann, A., Merrifield, M. A., Milne, G. A., Nerem, R. S., Nunn, P. D., Payne, A. J., Pfeffer, W. T., Stammer, D., & Unnikrishnan, A. S. (2013). Sea-Level Rise by 2100. *Science*, *342*(6165), 1445–1445. https://doi.org/10.1126/science.342.6165.1445-a

COMSOL. (2019). COMSOL Multiphysics - user manual.

Constantinescu, G., Rodi, W., & Stoesser, T. (2013). *Large-eddy simulation in hydraulics*. https://doi.org/10.1201/b15090

Courant, R., & Hilbert, D. (1962). Methods of Mathematical Physics. *Interscience*, *137*(3527), 334. https://doi.org/10.1126/science.137.3527.334

Dekker, F., Bijlsma, A., de Jong, M., & Boot, M. (2009). Integration of a cooling water outflow in the rotterdam harbour extension. ResearchGate.

Deltares. (2021). Delft3D-FLOW - user manual.

di Martino, B., Giacomoni, C., & Orenga, P. (2001). Analysis of some shallow water problems with rigid-lid hypothesis. *Mathematical Models and Methods in Applied Sciences*, *11*(6), 979–999. https://doi.org/https://doi.org/10.1142/S0218202501001203

Dronkers, J. (2011). Investigations of the tides and storm surges for the deltaworks in the southwestern part of the netherlands. *Coastal Engineering Proceedings*, *1*(7), 32. https://doi.org/10.9753/icce.v7.32

Dujardin, A., Vanlede, J., Verwilligen, J., Verwaest, T., Peeters, P., & Mostaert, F. (2017). Nautische optimalisatie ontwerp Halve Maandijk te Oostende - technical report.

EPA. (2021). Environmental fluid dynamics code (efdc). https://www.epa.gov/ceam/environmental-fluid-dynamics-code-efdc

Erdbrink, C. D., Krzhizhanovskaya, V. V., & Sloot, P. M. (2014). Free-surface flow simulations for discharge-based operation of hydraulic structures gates. *Journal of Hydroinformatics*, *16*(1), 189–206.

Fan, F., Liang, B., Li, Y., Bai, Y.-c., Zhu, Y., & Zhu, Z. (2017). Numerical investigation of the influence of water jumping on the local scour beneath a pipeline under steady flow. *Water*, *9*, 642.

Ferziger, J. H., & Perić, M. (1996). *Computational methods for fluid dynamics*. Springer.

Fletcher, C. A. (1984). *Computational Galerkin Methods*, 72–85. https://doi.org/10.1007/978-3-642-85949-6_2

Genic, S., Aranđelović, I., Kolendić, P., Jarić, M., Budimir, N., & Genić, V. (2011). A Review of Explicit Approximations of Colebrook's Equation.

Gessner, F. B., & Jones, J. B. (1965). On some aspects of fully-developed turbulent flow in rectangular channels. *Journal of Fluid Mechanics*, *23*(4), 689–713. https://doi.org/10.1017/S0022112065001635

Goossens, E., & Moerkerke, C. (2019). Project-MER Overstromingsmaatregelen achterhaven Oostende - technical report.

Havencommissie, V. (2019). Haven van Oostende. https://www.vlaamsehavencommissie.be/vhc/pagina/haven-oostende

HIC. (2021). Hydrologisch Informatie Centrum. https://www.waterbouwkundiglaboratorium.be/nl/hydrologisch-informatie-centrum-hic-modernisering-hic-meetnet

Idel'chik, I. E. (1966). *Handbook of hydraulic resistance: Coefficients of local resistance and of friction*. Israel Program for Scientific Translations.

Imao, S., Kikuchi, S., Kozato, Y., & Hayashi, T. (2005). Flow characteristics of plane wall jet with side walls on both sides(wall jet and wall flow). *The Proceedings of the International Conference on Jets, Wakes and Separated Flows (ICJWSF)*, *2005*, 73–78. https://doi.org/10.1299/jsmeicjwsf.2005.73

Inventaris, V. (2019). Oostende Haven. https://inventaris.onroerenderfgoed.be/themas/14517

Jirka, G. H., Doneker, R. L., & Hinton, S. W. (1996). User's manual for Cormix.

Jørgensen, S. E. (2000). *Principles of pollution abatement: Pollution abatement for the 21st century*. Elsevier.

Konter, J., & Klatter, L. (1991). Hydraulic Aspects of the Construction of the Eastern Scheldt Storm Surge Barrier. *Coastal Engineering 1990*. https://doi.org/10.1061/9780872627765.225

Kranenburg, W. M., Morelissen, R., Schueder, M. R., Groenenboom, J., van der Hout, A. J., & van der Kaaij, T. (2016). Effect IZZS spuitmiddel op stroming Voorhaven Krammersluizen.

Lee, J. H. W., & Cheung, V. (1990). Generalized lagrangian model for buoyant jets in current. *Journal of Environmental Engineering*, *116*(6). https://doi.org/https://doi.org/10.1061/(ASCE)0733-9372(1990)116:6(1085)

Lesser, G. R., Roelvink, J. A., van Kester, J. A., & Stelling, G. S. (2004). Development and validation of a three-dimensional morphological model. *Coastal Engineering*, *51*. https://doi.org/doi:10.1016/j.coastaleng.2004.07.014

Liu, S.-h., Liao, T.-t., & Luo, Q.-s. (2015). Numerical simulation of turbulent flow behind sluice gate under submerged discharge conditions. *Journal of Hydrodynamics*, *27*(2), 257–263. https://doi.org/10.1016/s1001-6058(15)60480-2

Luijendijk, A., De Vries, S., Van het Hooft, T., & De Schipper, M. (2019). Predicting dune growth at the sand engine by coupling the Delft3D flexible mesh and aeolis models. *Coastal Sediments 2019*. https://doi.org/10.1142/9789811204487_0115

Luijendijk, A., Ranasinghe, R., De Schipper, M., Huisman, B., Swinkels, C., Walstra, D.-J., & Stive, M. (2017). The initial morphological response of the sand engine: A process-based modelling study. *Coastal Engineering*, *119*, 1–14. https://doi.org/10.1016/j.coastaleng.2016.09.005

Maas, A. (2002). *Optimalisatie van afmetingen spuiopeningen in huidig voorontwerp van open spuisluis in Afsluitdijk* (Doctoral dissertation).

Marriott, M., & Jayaratne, R. (2010). Hydraulic roughness – links between Manning's coefficient, Nikuradse's equivalent sand roughness and bed grain size. *Proc. 5th Annual Conf. on Advances in Computing and Technology*.

McSherry, R. J., Chua, K. V., & Stoesser, T. (2017). *Large-eddy simulation of free-surface flows* (Doctoral dissertation).

Miozzi, M., Lalli, F., & Romano, G. (2010). Experimental investigation of a free-surface turbulent jet with Coanda effect. *Exp Fluids*, *49*, 341–353. https://doi.org/10.1007/s00348-010-0885-1

Montagna, P. A., Palmer, T. A., & Pollack, J. B. (2013). *Hydrological Changes and Estuarine Dynamics*. Springer.

Navisworks. (2021). Navisworks 2021 - user manual.

Persoone, G., & de Pauw, N. (1968). Pollution in the harbour of Ostend (Belgium). Biological and hydrographical consequences. *Helgoländer wiss. Meeresunters*, *17*, 302–320.

PIANC. (2017). Guidelines for marina design.

Pietrzak, J. (2017). An Introduction to Stratified Flows for Civil and Offshore Engineers "From Shelf to Shore".

Pietrzak, K. (2013). An Introduction to Oceanography for Civil and Offshore engineers - lecture notes CIE5317.

Rajaratnam, N., & Subramanya, K. (1967). Flow Equation for the Sluice Gate. *Journal of the Irrigation and Drainage Division*, *93*(3), 167–186. https://doi.org/10.1061/JRCEA4.0000503

Rajatratnam, N. (1976). *Turbulent Jets*. Elsevier.

Ramos, P. X., Schindfessel, L., Pêgo, J. P., & De Mulder, T. (2019). Flat vs. curved rigid-lid LES computations of an open-channel confluence. *Journal of Hydroinformatics*, *21*(2), 318–334.

Rapp, B. E. (2017). Chapter 9 - fluids. In B. E. Rapp (Ed.), *Microfluidics: Modelling, mechanics and mathematics* (pp. 243–263). Elsevier.

Ridderinkhof, W., van den Berg, B., Berkhout, B., van der Valk, R., Carree, P., Broere, P., Spasov, K., Versluys, M., & Verscheuren, J. (2019).

Rijkswaterstaat. (2000). Ontwerp van schutsluizen - manual.

Rijkswaterstaat. (2020). Richtlijnen Vaarwegen 2020 - manual.

Ryco. (2021). Ryco History. http://www.ryco.be

Schiereck, G. J., & Verhagen, H. (2019). *Introduction to bed, bank and shore protection*. Delft Academic Press / VSSD.

Shin, J. O., Dalziel, S. B., & Linden, P. F. (2004). Gravity currents produced by lock exchange. *Journal Fluid Mechanics*, *521*, 1–34. https://doi.org/10.1017/S002211200400165X

Shires, G. L. (2021). Peclet number. *A-to-Z Guide to Thermodynamics, Heat and Mass Transfer, and Fluids Engineering*. https://doi.org/10.1615/atoz.p.peclet_number

Swamee, P. K. (1992). Sluice-Gate Discharge Equations. *Journal of Irrigation and Drainage Engine*, *118*(1).

Talstra, H. (2011). *Large-scale turbulence structures in shallow separating flows* (Doctoral dissertation).

Thijsse, J. T. (1960). Collegediktaat hydraulica deel 1 en 2.

Turan, C., Politano, M. S., Carrica, P. M., & Weber, L. (2007). Water entrainment due to spillway surface jets. *International Journal of Computational Fluid Dynamics*, *21*(3-4), 137–153. https://doi.org/10.1080/10618560701525954

Uijttewaal, W. (2018). Collegedictaat CIE5312 Turbulence in Hydraulics - lecture notes.

Uittenbogaard, R. E., Stolker, C., de Goede, E. D., van Kester, J. A. T. M., Jagers, H. R. A., & Wijbenga, J. H. A. (2005). Eddy Viscositeit in WAQUA modellen van Rijntakken en Maas.

van der Hout, A. (2011). Nautical interpretation of stratified flow fields - technical report. *Deltares*.

van der Hout, A. (2020). Ports and Waterways 2 CIE5306 - lecture notes.

van der Wal, M. (2000). Cursus moderne rivierkunde.

van Reeken, H. (1988). Spuisluis bij Bath luchtfoto ID304032. https://beeldbank.rws.nl/MediaObject/Details/304032

Vliz. (2021). Metingen | de spuikom oostende. http://www.vliz.be/spuikom/metingen

Westin, K. J. A., & Henkes, R. A. W. M. (1988). Prediction of Bypass Transition with Differential Reynolds Stress Models.

Witteveen+Bos. (2019). Stromingsmodellering Delft3D achterhaven Oostende - technical report.

Zijlema, M. (2020). CIE4340 Computational modelling of flow and transport - lecture notes.